



This is to certify that the
thesis entitled

Physicochemical studies of
magnesium complexes
presented by

Pierre-Henri C. HEUBEL

has been accepted towards fulfillment of the requirements for

Ph. D. degree in <u>Chemistry</u>

Major professor

Professor Alexander I. POPOV

Date July 18, 1978

O-7639

PHYSICOCHEMICAL STUDIES OF MAGNESIUM COMPLEXES

Ву

Pierre-Henri C. Heubel

A DISSERTATION

Submitted to

Michigan State University

in partial fulfillment of the requirements

for the degree of

DOCTOR OF PHILOSOPHY

Department of Chemistry

ABSTRACT



PHYSICOCHEMICAL STUDIES OF MAGNESIUM COMPLEXES

Ву

Pierre-Henri C. Heubel

Magnesium-25 NMR measurements were made in a variety of solvents on several magnesium salts as a function of salt concentration.

Magnesium chloride and bromide were prepared following the method described by Ashby and Arnott [redox reaction between magnesium turnings and a mercury (II) halide in tetrahydrofuran (THF)]. When ion pairing takes place in solution, a chemical shift change (up to 30 ppm in propylene carbonate [PC]) and a broadening of the NMR signal (up to 260 Hz in PC) are observed.

The limiting chemical shift of magnesium-25 in different solvents was determined by studying solutions of $MgCl_2$, $MgBr_2$, $MgCl_2I_4$ and $MgBr_2I_4$ in acetone, acetonitrile, dimethylformamide, dimethylsufoxide, methanol, PC, THF and water.

Complexation of magnesium ions by the cryptand C211 in dry methanol results in a small line broadening, while the complexation by phosphonoacetate (PA) in water broadens the signal to such an extent that the NMR signal disappears. The larger distortion of the electric field by the ligand PA is thought to be responsible for this behavioral difference.

Infra-red studies of acetonitrile solutions of MgBr₂ showed complexation of the magnesium ion by the solvent.

The acidity functions of phosphonoacetic acid (PAA) and its complexation with magnesium ion were also investigated by other physicochemical techniques. The behavior of the phosphorus-31 and carbon-13 NMR signals \underline{vs} pH, as well as the accompanying change in J_{C-P} coupling constant show evidence for a relationship between the acetic acid moiety of PAA and its second acid dissociation constant (pK_2) .

The pK $_a$'s of PAA were studied potentiometrically by coulometric titration at ionic strengths from 0.1 to 0.02 and numerical values were obtained by using the computer program MINIQUAD 76A. Tetramethylammonium bromide was used as a supporting electrolyte. Thermodynamic pK $_a$'s of 2.0, 5.11 \pm 0.04 and 8.69 \pm 0.05 were obtained by linear least squares fitting and extrapolation to zero ionic strength.

The thermodynamic quantities for the second and third protonation of PAA were obtained by studying the temperature dependence of the formation constants. These two protonations of PAA are entropy and enthalpy stabilized (entropy stabilization strongly dominant) as shown below:

$$\Delta G_2^0 = -6.9 \pm 0.3 \text{ kcal/mole}$$
 $\Delta G_3^0 = -11.7 \pm 0.4 \text{ kcal/mole}$ $\Delta H_2^0 = -0.2 \pm 0.3 \text{ kcal/mole}$ $\Delta H_3^0 = -1.3 \pm 0.4 \text{ kcal/mole}$ $\Delta S_2^0 = 22.6 \pm 0.9 \text{ cal/mole,}$ $\Delta S_3^0 = 35 \pm 1 \text{ cal/mole,}$ $\Delta S_3^0 = 35 \pm 1 \text{ cal/mole,}$

In the case of K_1 , the experimental results were not sufficiently precise for thermodynamic calculations.

The stoichiometry of the completely deprotonated PAA-cadmium complexes was investigated by cyclic voltammetry. A 1:1 and a 2:1 (ligand:metal) complex were found. The respective formation constants of 8×10^3 and 8×10^1 were determined at 0.4 ionic strength.

Different complexes (namely mono- and completely deprotonated ones) were observed by potentiometry in the case of alkali and alkaline earth metal ions. Thermodynamic values of the magnesium-PAA complexes were determined in the same manner as the thermodynamic pK_a 's. Log K_f values of 3.0 \pm 0.3 and 5.58 \pm 0.09 were obtained for the mono- and deprotonated complexes, respectively.

The thermodynamic quantities:

$$\Delta G^{O}$$
 = -7.2 ± 0.7 kcal/mole
 ΔH^{O} = 3.0 ± 0.7 kcal/mole
 ΔS^{O} = 35 ± 2 cal/mole, °K

were calculated from the temperature dependence of the deprotonated complex formation constant. The change in charge-to-size ratio of the different ions upon complexation is thought to be responsible for the entropy stabilization observed.

The stability of the deprotonated complex decreases when the size of the alkaline earth ion increases (log K_f from 4.50 \pm 0.02 for magnesium ion to 3.67 \pm 0.02 for barium ion at 0.05 ionic strength), or when the charge of the ion decreases (log K_f of 1.43 \pm 0.02 for sodium ion at 0.07 ionic strength).

The pK_a 's and magnesium complex formation constants of several PAA analogs: phosphonoformic acid, 2-phosphonopropionic acid, and

3-phosphonopropionic acid were determined. The results show evidence for a relationship between the amount of magnesium complexed at pH 7 (physiological pH) and the biochemical activity of the ligand.

AUX "QUATRE AUTRES" ET A NANCY

ACKNOWLEDGMENTS

The author wishes to thank Professor Alexander I. Popov for his counseling and for his guidance into the field of chemical research and scientific writing. Thanks are also extended to Professor Bernard Tremillon for introducing me to the analytical field and for his friendship.

Financial aid from the Department of Chemistry, Michigan State University, and the National Science Foundation was appreciated.

The help of Frank Bennis and Wayne Burkhardt in keeping the NMR spectrometers in operating condition is acknowledged.

Dr. John G. Hoogerheide (also known as Long John, Mutt, the siamese brother, etc.) is thanked for his friendship and constant encouragement during this whole research project. The friendship of Dr. Jenshang Shih is also acknowledged.

The author would like to extend his appreciation to Dr. Neil Armstrong for being the second reader, to Dr. Andrew Timnick for his willingness to discuss technical problems, and to Dr. Donald Ward for his help in computer programming and usage.

The author wishes to thank Nancy A. Fedewa for her love, patience and concern throughout this research project. Her everyday smile was greatly appreciated.

Finally, the author is deeply grateful to his family. The love, consideration and encouragement of the "four others" contributed to a large extent to the successful completion of this research project.

TABLE OF CONTENTS

Chapter	Page
LIST OF TABLES	. ix
LIST OF FIGURES	. xi
PART I: MAGNESIUM-25 NMR STUDIES	. 1
1 HISTORICAL REVIEW	. 2
1.1. Introduction	. 3
1.2. Magnesium-25 NMR	. 3
1.3. Proton NMR	. 3
1.4. Ligands	. 6
1.5. Conclusion	. 9
2 MATERIALS AND METHODS	. 10
2.1. Materials	. 11
2.1.1. Reagents	. 11
2.1.2. Solvents	. 13
2.1.3. Molecular Sieves	. 15
2.2. Instruments	. 15
2.2.1. Flame Emission	. 15
2.2.2. Nuclear Magnetic Resonance	. 15
2.2.2.1. DA-60 NMR Spectrometer	. 16
2.2.2.2. Bruker HFX-90 NMR Spectrometer	. 16
2.2.2.3. Bruker WH-180 Superconducting NMR Spectrometer	. 16
2.2.2.4. Operating Procedures	. 17
2.2.3. Infra-red Spectra	. 18

	2.3.	NMR Sample Preparation	18
	2.4.	Data Handling and Miscellanei	19
3	RESULT	S AND DISCUSSION	20
	3.1.	Introduction	21
	3.2.	Problems Specific to Magnesium-25 NMR	21
	3.3.	Solubilities of Magnesium Salts in Nonaqueous Solvents	23
	3.4.	Study of Magnesium Salts	24
		3.4.1. Water	24
		3.4.2. Nonaqueous Solvents	24
		3.4.2.1. Chemical Shift	24
		3.4.2.2. Line-Width	33
	3.5.	Donor Number Correlation	36
	3.6.	Complexation	39
	3.7.	I.R. Studies	42
	3.8.	Conclusion	42
PAR	T II:	PHOSPHONOACETIC ACID STUDIES	44
1	HISTOR	RICAL REVIEW	45
	1.1.	Introduction	46
	1.2.	Phosphonoacetic Acid	47
	1.3.	Analytical Techniques	49
	1.4	Nuclear Magnetic Resonance Studies	49
	1.5.	Acidities and Actinide Complexes of PAA	50
	1.6.	Industrial Applications	52
	1.7.	Biological Properties of PAA	52
		1.7.1. Herpesviruses	52
		1.7.2 Hernesvirus DNA nolymerase	53

		1.7.3.	Herpesvirus	Mode	of	Actio	on .	•	•		•	•	•	53
		1.7.4.	Inhibitory	Power	of	PAA			•			•	•	54
		1.7.5.	Drugs Agair	nst He	rpes	virus	ses					•	•	57
		1.7.6.	Toxicologic	al Ef	fect	s of	PAA		•		•	•	•	57
	1.8.	Phosphone	oacetic Acid	d Deri	vati	ves		•	•		•	•	•	60
	1.9.	Concl us i	on					•	•		•	•	•	61
2	MATER	IALS AND	METHODS					•	•		•	•	•	62
	2.1.	Reagents							•		•	•	•	63
	2.2.	Resins						•			•	•	•	64
	2.3.	Spectros	сору					•	•		•	•	•	64
		2.3.1.	Visible Spe	ectros	сору	• •		•	•			•	•	64
		2.3.2.	Nuclear Mag Spectroscop		Res	onand • •	ce	•	•			•		64
	2.4.	Cyclic Vo	oltammetry					•	•		•	•	•	65
	2.5.	Potention	metry						•		•	•	•	65
	2.6.	Coulomet	er						•			•	•	67
	2.7.	Sample P	reparation					•	•	•	•	•	•	70
		2.7.1.	Cyclic Vol	tammet	ry .			•	•			•	•	70
		2.7.2.	Sodium Ion	Elect	rode	Meas	sure	ne r	its			•	•	70
		2.7.3.	pH Measurer	nents				•	•			•		70
	2.8.	Data Han	dling					•				•	•	72
3	RESUL	TS AND DIS	SCUSSION .					•					•	73
	3.1.	Acidity S	Studies of F	PAA .				•	•				•	74
		3.1.1.	Spectroscop	oic St	udie	s of	PAA	•					•	74
			3.1.1.1.	Phosp NMR .		s-31	and	Pr	ot •	on		•	•	74
			2112	Cambo	~ 12	NMD								01

		3.1.2.	of PAA	37
			3.1.2.1. Coulometric Titrations 8	87
			3.1.2.2. pK's of PAA	90
			3.1.2.3. Thermodynamics of Protonation	99
	3.2.	Complexa	tion Studies of PAA 10)2
		3.2.1.	Spectroscopic Studies 10)2
			3.2.1.1. Visible Spectra 10)2
			3.2.1.2. Sodium-23 NMR 10)3
			3.2.1.3. Phosphorus-31 NMR 10)3
		3.2.2.	Cyclic Voltammetry)5
		3.2.3.	Potentiometric Studies of Complexation	11
			3.2.3.1. Sodium Ion Electrode Study 11	11
			3.2.3.2. Glass Electrode Study 11	11
			3.2.3.3. Thermodynamics of Magnesium Complexation 12	20
	3.3.	Phosphon	oacetic Acid Analogs 12	20
		3.3.1.	Spectroscopic Studies of PFA 12	21
		3.3.2.	Determination of the pK's 12	21
		3.3.3.	Complexation	22
	3.4	Conclusi	on	25
APP	ENDICE	S		
A	SODIU	M-23 NMR		26
	A.1.	Introduc	tion	2
	A.2.	Results	and Discussion	2
В	APPLI	CATIONS O	OF THE COMPUTER PROGRAM KINFIT4 1	3

	B.1.	Calibrat	ion of a pH	Glass	Elect	rode		•		•	•	•	•	136
		B.1.1.	Program Fun	ction						•	•	•	•	136
		B.1.2.	Subroutine	EQN				•		•	•	•		137
		B.1.3.	Data Sample					•	•	•	•	•		137
	B.2.		ation of the nd 2:1 Compl						•	•	•	•		137
		B.2.1.	Program Fun	ction					•	•	•	•	•	137
		B.2.2.	Subroutines					•	•		•	•	•	1 39
			B.2.2.1.	Subrou Data S				•	•	•	•	•		139
			B.2.2.2	Subrou	ıtine	EQN				•	•	•	•	140
		B.2.3.	Data Sample					•	•	•	•	•	•	140
С	TO TH	E DETERMI	THE COMPUTE	UILIBE	RIUM C	CONST	ANTS	FR	MO					7.47
	PUIEN	ITOMETRIC	DATA	• • •	• • •	• •	• •	•	•	•	•	•	•	141
	C.1.	Program I	MINIQUAD 76A	٠.		• •		•	•	•	•	•	•	142
	C.2.	Data Inp	ut Instructi	ons fo	or MIN	NIQUA	76 <i>P</i>	4	•	•	•	•	•	143
	C.3.	Data Sam	ple				• •	•		•	•	•	•	148
BIB	LIOGRA	PHY						•						149

LIST OF TABLES

Table		Page
I	Key Solvent Properties and Correction	
	for Magnetic Susceptibility	14
II	Line-Width of the Magnesium-25 NMR	
	Signal in Different Solvents	34
III	Limiting Chemical Shift of Magnesium-25	
	in Various Solvents	38
IV	Vibrational Frequencies of Free and	
	Complexed Acetonitrile	43
٧	Carbon-13 Chemical Shift of 0.7 M	
	PAA <u>vs</u> pH	84
VI	Acidity Functions of Citric Acid at	
	Ionic Strength 0.1	91
VII	Acidity Functions of PAA at Various	
	Ionic Strengths at 25°C	97
VIII	Thermodynamic Quantities for Acid	
	Association and for the Mg-PA	
	Complex	101
IX	Half-wave Potential of the Cd(II)/Cd	
	Couple in the Presence of PA	
	<u>vs</u> Thallium Amalgam	110

X	PAA Complexes With Metal	
	Ions	112
ΧI	Formation Constants for PAA-Magnesium	
	Complexes at Various Ionic	
	Strengths at 25°C	115
XII	Complexation Formation Constants	
	of PAA Analogs at 25°C and 0.05	
	Ionic Strength	123
IIIX	Formation Constants of Sodium-(12-C-4)	
	Complexes and Their Chemical Shifts	134

LIST OF FIGURES

Figure		Page
1	Structures of Representative Cryptands and	
	Crowns (Cryptand: The Numbers Represent the	
	Number of Oxygens in Each Bridge, Crown: The	
	First Number is the Number of Atoms in the	
	Cycle, and the Second, the Number of Oxygens	7
2	Magnesium-25 Chemical Shifts of MgBr ₂	
	in Acetonitrile	26
3	Magnesium-25 Chemical Shifts of MgCl ₂ (▲)	
	and MgCl $_2$ I $_4$ (\blacksquare) in PC	27
4	Magnesium-25 Chemical Shifts in THF [MgCl ₂ (X),	
	$MgCl_2I_4$ ($lacktriangle$) and Acetone [MgCl ₂ ($lacktriangle$),	
	MgCl ₂ I ₄ (m)]	28
5	Magnesium-25 Chemical Shifts of MgCl ₂ in	
	Methanol (♠), DMSO (♠) and DMF (♠) and of	
	MgCl ₂ I ₄ in DMF (x)	29
6	Magnesium-25 Chemical Shift of MgCl ₂ <u>vs</u>	
	Mole Ratio of Iodine in Acetonitrile	31
, 7	Magnesium-25 Chemical Shift of MgCl ₂ vs	
	Mole Ratio of Iodine in PC	32
8	Limiting Magnesium-25 Chemical Shift in Various	
	Solvents <u>vs</u> Their Gutmann Donor Number	37

9	Structures of Various Phosphonic Acids:	
	Phosphonoacetic Acid, Phosphonoformic Acid,	
	2-Phosphonopropionic Acid, and	
	3-Phosphonopropionic Acid	4 8
10	DNA Synthesis and Mode of Action	
	of PAA	55
11	Block Diagram of the Constant	
	Current Coulometer	6 8
12	Phosphorus-31 Chemical Shift of 0.3 M	
	PAA <u>vs</u> pH	76
13	Comparison of the Phosphorus-31 Chemical Shifts	
	and the Species Distribution of PAA \underline{vs} pH	77
14	Carbon-13 Chemical Shift (Referenced to Dioxane,	
	Which is 68.1 ppm Downfield of TMS) of the $\underline{\text{CH}}_2$	
	Carbon of 0.7 M PAA vs pH	83
15	Change in J_{C-P} Coupling Constant of the \underline{CH}_2	
	Carbon of PAA <u>vs</u> pH	86
16	Plot of the pK_2 of PAA \underline{vs} Ionic Strength,	
	the Line is a Linear Least Squares Fit	95
17	Plot of the pK_3 of PAA \underline{vs} Ionic Strength,	
	the Line is a Linear Least Squares Fit	96
18	Species Distribution Plot of PAA at 0.05	
	Ionic Strength	98
19	Temperature Dependence of ln K_f for Three PAA	
	Complexes, the Lines are Linear Least Squares Fits	100

20	Phosphorus-31 Chemical Shift of 0.3 M PAA and	
	of a 1:1 Mg:PAA Solution <u>vs</u> pH)4
21	Phosphorus-31 Chemical Shift of 0.3 M PAA vs	
	Mole Ratio of Magnesium at pH Above 9 10)6
22	Plot of $E_{1/2}$ as a Function of Log [PA] for	
	the ${\rm Cd}^{2+}$ -PA System (Reference: Thallium Amalgam) 10)9
23	Coulometric Titration Curves of the PAA and	
	PAA-Mg ²⁺ Systems	3
24	Plot of Log K_f of the Monoprotonated PAA-Mg $^{2+}$	
	Complex <u>vs</u> Ionic Strength, the Line is a	
	Linear Least Squares Fit	6
25	Plot of the Log K_f of the Completely	
	Deprotonated PAA-Mg $^{2+}$ Complex <u>vs</u> Ionic Strength,	
	the Line is a Linear Least Squares Fit 11	۱7
26	Species Distribution Plot of the PAA-Mg ²⁺ System	
	at 0.05 Ionic Strength 11	19
27	Species Distribution Plot of the PFA-Mg ²⁺ System	
	at 0.05 Ionic Strength	24
28	Sodium-23 Chemical Shift vs Mole Ratio of 12-C-4.	
	NaBPh ₄ : (\diamondsuit) : 0.1 \underline{M} in PC, (\blacksquare) : 0.034 \underline{M} in THF;	
	(O): 0.04 \underline{M} NaI in Methanol; (\square): 0.04 \underline{M}	
	NaClO ₄ in Water	29
29	Sodium-23 Chemical Shift vs Mole Ratio of 12-C-4.	
	NaBPh ₄ : (\bullet): 0.04 \underline{M} in Pyridine, 0.1 \underline{M} in DMSO	
	(△), Acetone (X), DMF (▲), Acetonitrile (○) 1	30

PART I

MAGNESIUM-25 NMR STUDIES

CHAPTER 1

HISTORICAL REVIEW

1.1. INTRODUCTION

The main purpose of this thesis was to study the complexes formed between magnesium ion and phosphonoacetic acid (PAA) by different physicochemical techniques. Techniques such as visible UV spectroscopy are not very useful to study the environment of group I or group II metal ions in their stable oxidation states. In the case of most of the alkali metal ions, the observation of the metal nuclide resonance and the study of both the line-width and the chemical shift of the signal gave interesting information about the chemical environment and the complexation of these nuclei in their first oxidation state (1). For these reasons, the magnesium-25 nuclear magnetic resonance (NMR) technique was applied to the magnesium-phosphonoacetic acid system.

1.2. MAGNESIUM-25 NMR

However, the properties of the magnesium-25 nucleus are not very favorable for NMR studies. The magnesium-25 nucleus has a low nuclear magnetic sensitivity (the senstivity per nucleus at constant field is only 2.68 x 10⁻² of the sensitivity of the proton), a low natural abundance (10.05%), a low resonance frequency and a quadrupolar momentum (the nuclear spin is 5/2). In 1951, Alder and Yu (2) located the resonance frequency of magnesium-25 in a 4.6 M solution of magnesium chloride in water near a frequency of 3.9 MHz, in a magnetic field of 11 kG. They also measured the magnetic moment of magnesium-25 by NMR. However, because of the poor properties of the magnesium-25 nucleus mentioned earlier, few studies of magnesium-25 NMR have been performed.

Using continuous wave technique, Ellenberger and Villemin (3) reported magnesium-25 NMR studies of aqueous solutions. They found line-widths of 40 to 45 Hz for the different solutions used. However, within the precision of the measurements, the resonance frequency seemed to be independent of the salt concentration.

Subsequently, Dougan et al. (4) and Dickson and Seymour (5) determined the Knight shift of magnesium-25 in magnesium metal, that is the paramagnetic shift of the nuclear resonance due to the delocalized conduction electrons of a metal (named after W. D. Knight who was the first one to observe it in copper in 1949). Bryant (6) used magnesium-25 NMR to study aqueous solutions and reported a linewidth (full width at half height of the peak) of 3.8 ± 0.5 Hz for a $1.5 \ \underline{\text{M}} \ \text{MgCl}_2$ solution, which is an order of magnitude smaller than the one reported by Ellenberger and Villemin (3). Bryant's use of magnesium-25 NMR was essentially to determine the chemical rate of exchange (based on measurements of the line-width) of magnesium between complexed and uncomplexed sites of ATP type phosphate solutions.

In the absence of chemical shift change in aqueous magnesium solutions, Magnusson and Bothner-By (7) used the change in line-width <u>vs</u> pH of acidic ligand solutions (e.g., citric acid, ATP) to approximate the formation constants of the corresponding complexes. Although this method seems unsound because of the various factors affecting the line-width of the signal and because of the precision of such measurements, their values are within one order of magnitude of other published values. The above authors reported a variation of the line-width from 5 to 9 Hz when the concentration of magnesium

ions was increased from 1.0 to 4.0 $\underline{\text{M}}$. They also reported that above pH 7, a solution of magnesium ions and EDTA gave one broad peak, thus showing that the exchange was fast compared to the NMR time scale. The widest line-width reported for magnesium-25 NMR was in the case of complex formation with ATP (1300 Hz).

Simeral and Maciel (8) are among the last ones so far to have reported magnesium-25 NMR studies, and those were also done in aqueous solutions. After having taken the viscosities of the different solutions into account, the line-width data have been discussed in terms of four models for quadrupolar nuclear spin relaxation in the systems studied. The line-widths reported vary from 3 to 11 Hz, but once again, no chemical shift change either with the concentration or the counterion was observed.

1.3. PROTON NMR

Proton magnetic resonance has been used to study the solvation number of magnesium ion in acetone-water and methanol-water mixtures (9-15). The inner solvation shell consisted of six water molecules as long as the mole ratio of water to magnesium was equal to or higher than 6. Matwiyoff and Taube (10) also determined that in methanol-acetone mixtures, methanol was a much better solvating agent than acetone. In all those solutions the total solvation number was 6.

The preparation of anhydrous magnesium salts presents a difficult problem. With one exception [16, redox reaction between magnesium and mercury (II) halide in tetrahydrofuran], all the purifications or synthesis (17) of magnesium chloride or bromide

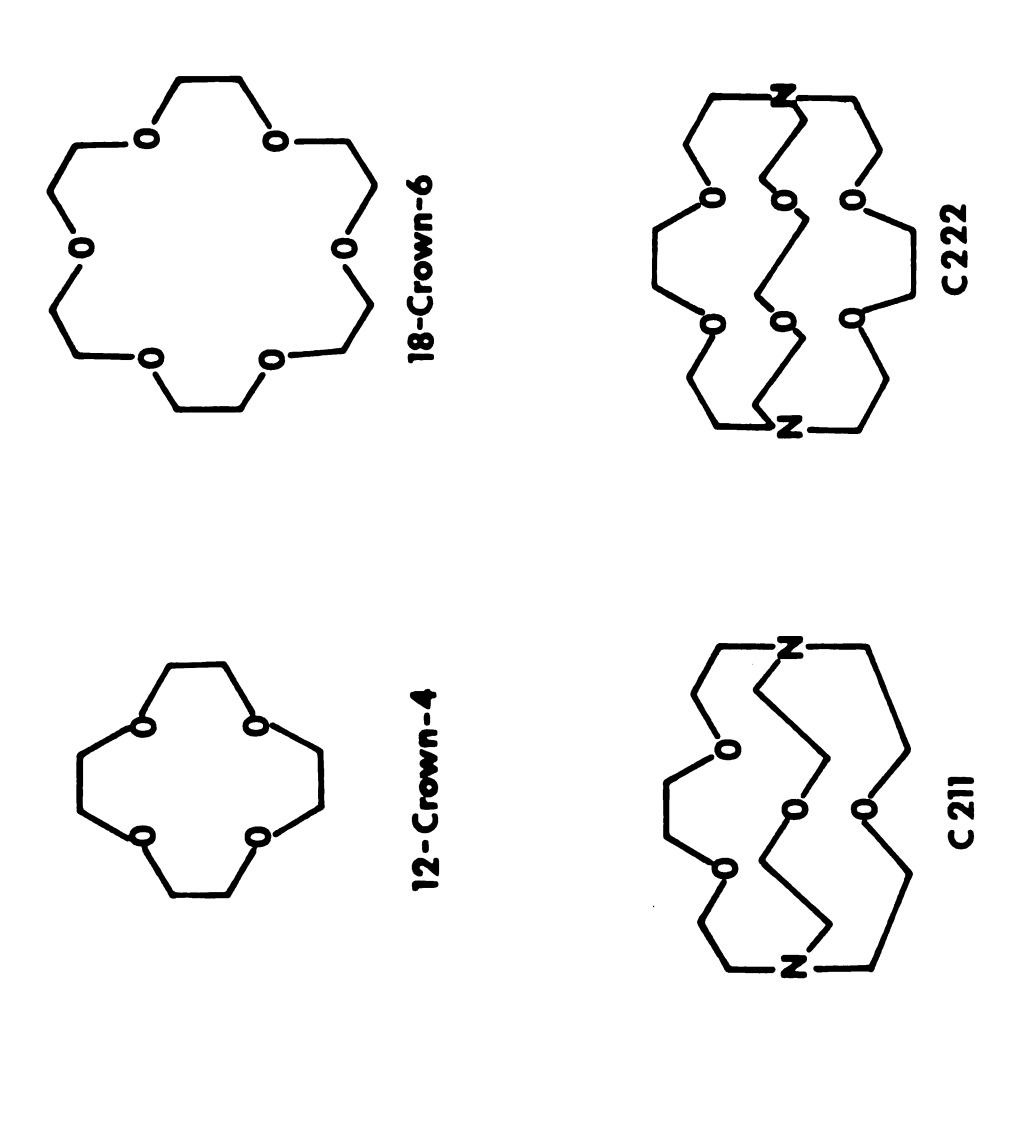
found in the literature involve the fusion of the halide and its separation from magnesium oxides by filtration in a stream of dry nitrogen in a quartz tube (the melting points of $MgCl_2$ and $MgBr_2$ are 708° and 700° C, respectively).

The affinity of magnesium ions for water is such that direct heating of the hydrated salt under active vacuum leads to the formation of magnesium oxides. Thus, according to Halliwell and Nyberg (18), the hydration enthalpy of magnesium is -459 kcal/mole, respectively four, five, six and seven times the ones of lithium (-124 kcal/mole), sodium (-97 kcal/mole), potassium (-77 kcal/mole) and cesium (-63 kcal/mole). Since all of the above magnesium-25 studies were restricted to aqueous solutions, it was of interest to us to study this resonance in nonaqueous solvents.

1.4. LIGANDS

Cyclic polyethers, or crown ethers, were developed by Pedersen (19 and references therein). They have a remarkable ability to form stable two-dimensional complexes with alkali metal cations. Structural formulae of some typical crown ethers are shown in Figure 1. Formation of such complexes distorts the spherically symmetrical electric field around the solvated metal ion which may result in a broadening and/or a chemical shift change of the metal NMR signal.

There are (19-23) several reports of syntheses, spectroscopic and crystallographic studies of the ligand 12-crown-4 (12-C-4), also known as the ethylene oxide cyclic tetramer (1,4,7,10 tetraoxacyclododecane). The ligand 12-C-4 is a liquid at room temperature with a specific gravity of 1.104, a boiling point of 238°C at 760 mm



Structures of Representative Cryptands and Crowns (Cryptand: The Numbers Represent the Number of Oxygens in Each Bridge, Crown: The First Number is the Number of Atoms in the Cycle, and the Second, the Number of Oxygens). Figure 1.

of mercury and a vapor pressure of 0.03 mm at room temperature (24). The cavity size of this crown is 1.2 to 1.5 $^{\rm A}$, which is approximately the size of the magnesium ion (1.3 Å diameter from crystallographic measurements). In a study of the complexation of crown ethers, Chock (25) found that the enthalpy of hydration involved in the desolvation step and the binding energy for a given ligand were the most important factors in the mechanism of complexation and the stability of the resulting complex. These observations, added to the great affinity of magnesium ion for water, probably explain why the crystal structure of MgCl₂, 6H₂O-12-C-4 complex (20) consists of octahedral $Mg(H_20)_6^{2+}$ units very similar to those in $MgCl_2$, $6H_20$, located on crystallographic axes, with 8 of the 12 water hydrogens forming hydrogen bonds to six different chloride ions, which are located in tetrahedral holes, while the remaining four hydrogens of the $Mg(H_20)_6^{2+}$ unit form hydrogen bonds to ether oxygens from four different cyclomer molecules.

Leong <u>et al</u>. (24, 26) reported some toxicological studies of 12-C-4. Rats exposed to the vapors of 12-C-4 for six hours daily for six to eight days exhibited variable degrees of anorexia, loss of body weight, asthenia, hindquarter incoordination, testicular atrophy, auditory hypersensibility, tremors, convulsions, moribond conditions and death, depending on the exposure concentration.

Cryptands are diaza-polyoxamacrocycles. These ligands with bridging nitrogens were first synthesized by Lehn et al. (27, 28). They can form very stable complexes with alkali and alkaline-earth cations. The length and number of ether bridges may be changed to vary the size of the inner cavity of the cryptand. The term cryptand

refers to the ligand and cryptate to the complex. The stability of the cryptate complexes depends to a large extent on the size relationship between the three-dimensional cavity of the cryptand and the diameter of the complexed ion.

In general, cryptands form much stronger complexes with the alkali metal ions than the crown ethers, provided that ligands with approximately the same cavity size are compared. Recent reviews (29-33) contain extensive compilations of complexation stability constants.

Cryptand C211 is shown in Figure 1 (211 refers to the number of oxygens in each hydrocarbon chain). Its cavity size is approximately 1.6 Å. Very little work has been done on the complexation of ${\rm Mg}^{2+}$ ion by C211. Lehn and Sauvage (29) reported log ${\rm K}_{\rm f}$ for a 1:1 complex to be 2.5 \pm 0.3 and 4.0 \pm 0.8 in water and in 95/5 methanol/water mixture respectively, while Morf and Simon (30) found a log ${\rm K}_{\rm f}$ value of less than 2 in water.

1.5. CONCLUSION

Very little work has been done concerning the NMR properties of magnesium-25. In order to use this technique to study the magnesium-PAA complexes, it is necessary to perform preliminary studies of the influence of the environment of the magnesium ion upon its NMR properties.

CHAPTER 2

MATERIALS AND METHODS

2.1. MATERIALS

2.1.1. <u>REAGENTS</u> - The following chemicals were all reagent grade and used without further purification. The code is: Aldrich (A), Alfa inorganics (AI), J. T. Baker (B), Drake brothers (D), Fisher scientific company (F), Mallinckrodt (M), Matheson Colleman and Bell (MCB) and G. F. Smith Company (S):

Barium chloride (M), barium oxide (MCB,F), cadmium nitrate tetrahydrate (B), citric acid monohydrate (F), cobalt chloride (AI), cobalt sulfate (B), copper sulfate (AI), dioxane (F), ethylene diammine tetraacetic acid, disodium salt (MCB), glacial acetic acid (M), hydrochloric acid (M), lithium bromide (MCB), magnesium acetate tetrahydrate (B), magnesium bromide hexahydrate (F), magnesium chloride hexahydrate (MCB), Magnesium perchlorate (S), magnesium sulfate (M), manganese chloride (AI), nickel bromide (AI), potassium hydroxide (MCB), potassium iodide (F), potassium permanganate (B), 3(trimethylsilyl)-l-propanesulfonic acid, sodium salt hydrate (known as DSS, the water soluble TMS: $(CH_3)_3Si(CH_2)_3So_3Na$, nH_2O , is an internal standard for use with D_2O) (A), sodium carbonate (F), sodium hydroxide (D), sodium iodide (F), tetraphenylarsonium chloride (S) and zinc chloride (M). Tetramethyl ammonium hydroxide was from either Eastman organics or MCB and was obtained as a 10% solution in water. Phosphonoformic acid, trisodium salt hexahydrate and 3-phosphonopropionic acid were kindly furnished by J. Reno from Dr. J. Boezi's group (Biochemistry Department) and used as received. Cryptand 211 was from E. M. Lab, and 12-crown-4 from Aldrich; 3-phosphonopropionic acid was from Richmond Organics.

Several indicators have been used: bromocresol green and eriochrome black T (F), phenol red (A), and phenolphthalein (F).

The following chemicals were dried in the vacuum oven, unless otherwise specified (Company, time, temperature): magnesium metal (B, 6h., 60°C), sodium tetraphenylborate (B, 48h., 25°C), lithium perchlorate (F, 96h., 190°C, regular oven), mercuric chloride, bromide and nitrate (M, 6h., 60°C), sodium chloride (M, 24h., 150°C), sodium perchlorate (S, 24h., 110°C) and mercuric thiocyanate (Ventron Alfa Products, 6h., 60°C).

A flame and K. Fischer analysis of 12-crown-4 showed that the mole ratios of Na⁺ ion and water to 12-crown-4 were 0.26% and 2%, respectively. No traces of lithium or potassium were detected.

Iodine (Baker Analyzed reagents, ACS or USP grade) was purified by double sublimation: 10 g of iodine are first sublimed with 5 g of potassium iodide (in order to eliminate the iodine chloride and iodine bromide) at 70-80°C. It takes about 10 hours to sublime 10 g of iodine. Then the obtained iodine is sublimed with 4.3 g of granulated barium oxide (in order to remove the water) under the same conditions.

Bromine (Dow Chemical) was dried over P_2O_5 for 24 hours and then distilled under atmospheric pressure.

Magnesium salts: anhydrous magnesium bromide was first prepared by direct reaction of bromine over magnesium in ether, but contamination of the solution by bromine made the solution useless for NMR purposes. Therefore, magnesium chloride and bromide were prepared by using the method described by Ashby and Arnott (10).

A redox reaction between a mercury (II) halide and an excess of magnesium metal in a tetrahydrofuran (THF) diethylether mixture

(kept under reflux for 4 to 6 hours) leads to the formation of the corresponding magnesium salt and a magnesium amalgam. It was found here that THF alone gave better results for MgCl₂ and MgBr₂ than the THF-ethylether mixture. Mercury (II) bromide (86 g., 0.24 mole) and metallic magnesium turnings (6 g., 0.25 mole) were refluxing in 1.4 l. of THF for 6 hours (in the case of magnesium chloride, the concentrations were doubled: 0.5 mole in 1.4 l.). The solution then was transferred to a dry box and the amalgam and excess of magnesium were removed by filtration through filter paper (because of the presence of liquid mercury and of clogging problems, a glass frit could not be used).

Tetrahydrofuran is then evaporated on a rotavap under vacuum and the salt is dried under vacuum at 80°C overnight. Omission of this step lead to supersolubility problems, due to the contamination of the solution by the small amounts of THF remaining in the salt. The salt was stored in a dry box where the nonaqueous solutions were prepared.

Attempts to prepare $\mathrm{Mg(NO_3)_2}$, $\mathrm{Mg(SCN)_2}$ or $\mathrm{Mg(BPh_4)_2}$ by the same technique failed, as well as attempts to prepare $\mathrm{Mg(BPh_4)_2}$ by either using the method given in the literature for the lithium salt (34), or the potassium salt (35). This latter method was used to prepare $\mathrm{Hg(BPh_4)_2}$.

2.1.2. <u>SOLVENTS</u> - The solvents were obtained from the following companies: Acetone (F), acetonitrile (MCB), dimethylformamide (DMF, F), dimethylsulfoxide (DMSO, F), methanol (F), propylene carbonate (PC, A), tetrahydrofuran (THF, M). (See code in Part II.2.1.1.). Useful solvent parameters are listed in Table I.

Table I. Key Solvent Properties and Correction for Magnetic Susceptibility.

Solvents	Dielectric Constant	Gutmann's Donor Number	Correction on DA-60 (ppm)	Correction on B-180 (ppm)
Acetone	20.7	17.0	-0.545	+1.09
Acetonitrile	37.5	14.1	-0.390	+0.780
Dimethylformamide (DMF)	36.71	26.6	-0.308	+0.616
Dimethylsulfoxide (DMSO)	46.68	29.8	-0.241	+0.482
Methanol	32.7	25.7	-0.429	+0.858
Propylene Carbonate (PC)	65.0	15.1	-0.180	+0.360
Tetrahydrofuran (THF)	7.58	20.0	-0.224	+0.448
Water	78.54	33.0	0.000	0.000

All solvents except methanol were dried over calcium hydride or activated 3A and 4A molecular sieves (3A has a cavity size that just fits the water molecule) for 5 hours, followed by a distillation at atmospheric pressure (except for DMSO for which a static low pressure was applied). Usually 10 g of CaH₂ or 100 ml of sieves were used for one liter of solvent. Methanol was dried by double distillation over magnesium (36). The water contents of the solvents used were measured with the help of a Karl Fischer automatic titrator and were found to be always less than 50 ppm's.

2.1.3. MOLECULAR SIEVES - Molecular sieves 3A (Davison Chemical Company, W. R. Grace and Co.) and 4A (MCB) were activated by drying at a maximum of 400°C for 6 hours under nitrogen which was dried by passing it through concentrated sulfuric acid.

2.2. INSTRUMENTS

- 2.2.1. <u>FLAME EMISSION</u> Flame emission experiments were performed using a Heath EU-703-70 flame unit, an EU 700 scanning monochromator and EU-701-30 photomultiplier module containing an R-44-UR Hammamatsu photomultiplier tube. Output from the P.M. tube was recorded through a Heath EU-703-31 photometric readout amplifier. The total consumption burner used hydrogen at 1 psi and air at 15 psi. Samples were aspirated for at least 30 seconds with distilled water blanks between samples. Duplicate runs were made for each standard and unknown.
- 2.2.2. <u>NUCLEAR MAGNETIC RESONANCE</u> The NMR spectra were collected on three different instruments, all operated in the Fourier transform mode.

2.2.2.1. <u>DA-60 NMR Spectrometer</u> - A modified Varian DA-60 NMR spectrometer was used for magnesium-25 and sodium-23 NMR measurements. The instrument consists of the magnet of a Varian DA-60 spectrometer equipped with a wide band probe capable of multinuclear operation, as described by Traficante <u>et al</u>. (137). The field is at 14.09 kG and the frequency of the RF unit is 56.44 MHz. A detailed description of the spectrometer has been given elsewhere (138). The resonance frequency of the sample can be obtained by changing the synthesizer frequency, instead of changing the magnetic field.

Before each experiment, the probe and image filter were tuned to the resonance frequency of the nucleus under consideration (3.672 MHz for magnesium-25 and 15.87 MHz for sodium-23). The field is locked by a home-built lock probe on the proton resonance of the upfield sideband of H_2O). Pulse generation and data collection were performed with the help of a Nicolet 1083 computer with 12K of memory. The tubes were 25 and 15 mm OD (magnesium-25 NMR) and 10 mm OD (sodium-23 NMR).

- 2.2.2.2. <u>Bruker HFX-90 NMR Spectrometer</u> The phosphorus-31 and sodium-23 NMR spectra were obtained by using a Bruker HFX-90 NMR spectrometer equipped with a Nicolet 1083 computer with 12K of memory, a Diablo disc memory unit and a Nicolet 293 I/O controller. The spectra were obtained at a frequency of 36.44 MHz (phosphorus-31) and 23.81 MHz (sodium-23). Spinning tubes of 10 mm 0D were used.
- 2.2.2.3. <u>Bruker WH-180 Superconducting NMR Spectrometer</u> This instrument was used to collect magnesium-25 NMR spectra at
 11.01 MHz, and proton spectra at 180 MHz. The field strength is

42.28 kG. An external D_2 0 lock was used. Due to the superconducting magnet, the field was very stable, and results were obtained without using an internal lock for the nonaqueous samples.

Solutions were run in 20 mm OD nonspinning tubes, the minimum amount of solution for each tube is 8 ml. Preliminary studies showed that due to the broadening of the peak by quadrupolar relaxation, the absence of spinning did not affect the line width to a measurable extent.

2.2.2.4. Operating Procedures - The chemical shifts were measured against external references. A 4.0 $\underline{\text{M}}$ solution of aqueous NaCl was used for sodium-23, and a 4.0 $\underline{\text{M}}$ solution of aqueous MgCl₂ (DA-60) or a 4.0 $\underline{\text{M}}$ 75/25 H₂0/D₂0 MgCl₂ solution (B-180) for magnesium-25. As shown by Maciel (8), there is no difference in chemical shift for these last two solutions. The phosphorus-31 NMR chemical shifts are reported relative to 85% phosphoric acid.

According to the convention used in this thesis, a positive change in chemical shift of sodium-23, magnesium-25 and phosphorus-31 NMR signals corresponds to a shift to higher field strength than that of the reference signal.

All chemical shifts are corrected for the bulk diamagnetic susceptibility difference between water and the pure nonaqueous solvent. For each solution, the contribution of the salt to the susceptibility of the solution is assumed to be negligible: a reasonable assumption as shown by Templeman and Van Geet (37). The formulae given by Live and Chan (38) for normal (equation 1) and superconducting (equation 2) magnet were used:

$$\delta_{corr} = \delta_{obs} - \frac{4}{3}\pi (x_v^{ref} - x_v^{sample})$$
 (1)

$$\delta_{corr} = \delta_{obs} + \frac{2\pi}{3}(x_v^{ref} - x_v^{sample})$$
 (2)

In the case of magnesium-25 and phosphorus-31 NMR, when the top of the peak was too flat to allow precise determination of the chemical shift change, the precise frequency of the peak was obtained by averaging the two frequencies at half height.

2.2.3. INFRA-RED SPECTRA - Infra-red spectra covering a range of 4000-600 cm⁻¹ were collected on two Perkin-Elmer grating IR spectrophotometers: models 237 B and 457. The frequencies were calibrated using polystyrene reference peaks. Solutions and nujol mulls of solid samples were placed between sodium chloride mull plates.

2.3. NMR SAMPLE PREPARATION

Nonaqueous solutions of magnesium salts were prepared in a dry box. When the dissolution of the magnesium salt lead to the formation of a light precipitate [presumably $Mg(OH)_2$], the solution was filtered in the dry box. Since magnesium has a large affinity for water, the water content for each sample was measured after each NMR measurement, and data points were kept only if the mole ratio of water to magnesium was less than 20%. In these conditions, the lowest concentration studied in nonaqueous solvents was $10^{-2} \, \underline{M}$, which corresponds to a water content for the solution of 36 ppm. In most cases, the lowest concentration was 3 x $10^{-2} \, \underline{M}$. The magnesium concentration in the different solvents was measured

by diluting a small sample (usually 1 ml) of solution with distilled water followed by the usual titration by EDTA in NH_3/NH_4Cl buffered medium.

Since 12-crown-4 and cryptand 211 are liquid at room temperature, the preparation of the solutions containing them was completed outside the dry box. The amounts of the above ligands or sodium salts used were determined by weight. Suitable diultions were performed using 2, 5, 10, 25 and 50 ml volumetric flasks.

2.4. DATA HANDLING AND MISCELLANEI

Extensive use was made of the CDC 6500 computer with several Fortran IV programs (see Appendices B and C). Elemental analyses were done by Chemalytics Inc. of Tempe, Arizona, and/or by Spang Microanalytical Laboratory, Eagle Arbor, Michigan; the latter giving more precise results. Melting points were determined on the Fisher-Johns melting point apparatus. The instrument was calibrated from 40°C to 300°C by means of melting point standards (Hoover). Analyses for water were accomplished with a Photovolt Aquatest II automatic Karl Fischer titration apparatus.

CHAPTER 3

RESULTS AND DISCUSSION

3.1. INTRODUCTION

Previous studies in this laboratory and elsewhere have shown that the NMR of alkali metal ions offers a sensitive probe of the environment of these ions in different solvents and solvent mixtures. The purpose of this study is to determine whether magnesium-25 NMR would be a suitable technique to study the influence of the cation on the ionic equilibria and ionic species present in various solvents. The exchange of ions between different environments is usually rapid with respect to the NMR time scale, resulting in only one resonance signal at an average frequency determined by the magnetic shielding and nucleus population in each of the sites. Alteration of parameters such as concentration, counterions and solvent produces changes in the relative proportion and type of environment which may be reflected by a change in chemical shift and/or line-width of the observed resonance.

3.2. PROBLEMS SPECIFIC TO MAGNESIUM-25 NMR

In the first place, magnesium ion has a very large affinity for water. Since most organic solvents cannot be obtained completely anhydrous, it is obvious that in such cases meaningful chemical shifts for magnesium can only be obtained if the concentration of water is much smaller than the concentration of the salt. We found that in the present study a mole ratio of water to magnesium of 20% was the upper water content limit. For example, a solution of magnesium chloride in acetonitrile, with a mole ratio of water to magnesium of 50% gave rise to a change in chemical shift of 2 ppm, compared to a solution with a mole ratio of 10%.

Secondly, prior to this study no one had performed any magnesium-25 NMR studies of nonaqueous solutions of magnesium salts, and, therefore, one of the problems was to determine whether the change in chemical shift would be large enough to be detected easily with our instruments (after all, lithium ion which has approximately the same size as magnesium ion has a chemical shift range of only a few ppm).

Thirdly, several instruments have been used in this study, with a large increase in sensitivity for each change of instrument: thus, with the first insert and probe, the sensitivity of the DA-60 was such that the magnetic field did not need to and could not be tuned: in these conditions a $0.05~\underline{\text{M}}$ aqueous solution of magnesium chloride required 8000 scans (50 minutes of time with 4K of memory and 5000 Hz sweepwidth for the computer) for a signal to noise ratio of 2.5 (the signal to noise ratio is defined as the ratio of the signal over the largest noise, multiplied by 2.4). The first improvement was to use a better probe, which allowed to study the same solution in much better conditions (6000 scans gave a signal to noise ratio of 8). The second and best improvement was to use the Bruker 180 spectrometer with which a $0.046~\underline{\text{M}}$ aqueous solution of MgCl₂ can be analyzed in 10 minutes.

Finally, another major problem specific to magnesium is the following - either the ion is strongly solvated and does not form contact ion pairs, resulting in no chemical shift change with salt concentration, and small line-width change (due to the change in viscosity of the solution), or there is ion pairing, which, if it results in a change in chemical shift, also significantly increases the line-width.

For this latter reason and because of the low sensitivity of the instrument, only few solutions could be studied with the DA-60 (mainly aqueous, methanol and acetonitrile solutions).

3.3. SOLUBILITIES OF MAGNESIUM SALTS IN NONAQUEOUS SOLVENTS

The solubilities of ${\rm MgCl}_2$ and ${\rm MgBr}_2$ in nonaqueous solvents are fairly small. The best cases studied are represented by acetonitrile (2.0 M), acetone (1.2 M), methanol (1.0 M) and dimethylformamide (DMF, 0.9 M). For propylene carbonate (PC) and tetrahydrofuran (THF), the solubility is approximately 0.3 M, while it decreases to 0.1 M for dimethylsulfoxide (DMSO), and to 10^{-3} M for pyridine and nitromethane. It was first thought that the solubility in nitromethane was around 1.0 M, but it was found later on that THF impurity in the salt (from its synthesis) was responsible for this high value. At the time the salt was only dried at room temperature under vacuum for 24 hours. Upon dissolution in a given solvent, the THF molecules solvate the cation thus increasing the "solubility" of the salt. On occasion, after the preparation of a 1.0 \underline{M} solution of MgCl₂, the salt would precipitate out, leading to a final solubility of the salt of less than 10^{-2} M.

The solubility of magnesium acetate $(Mg(OAc)_2)$ was found much smaller as a rule than the solubility of $MgCl_2$ or $MgBr_2$, since except in methanol $(0.1 \ \underline{M})$ all the other solvents tested (aminoethanol, formic acid, formamide, DMF, ethylenediamine, DMSO, THF, nitromethane, pyridine, acetone) dissolved at most $10^{-2} \ \underline{M} \ Mg(OAc)_2$, which is not suitable for a magnesium-25 NMR study in the present conditions.

3.4. STUDY OF MAGNESIUM SALTS

WATER - Five different magnesium salts have been 3.4.1. studied in water, $Mg(OAc)_2$, $MgCl_2$, MgI_2 , $Mg(NO_3)_2$, and $Mg(ClO_4)_2$. No change in chemical shift was observed when the concentration of each of these salts was changed. In the case of four of these salts [MgCl₂: 4.6 to 0.1 \underline{M} , MgI₂: 1.8 to 0.1 \underline{M} , Mg(NO₃)₂: 3.0 to 0.05 \underline{M} and Mg(ClO₄)₂: 3.2 to 0.05 \underline{M}] the change in line-width was small: from 17 to 7 Hz, while for $Mg(OAc)_2$ the line-width changed from 43 to 8 Hz for a corresponding change in concentration of 2.0 to 0.24 M. However, in the latter case, the concentrated solution was much more viscous than the other salts solutions, and this fact is probably responsible for the broadening of the peak. These results are similar to the ones reported by Maciel et al. (8). As expected, magnesium ion is strongly solvated by water, and from these measurements, it appears that if ion pairs are formed between the different ions in solution, these are at least solvent shared ion pairs.

3.4.2. NONAQUEOUS SOLVENTS

3.4.2.1. <u>Chemical Shift</u> - It has been previously observed (39, 40) that the contact ion pair equilibria strongly depend on the donor ability of the solvent molecule as well as on the bulk dielectric constant of the medium. Although PC and acetonitrile have high dielectric constants (65 and 37.5, respectively), their donor abilities are low on Gutmann's scale (41) (15.1 and 14.1, respectively). Gutmann defined a donor ability scale for solvents as the negative

ΔH-value in kcal/mole for the interaction of the solvent with SbCl₅ in a highly diluted solution of dichloroethane. We see from Figures 2 and 3 that the magnesium-25 chemical shifts of MgBr₂ and MgCl₂ solutions are concentration dependent and, therefore, that there is contact ion pair formation. These results are in agreement with the data obtained by sodium-23 and lithium-7 NMR in PC and acetonitrile solutions where the chemical shifts of NaI and NaSCN or LiBr and LiI are strongly concentration dependent (42, 43).

Tetrahydrofuran and acetone are interesting solvents in that they have low dielectric constants (7.58 and 20.7, respectively), but reasonable donor abilities (20.0 and 17.0). As can be seen from Figure 4, there is contact ion pair formation even between ${\rm Mg}^{2+}$ and the ClI $_2^-$ ions.

On the other hand, solvents like methanol, DMSO or DMF that have both high dielectric constants and high donor numbers and are good solvating agents show no or very little ion pairing (see Figure 5). For the methanol and DMSO solutions, the chemical shift does not change with concentration (1.1 and 3.5 ppm, respectively), while for the DMF solutions, the chemical shift changes from -4 to 4 ppm for a concentration change of 0.9 to 0.03 M.

We mentioned above that we attribute the concentration dependence of magnesium-25 chemical shifts to the formation of contact ion pairs, i.e., to cases where the anion directly replaces a solvent molecule or molecules in the inner solvation shell of the cation. It seems reasonable to assume that gross variations in the chemical shift and/or the line-width of the magnesium-25

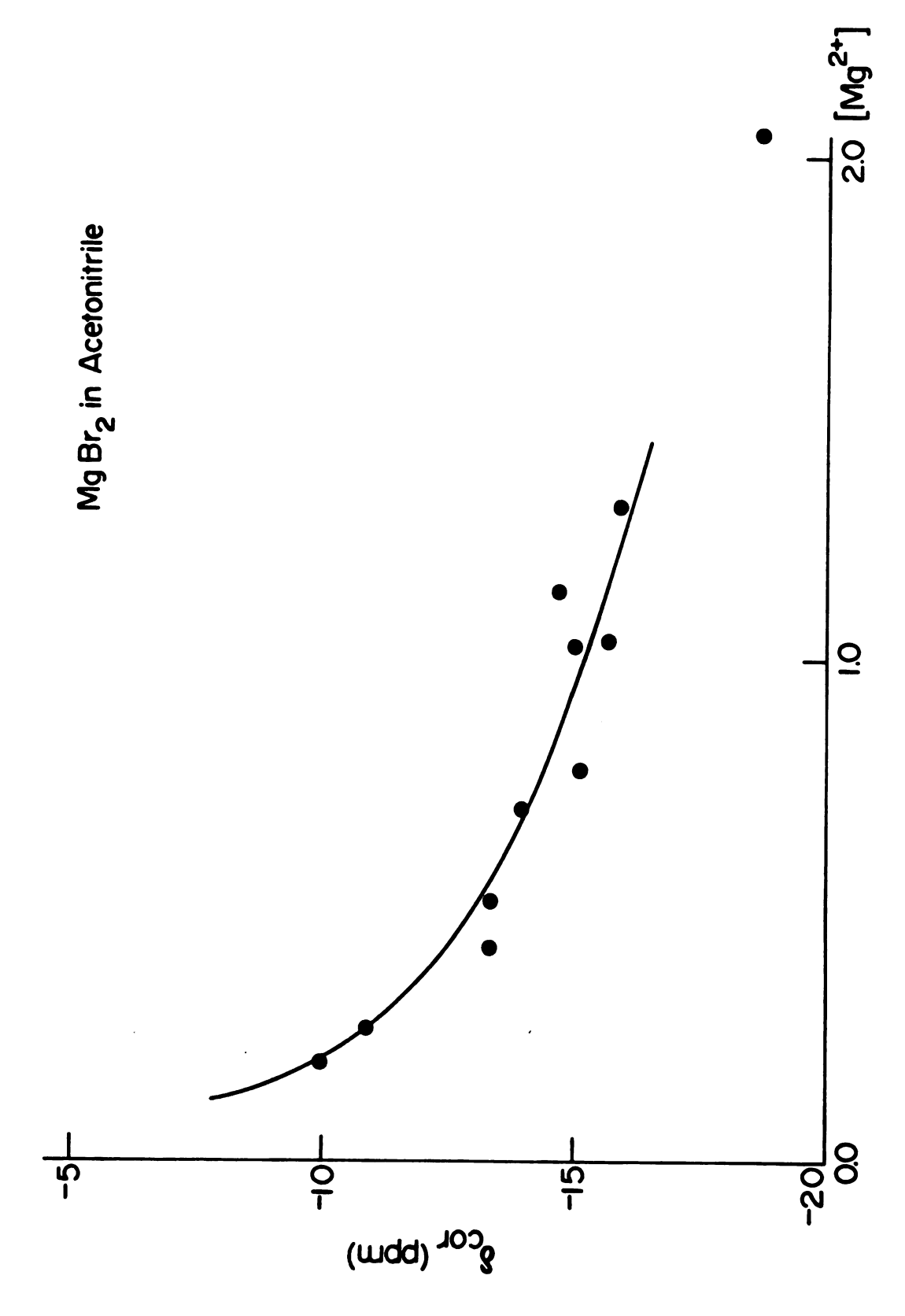


Figure 2. Magnesium-25 Chemical Shifts of MgBr $_{
m 2}$ in Acetonitrile.

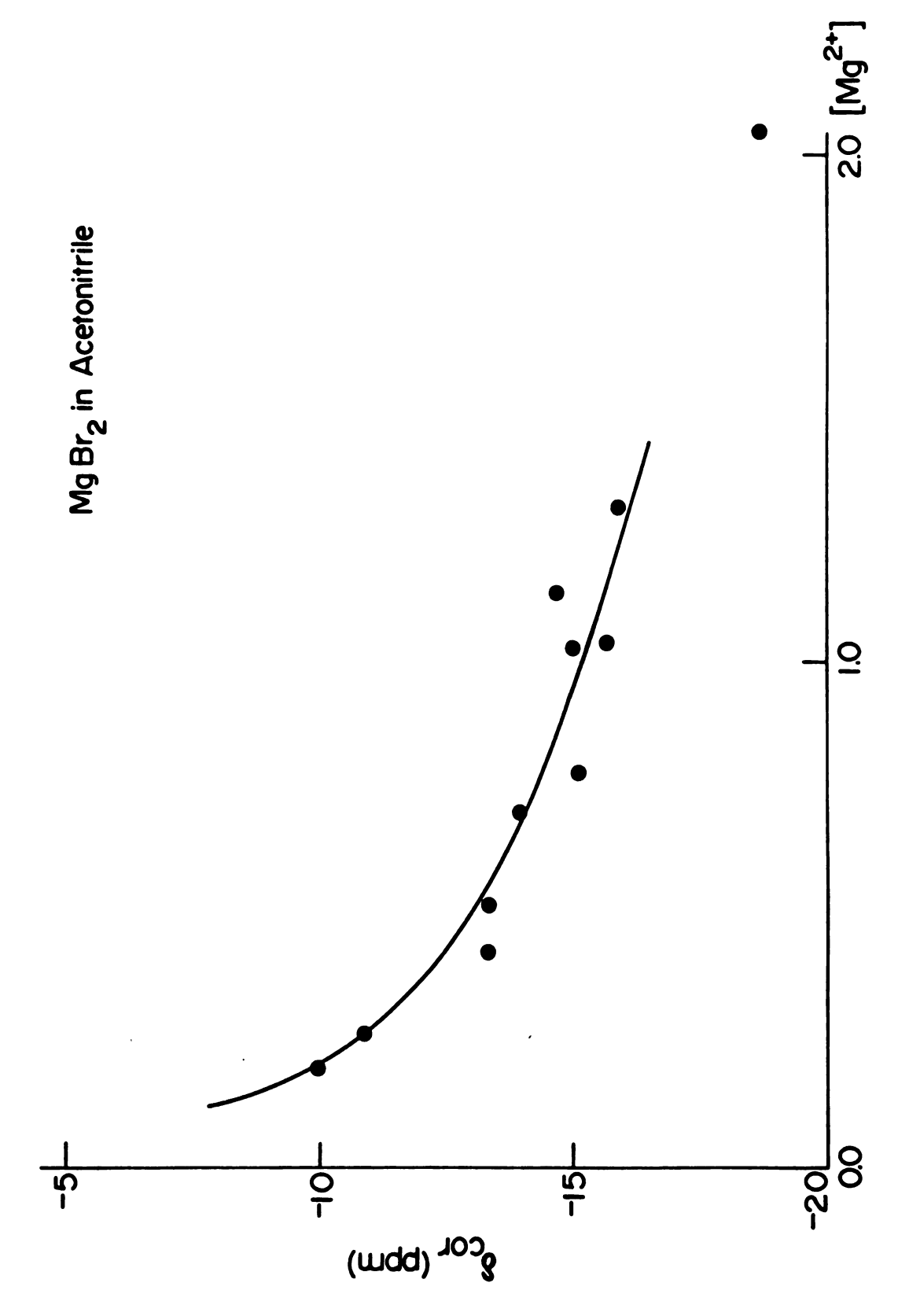
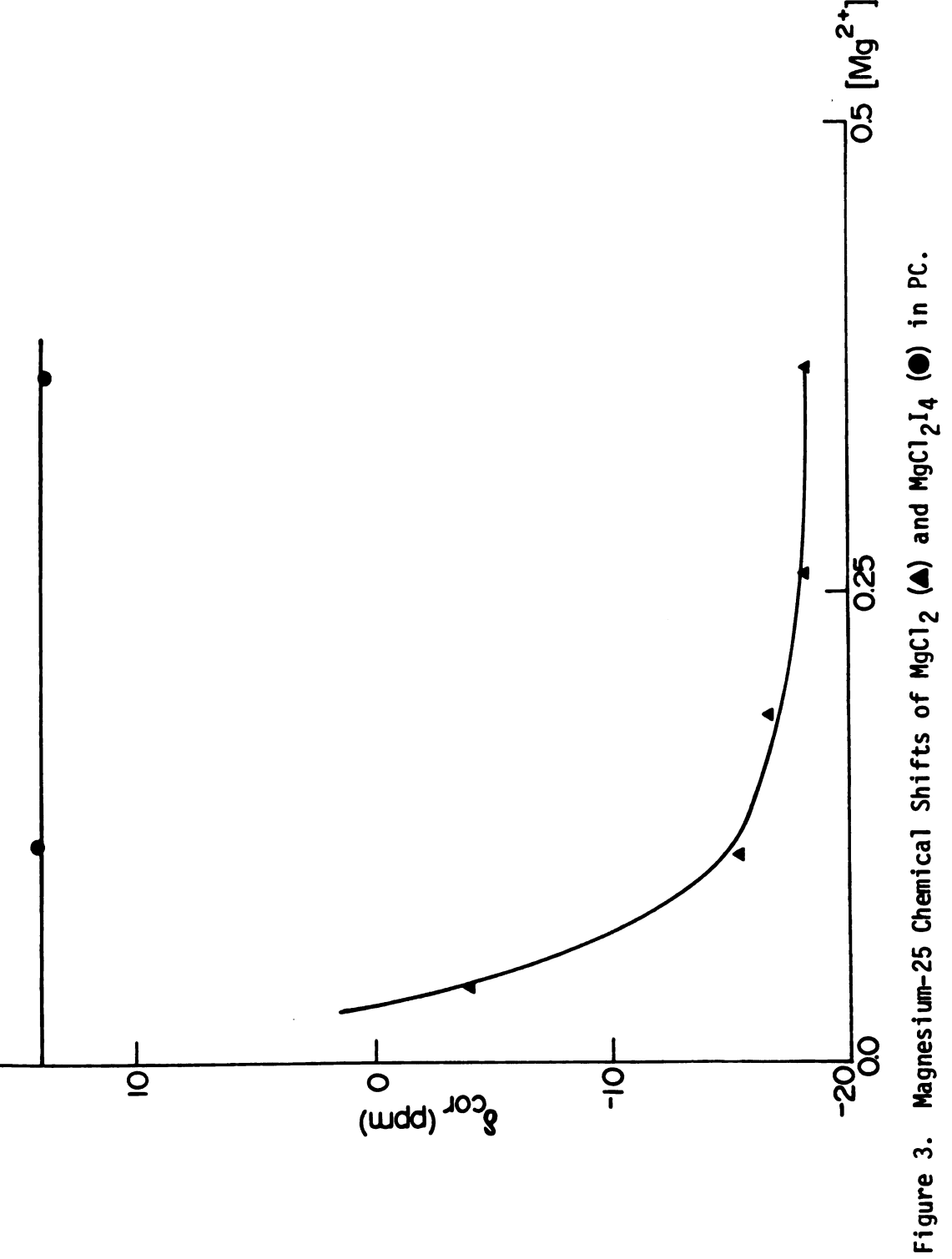
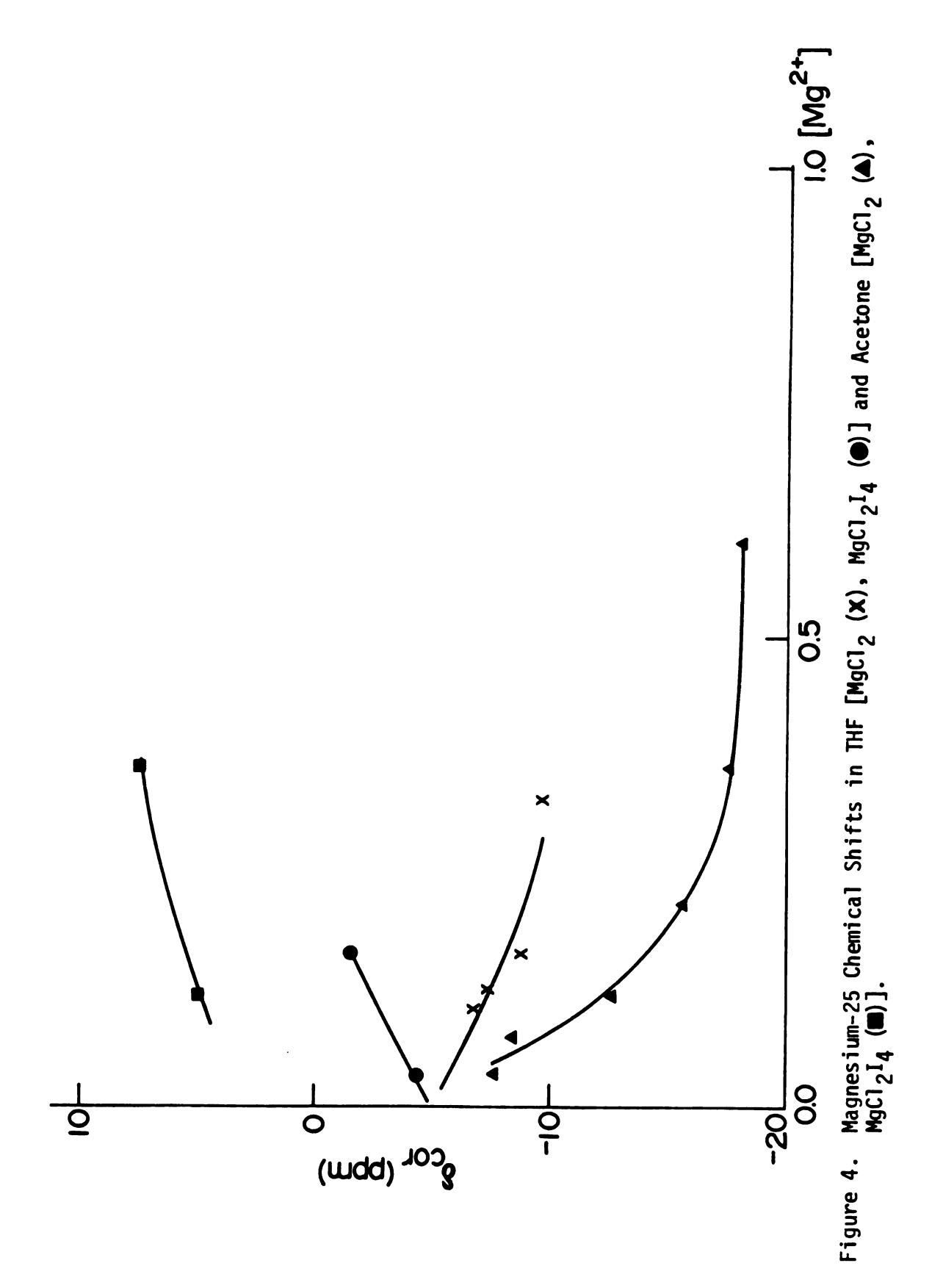


Figure 2. Magnesium-25 Chemical Shifts of ${\rm MgBr}_2$ in Acetonitrile.





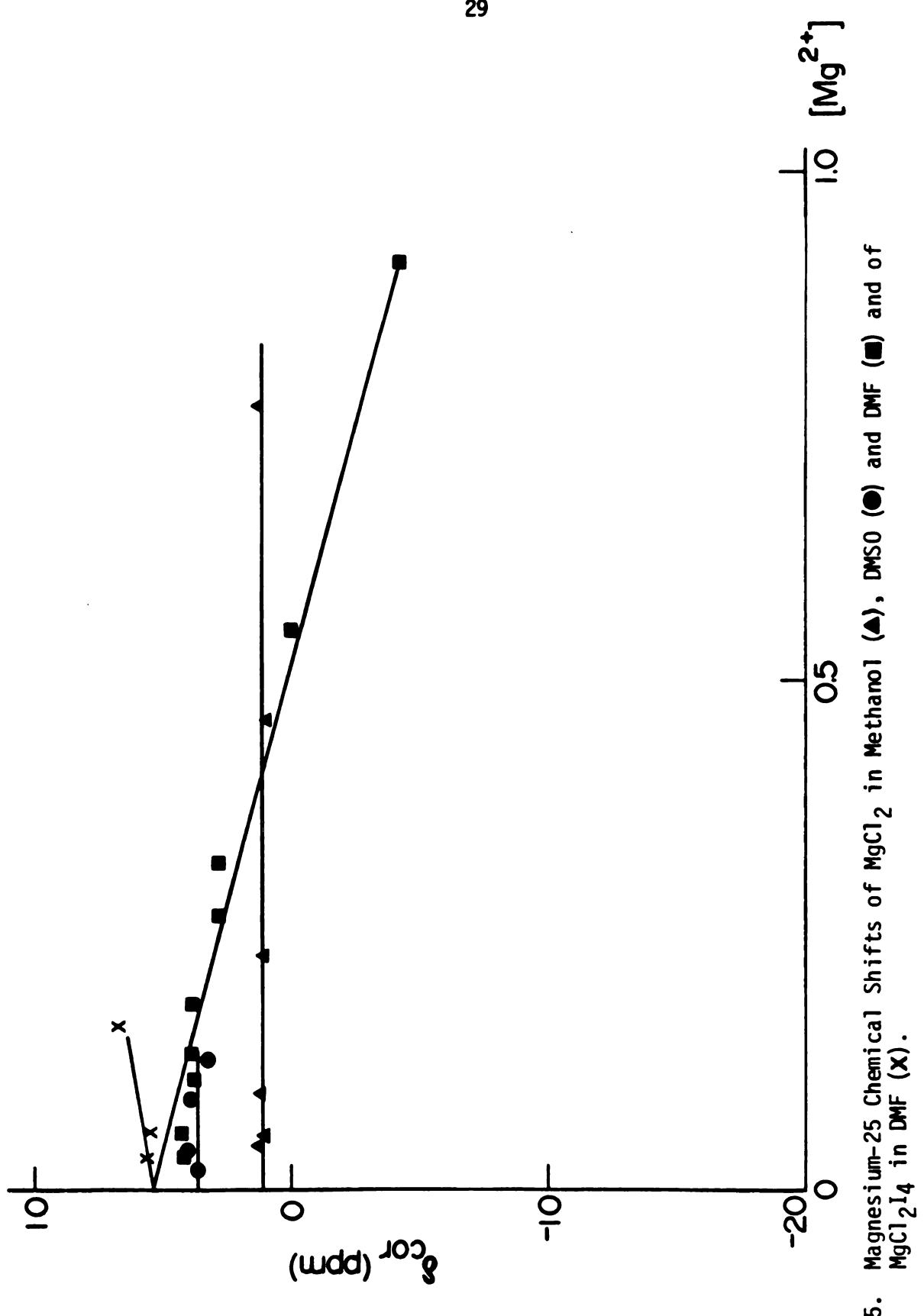


Figure 5.

NMR signal are related to a change of its direct chemical environment, that is, it reflects the influence of its nearest neighbors. It is well known that NMR gives information about the inner solvation shell of the nucleus under consideration. Replacement of the solvent molecule(s) by the anion may either increase or decrease the electron density of the cation. Replacement of solvent molecules by halide ions increases the electron density around the magnesium ion resulting in a downfield chemical shift of the Mg-25 resonance. Similar behavior has been previously observed with Li, Na, K, and Cs salts studied by Li-7, Na-23, K-39 and Cs-133 NMR (44).

Another evidence for the formation of contact ion-pair in the above solutions is the result obtained by studying the MgX_2 - I_2 mixtures in different solvents. It is well known (45) that halogen molecules interact with halide ions to form trihalide ions which are quite stable in nonaqueous solvents (e.g., K_f of $10^6 \cdot 6$, 10^7 and 10^{10} for I_3^- , Br_3^- and Cl_3^- ions respectively in acetonitrile). We can expect, therefore, the I_2Cl^- complexes to be stable, and, in the concentration range used (0.7 to 0.05 \underline{M}), we can assume that at a 1:1 mole ratio of iodine:halide ion, all the halide ions will be complexed. The size of the anion will become significantly larger and thus will have a much smaller tendency to form ion-pairs with magnesium ions.

The effect of iodine upon $Mg^{2+}-X^-$ ion-pairing is shown in Figures 6 and 7 - there is a linear change in chemical shift [similar to the one reported by Erlich and Popov (46) in the case of sodium-23 NMR] <u>vs</u> mole ratio of iodine to Mg^{2+} ion up to a value of 2 where all the halide ions are complexed. The largest

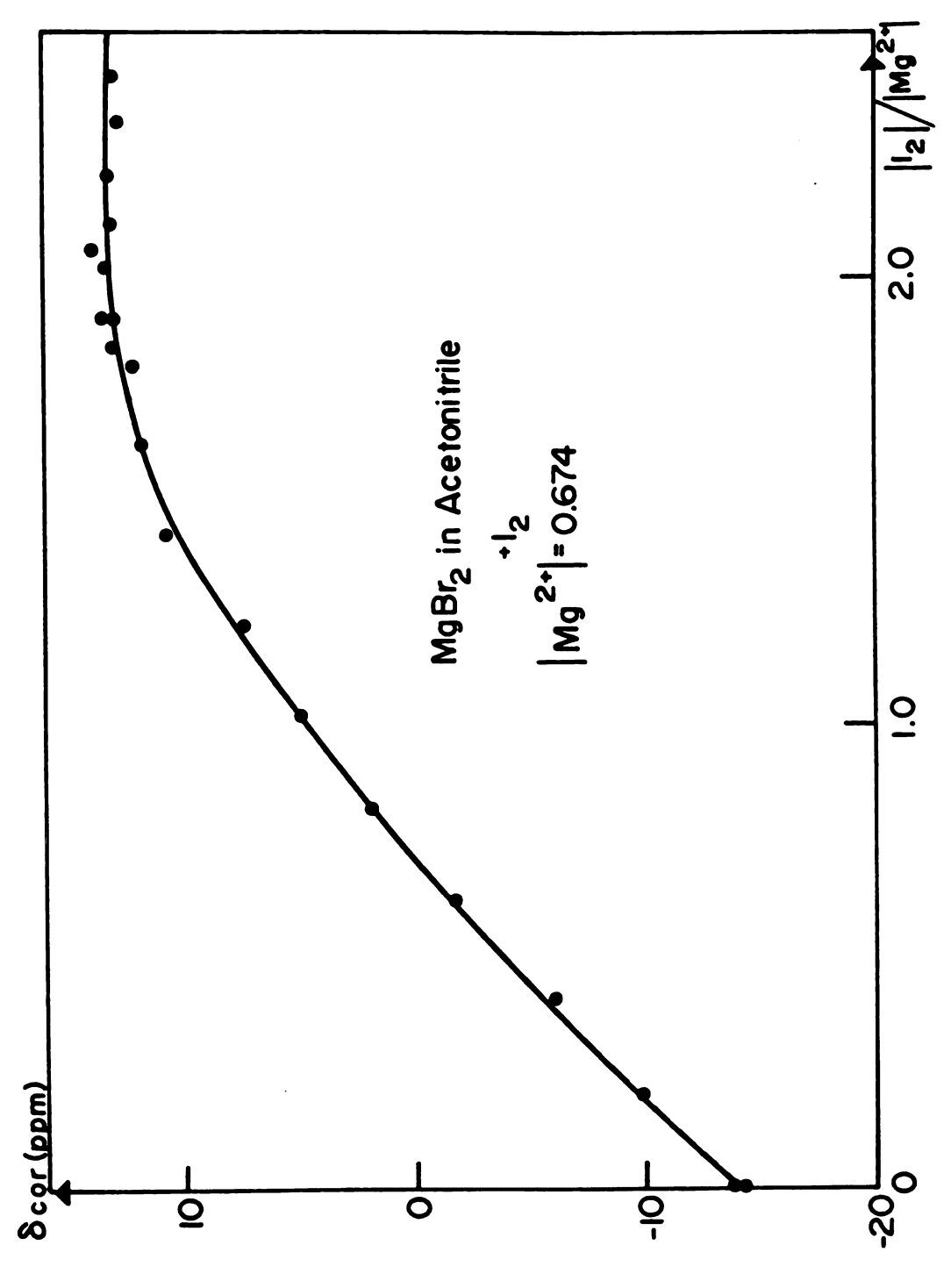


Figure 6. Magnesium-25 Chemical Shift of MgCl $_2$ <u>vs</u> Mole Ratio of Iodine in Acetonitrile.

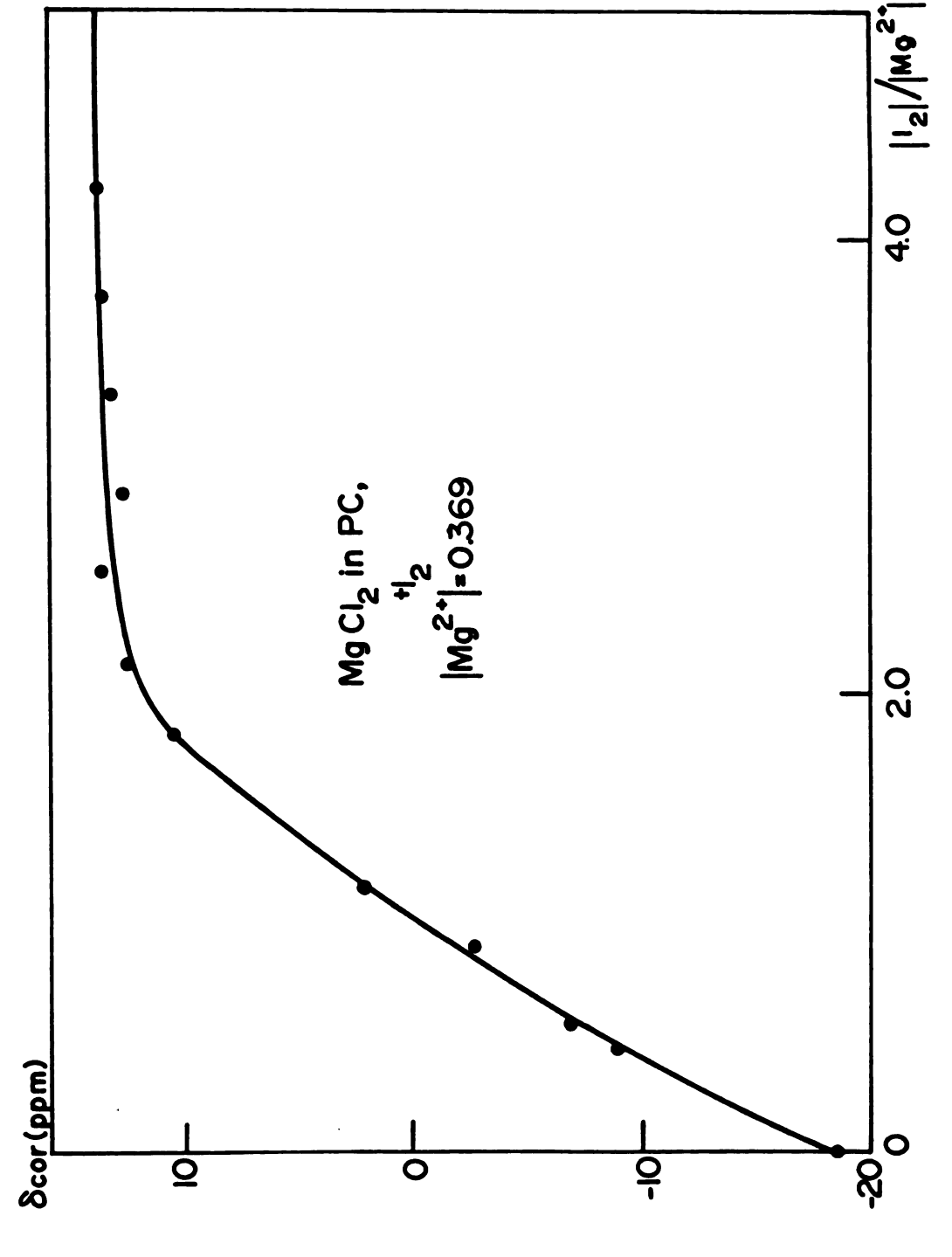


Figure 7. Magnesium-25 Chemical Shift of MgCl $_2$ vs Mole Ratio of Iodine in PC.

effect of ion-pairing was observed in the case of PC solutions, where the change in chemical shift due to ion-pairing was more than 30 ppm.

For solvents with a medium value of the dielectric constant (PC, acetonitrile, DMF), the interaction of the magnesium ion with the halide ion is decreased to such an extent that a magnesium-25 NMR concentration study of the complexed salt results in a constant chemical shift.

On the other hand, for solvents with a low dielectric constant (THF, acetone), the interaction between the two ions is decreased but is still noticeable, as shown by Figure 4. The poor solvating ability of acetone, and of THF had been shown by sodium-23 and lithium-7 NMR (47, 48).

3.4.2.2. <u>Line-Width</u> - Another interesting feature of the magnesium-25 NMR signal is the line-width. In the case of strong solvating agent (i.e., with both high dielectric constant and high donor number), the line-width of the signal is small. It is approximately 10 Hz in water, methanol and DMSO solutions. In DMF, concentration change from 0.03 to 0.9 M increases the line-width from 30 to 127 Hz.

As can be seen from Table II, the line-widths in other solvents are large, which also implies contact ion-pair formation. Indeed, although PC solutions are more viscous than aqueous solutions, this is not the case for acetone solutions, and, therefore, line-broadening of the signal must be due to other effects.

It is well known that the line-width of an NMR signal is related to the relaxation time T_2^* of the nucleus by the equation:

Table II. Line Width of the Magnesium-25 NMR Signal in Different Solvents

Solvent	Magnesium Concentration (<u>M</u>)	Line Width at Half Height (Hz
Methanol	0.768	12
	0.0543	10
THF	0.325	235
	0.1248	220
	0.0325 ^a	146
PC	0.369	460
	0.111	390
	0.111 ^a	134
DMF	0.913	127
	0.0319	30
	0.0319 ^a	15
DMSO	0.1227	37
	0.01227	11
Acetone	1.221	310
	0.1196	215
	0.1196 ^a	150
Acetonitrile	2.045	62
	0.423	27
	0.630 ^a	24

 $^{^{\}mathbf{a}}$ With a mole ratio of iodine to magnesium equal to or higher than 2.

$$\Delta v_{1/2} = \frac{1}{\pi T_2^*} \tag{3}$$

with

$$\frac{1}{T_2^*} = \frac{1}{T_2} + \frac{\gamma \Delta H_0}{2} \tag{4}$$

where $\frac{\Delta H_0}{2}$ represents the contribution to the line-width due to inhomogeneity of the magnetic field ΔH_0 , γ is the magnetogyric ratio, a constant for a given nucleus, and T_2 is the spin-spin relaxation time. Since the observed relaxation time is assumed to be in the motionally narrowed limit so that $T_1 = T_2$, with T_1 being the spin lattice relaxation time, we can relate the line-width of the signal to the five categories of spin lattice relaxation mechanisms: dipole-dipole relaxation, chemical shift anisotropy, scalar coupling, spin rotation and quadrupole relaxation.

We can then express the observed results as follows:

$$\frac{1}{T_1} = \frac{1}{T_2} = R_1, \text{ exp} = R_1, \text{ dip-dip} + R_1, \text{ chem shift an} + R_1, \text{ scal} + R_1, \text{ spin rot} + R_1, \text{ quad}$$
 (5)

It has been shown (49) that in the case of quadrupolar nuclide resonance, the line-width is generally determined by the quadrupolar interaction, the contributions from the other relaxation mechanisms being negligible. The interaction Hamiltonian for the quadrupole relaxation has the form: $H_q = I.Q.I$ and represents the interaction between the nuclear spin (I>1/2) and the electric field gradient at the nucleus. As reorientation occurs, the components of the quadrupole coupling tensor Q become random functions of time and provide a relaxation mechanism. We then have:

$$R_1 = R_2 = \frac{3}{40} \times \frac{2I+3}{I^2(2I-1)} (1 + \frac{\eta^2}{3}) (\frac{e^2Qq}{h})^2 \tau_c$$
 (6)

where η is the asymmetry parameter and (e^2Qq)/h is the quadrupole coupling constant, I is the nuclear spin of the observed species and τ_c is the translational correlation time.

Thus, the line-width of the NMR signal depends on three terms: $\eta,\,\tau_C$ and the quadrupole coupling constant. When ion-pairs are formed, the asymmetry parameter and the field gradient (and hence the quadrupole coupling constant) will change, and we will observe an increase in line-width. In the absence of ion-pairing, the line-width will be affected by the solvent cage. In a strongly solvating medium, the solvent molecules are held tightly around the metal ion, and the change in electric field around the nucleus is minimal, therefore, the line-width of the signal is small. On the other hand, when the magnesium ion is surrounded by a less solvating agent, like acetone or PC, the solvent molecules around the magnesium are held less tightly, and having more latitude to move, cause an increase in the inhomogeneity of the field, thus allowing the magnesium ion to relax faster, which in turn is reflected by a wider line-width.

3.5. DONOR NUMBER CORRELATION

It has been shown previously (50, 51) that in the case of the sodium-23 and potassium-39 resonances there is a roughly linear relationship between the magnitude of the chemical shift in a given solvent and the donicity of the latter expressed by the Gutmann donor number. Similar plot is shown in Figure 8 for the magnesium-25 resonance, and the data are given in Table III.

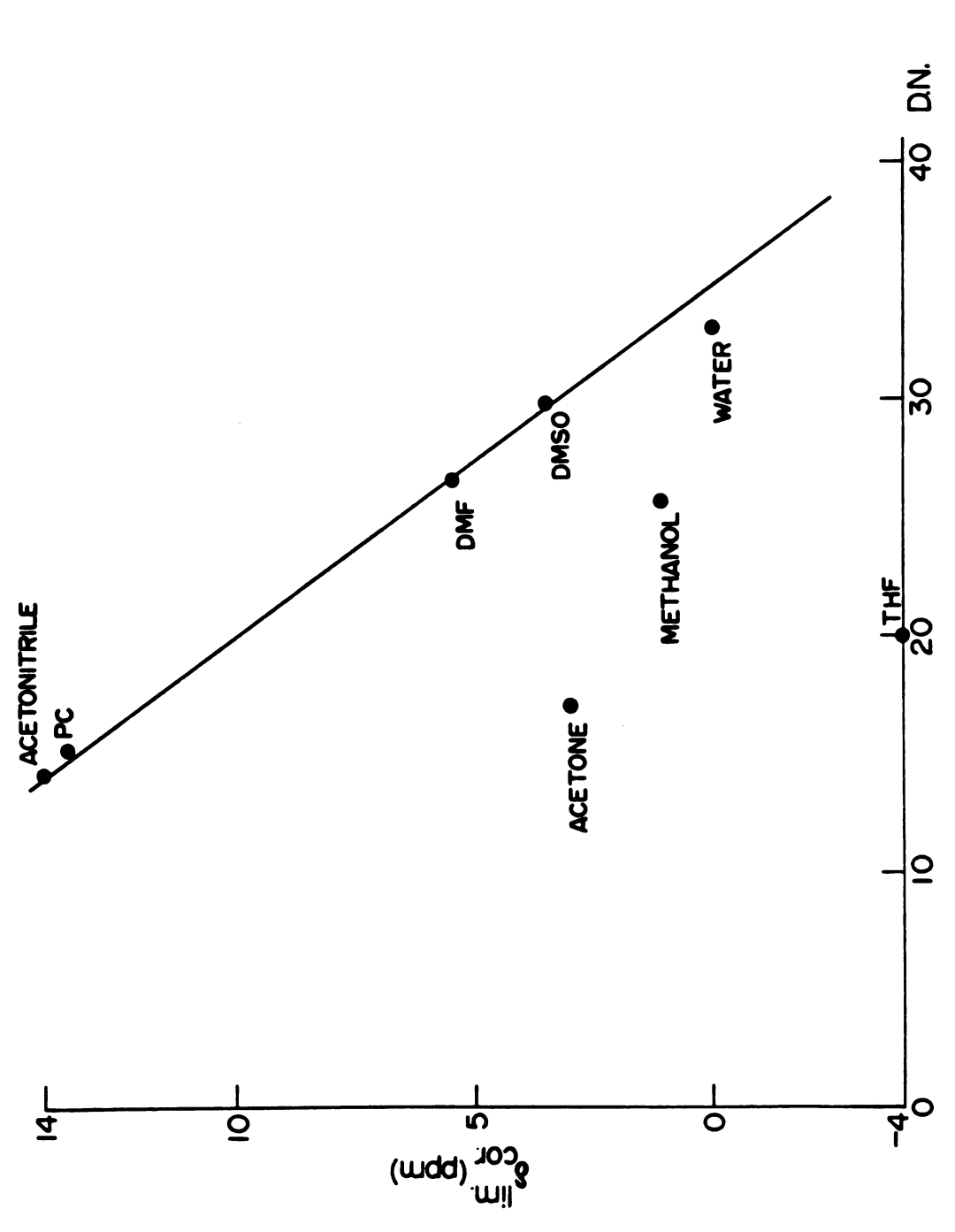


Figure 8. Limiting Magnesium-25 Chemical Shift in Various Solvents vs Their Gutmann Donor Number.

Table III. Limiting Chemical Shift of Magnesium-25 in Various Solvents.

Solvent	δ (ppm) ^a	Donor Number	Dielectric Constant
Acetone	3.0	17.0	20.7
Acetonitrile	14.0	14.1	37.5
DMF	5.5	26.6	36.71
DMS0	3.5	29.8	46.68
Methanol	1.1	25.7	32.7
PC	13.5	15.1	65.0
ГНБ	-4.0	20.0	7.58
Nater	0.0	33.0	78.9

 $[^]a\underline{\text{Vs}}$ 4.0 $\underline{\text{M}}$ aqueous MgCl $_2$ as external standard. Corrected for bulk susceptibility.

It is readily seen that for a majority of solvents there is a definite correlation between the magnitude of the downfield chemical shift and the donor number. Five of the eight solvents studied seem to fall on a reasonable straight line, but the correlation is not good in the case of THF, acetone and methanol. For the latter, a similar behavior was observed in the case of cesium-133 and potassium-39 resonances.

3.6. COMPLEXATION

Only preliminary studies have been performed in this area. An aqueous solution of phosphonoacetate and 0.05 M magnesium chloride at pH above 8 (so that all the PAA is under the deprotonated form) gave the following results: for a mole ratio of 0, 0.05, 0.1 and 0.2, the line-width changed from 7 to 16, 25 and 50 Hz, respectively, and no change in the chemical shift was observed. For higher mole ratios, the line-width was too large and the signal could not be detected within a reasonable amount of time.

It is seen from the above results that we have a fast exchange, compared to the NMR time scale, between the free and the complexed magnesium ion, therefore, the line-width and the chemical shift are the average of the free and complexed magnesium signals. If we define τ_a and τ_b as the lifetime of the magnesium nucleus in sites A and B, ν_a and ν_b as their resonance frequencies and τ as:

$$\tau = \frac{\tau_a \tau_b}{(\tau_a + \tau_b)} \tag{7}$$

we will have two resonance signals if

$$\tau > \frac{2}{\pi(\nu_a - \nu_b)} \tag{8}$$

otherwise, we will have the population average resonance.

Likewise, the line-width of the complexed magnesium ion is large, due to quadrupolar broadening since the ligand, being unsymmetrical, produces a nonuniform electrical field around the nucleus.

Similar studies performed with EDTA at pH 9-10 showed a somewhat different result, the line-width of the peak stays constant when the mole ratio ligand to metal increases from zero to close to one. At the same time, the signal becomes weaker and weaker, and finally for a mole ratio of one or above, it disappears. These results show that we have a slow exchange, compared to the NMR time scale, of free and complexed magnesium. The line-width of the complexed magnesium signal is again much too large to allow its detection. These results are in contradiction with the ones reported by Magnusson and Bothner-By (7).

Since the formation constant of the ${\rm Mg}^{2+}$ -C211 complex in water and in 95/5 methanol/water mixture was reported as $10^{2.5}$ and $10^{4.0}$, respectively (29), and since C211 and Li⁺ ion form a complex with an exchange between the free and complexed Li⁺ ion that is slow compared to the lithium-7 NMR time scale, the complexation between C211 and MgCl₂ has been studied in methanol. Kauffmann (52) from carbon-13 NMR studies of 0.1 $\underline{{\rm M}}$ solutions of C211 reported the formation of strong complex between magnesium and C211 in 95/5 methanol/water mixture. She found that in the 25°C-85°C temperature interval, the spectra of a 2:1 mixture of C211 and MgCl₂ contained two series of signals, one corresponding to the free ligand, while the other one was characteristic of the cryptate.

From equation (8), it can be seen that if the rate of exchange $(r = 1/\tau)$ between the free and complexed magnesium is slow compared to the C-13 NMR time scale, such is not necessarily the case for the magnesium-25 NMR time scale, since magnesium-25 resonates at a lower frequency and has a smaller chemical shift range than carbon-13.

Indeed, in the present case, the exchange between the two sites is fast since only one signal is observed. The line width increases from 10 to 22 Hz for the solutions of 5 x 10^{-2} M MgCl₂ with a mole ratio of ligand to magnesium of 0 and 1, respectively. The change in chemical shift, however, was small - from 1.1 to 0.7 ppm and, therefore, could be attributed to a random experimental error.

As an aside, the perchloric acid salt of C211 is insoluble in methanol. This property could be used to purify C211 or to recover it.

Another complexation study with 12-crown-4 (12-C-4, which has a cavity size comparable to the size of the magnesium ion) in DMF has been performed. In this case, no change in either line-width nor in chemical shift was observed. Either there is no complexation between Mg²⁺ ion and 12-C-4, or both free and complexed ions have the same chemical shift. The first hypothesis seems more reasonable in view of the solvating properties of DMF (ϵ = 36.71, donor number = 26.6).

On the other hand, at this early stage of development of magnesium-25 NMR in nonaqueous solutions, only qualitative results can be obtained as far as complexation is concerned, since there is no quantitative results concerning the ion-pairing in these solutions.

3.7. I.R. STUDIES

Some I.R. studies of 2.0 $\underline{\text{M}}$ solutions of MgBr $_2$ in acetonitrile showed a behavior of the solvent similar to the one observed by Janz et al. (53) by Raman spectroscopy in the case of silver ion. The splitting of the solvent bands corresponding to the C-C and C=N symmetric stretches (a₁) for complexed solvent molecules is shown in Table IV. The splitting is due to the presence in solution of both free and complexed acetonitrile.

3.8. CONCLUSION

We determined in this study that the chemical shift range of the magnesium-25 NMR signal is larger than 30 ppm, and that the NMR of magnesium-25 can be a useful tool to study solvent effect and ion-pairing of magnesium salt in nonaqueous solutions. The line broadening and chemical shift change have been explained by quadrupolar relaxation in terms of ion-pairing and solvent-magnesium interaction.

Table IV. Vibrational Frequencies of Free and Complexed Acetonitrile.

Solution	C-C Symmetric Stretch	C≡N Symmetric Stretch
Pure Acetonitrile	919 cm ⁻¹	2240, 2280 cm ⁻¹
Complexed Acetonitrile (2.182 M MgBr ₂ Solution)	880, 919, 935 cm ⁻¹	2240, 2280, 2305-10 cm ⁻¹

PART II

PHOSPHONOACETIC ACID STUDIES

CHAPTER 1

HISTORICAL REVIEW

1.1. INTRODUCTION

Just as the use of antibiotics revolutionized the treatment of bacterial disease in the 1940's, new antiviral agents promise to revolutionize the treatment of viral diseases in the 1970's and 1980's. For the first time, man will be able to combat viral infections, halting the replication of viruses and preventing their spread. The advent of this era may well be one of the most important milestones in the continuing battle against infectious diseases.

The genesis of the antiviral era has been quite different from that of the antibiotic era. The latter was launched by the discovery of penicillin, a relatively broad spectrum antibiotic whose value was readily apparent. The antiviral era is being launched with a number of narrow-spectrum agents whose value has been more difficult to establish. Antibiotics were introduced at a time when only a limited amount of testing was necessary to introduce a new drug to the market and when the need to treat wounded soldiers during a major war greatly accelerated that testing. Antiviral agents are being introduced at a time when consumer safety is the paramount concern, necessitating a great deal of expensive, time-consuming clinical testing.

The development and testing of antibiotics was largely subsidized by the federal government because of the national emergency, and the first antibiotics were quite profitable for the companies that put them on the market. The development of antiviral agents, in contrast, has been financed by the drug companies with

only limited support from the government, and no company has made a profit on one. In some ways, it is remarkable that the antiviral agents have been developed as rapidly as they have been.

1.2. PHOSPHONOACETIC ACID

Herpes viruses are a large family of deoxiribonucleic acid (DNA) viruses that are the causative factor of diseases, such as cold sores of the mouth, genital lesions, eye infections, varicella (chicken pox) and shingles. By some estimates as many as 10% of all Americans over the age of 18 have recurrent Herpes infections three or more times per year, and more than 70% of Americans are thought to have antibodies in their blood that indicate a prior Herpes infection. Some types of persistent Herpes infections are believed to be associated with initiation of cancer.

Few antiviral drugs exist against Herpesviruses, and most of them are nucleoside analogs, and, therefore, they are potential teratogenic agents (i.e., they could cause birth defects if injected during pregnancy). Phosphonoacetic acid (PAA), which is not a nucleoside analog, and has been found active against quite a few different Herpesviruses is, therefore, a very promising compound.

Phosphonoacetic acid (Chemical Abstract #4408-78-0) is an organophosphorus compound (see Figure 9), it has an inhibitory effect on the replication of Herpesviruses, and the mode of inhibition is thought to involve complexation with magnesium ion.

PHOSPHONO ACETIC ACID (PAA)

HO-P-CH2-C%

2-PHOSPHONOPROPIONIC ACID

PHOSPHONOFORMIC ACID (PFA)

3-PHOSPHONOPROPIONIC ACID

Structures of Various Phosphonic Acids: Phosphonoacetic Acid, Phosphonoformic Acid, 2-Phosphonopropionic Acid, and 3-Phosphonopropionic Acid. Figure 9.

This triacid, as well as several of its salts (calcium, barium, copper, manganese, zinc and silver), were first synthesized in 1924 by Nylen (54). Several syntheses have been proposed since then (55). Phosphonoacetic acid is a triacid; it is a white solid, with a molecular weight of 140.03, and has a sharp melting point at 142-143°C; it will also be referred to as phosphonoacetate (PA), its completely deprotonated salt.

1.3. ANALYTICAL TECHNIQUES

Several infra-red (IR) studies of PAA or its derivatives have been published in the literature (56-59). Its trimethylsilyl derivative has been studied by gas chromatography-mass spectroscopy and by gas chromatography (60); a single peak is obtained when examined in polar (OV-17) and nonpolar (SE-30) gas chromatographic phases. The above study is of importance for the biochemist, and the technique has been used to monitor the amount of PAA in blood. Phosphonic acid derivatives have also been separated by thin layer chromatography (61).

It has been found (62) that phosphonates can inhibit the transfer of copper ions or copper complexed ions to a mercury electrode because of their surface active properties. Investigations have been conducted on the adsorption of PA on hematite, silica and graphitized carbon (63, 64).

1.4. NUCLEAR MAGNETIC RESONANCE STUDIES

Nuclear magnetic resonance studies involving the measurement of the carbon-13 or phosphorus-31 chemical shift or of the coupling

constants between C and P or P and H have been conducted on PAA or its ethylester. For carbon-13 NMR studies, the acid was dissolved in methanol (65) and the chemical shifts \underline{vs} TMS are 35.8 and 168.6 ppm, for the \underline{CH}_2 and the $\underline{C}00H$ carbons, respectively, while the coupling constant between C and P is 132.0 Hz. The ester has been studied as a neat liquid (66).

Some phosphorus-31 NMR studies have been performed on PA (67). The solution was basic (pH=14) with tetramethylammonium hydroxide (TMAH). The chemical shift reported <u>vs</u> 85% phosphoric acid (contained in a capillary tube inside the sample tube) is -13.1 ppm, no indication being given whether it is a downfield or an upfield shift.

Riess <u>et al</u>. (67) found that a several fold change in either phosphorus or alkalinity concentrations caused less than 0.2 ppm change in the chemical shift. No mention was made by them of a triplet signal due to the coupling between the P and the CH_2 hydrogens. Complexes between lithium and two PAA esters have been studied in tetrahydrofuran (THF) (68).

1.5. ACIDITIES AND ACTINIDE COMPLEXES OF PAA

Aside from these industrial uses, all the other studies made so far were concerned with either the extraction of rare earth elements, or biological applications. It is interesting to note that most of the studies concerning the biological applications of PAA have been published in the last five years, and that they represent approximately 80% of all the studies ever performed on PAA.

Organophosphorus compounds have been found to be good extractants of rare earth elements (69), and more specifically, Elesin et al. (70, 71) investigated the complexation of PAA with americium, curium and promethium ions, as well as determined the acidity dissociation constants (pK's) of PAA.

Several comments can be made about this work: the dissociation constants of PAA were determined against a background of ammonium perchlorate at an ionic strength I=0.2, although ammonium perchlorate is known to be a weak acid. Moreover, sodium hydroxide was used as a titrant in this research, and since it has been shown (72, 73) that phosphate ions form weak complexes with alkali metal cations, the values of the pK's obtained (1.14, 4.33, and 7.31 at ionic strength 0.2, which, extrapolated to zero ionic strength gives 1.37, 4.84, and 8.50) are probably too small.

The investigation of the complex formation of Am^{3+} , Cm^{3+} , and Pm^{3+} was conducted by the method of ion exchange on the cation exchange resin KU-2, also against a background of ammonium perchlorate, at 0.2 ionic strength. Only protonated complexes were studied, and the log K_f values extrapolated to zero ionic strength are 2.75, 5.15 and 3.3 for the $M(H_2L)^{2+}$, $M(HL)^{+}$ and $M(HL)_{2}$ complexes, respectively (LH₃ represents the free PAA). The formation constants were found to be equal for the three cations.

Mao et al. (74) reported pK's of PAA of 2.6, 5.0 and 8.2 for the carboxylic and two phosphono groups, respectively. Their correlation between pK's and acidity functions is most probably

incorrect (see p 74), besides, the conditions under which those values have been determined are not specified.

1.6. INDUSTRIAL APPLICATIONS

The practical applications of PAA or its esters are numerous, and several patents mention it for widely different purposes: it has been used as a flame retardant in thermoplastics (75), as a corrosion inhibitor for iron-containing water conducting systems (76), to prevent the formation of spots in photographic materials due to the presence of particles of heavy metals or their derivatives (e.g., iron and rust) (77), as an insecticide (78), as an herbicide (79), or a plant growth regulator (80). Phosphonoacetic acid has also been proposed as a treatment against warts (81), or Herpesviruses (82, 83).

1.7. BIOLOGICAL PROPERTIES OF PAA

The popularity of PAA in the biochemical field lies in its ability to inhibit the replication of Herpesviruses. Three good reviews have been, or are going to be published on that matter (84-86).

1.7.1. <u>HERPESVIRUSES</u> - Herpesviruses (Herpesvirus in the U.S., Herpes virus in England) is the name of a genus of viruses that cause diseases affecting both man and animal. Some of these diseases are fatal, and it has been suggested recently that Herpesvirus may be directly or indirectly associated with cancer in several animals.

Herpesviruses have also been indirectly associated with naso-pharyngeal and cervical carcinomas in humans [carcinoma: solid tumor derived from epithelial tissues, is the major form (85%) of human cancer].

Other types of Herpesviruses are: Equine Herpesvirus,

Varicella-zoster virus (causes chicken pox, shingles), Marek's

disease Herpesvirus (the main cause of death among chicken in

commercial poultry, and the reason of the creation of the Poultry

Research Laboratory at M.S.U.), Epstein-Barr virus (responsible

for infectious mononucleosis), Cytomegalovirus (among the

diseases: pneumonitis, Cytomegalovirus mononucleosis), Herpes

Simplex virus [causing cutaneous lesions (Herpes Dermatitis),

mouth sores, cornea infection (Herpes Keratitis: responsible

for an estimated 18,000 cases of blindness each year in the

United States), venereal diseases]. The list is far from

being exhaustive.

- 1.7.2. <u>HERPESVIRUS DNA POLYMERASE</u> It has been found for several types of Herpesviruses that the virus induces its own DNA polymerase (DNA polymerase is an enzyme involved in the production of DNA). Three general classes of DNA polymerases are found in cells of all vertebrates: DNA polymerase α , β , and γ . The greek letters designate their order of discovery: α and β are the most important ones. Herpesvirus induced DNA polymerases have been reported for several Herpesviruses.
- 1.7.3. <u>HERPESVIRUS MODE OF ACTION</u> The mode of action of Herpesvirus is as follows: the virus enclosed in a capsid protein

comes in contact with a cell, at this point the protein opens and the viral DNA penetrates into the cell, it then travels through the cell to the nucleus, enters it, and uses the nucleus system to produce ribonucleic acid typical of the virus (RNA $_{HV}$). The RNA $_{HV}$ leaves the nucleus, and following the usual pattern, forms a DNA polymerase typical of the virus. This DNA polymerase goes back to the nucleus where it creates its own DNA (DNA $_{HV}$); from this point on, the loop is closed, the production of DNA $_{HV}$ increases a lot, and within a few hours or a few days, depending on the virus, the cell dies and many new viruses are then released.

1.7.4. INHIBITORY POWER OF PAA - Leinbach et al. (87) proposed two solutions to explain the inhibitory power of PAA on the Herpesvirus of turkey induced DNA polymerase. The basic pathway used by the enzyme to build up the Herpesvirus specific DNA is shown in Figure 10.

In the first step, the DNA $_{HV}$ binds to the enzyme, in the second step deoxynucleoside triphosphate (dNTP) binds to another site of the enzyme, upon which the length of the viral DNA $_{HV}$ molecule is increased and inorganic pyrophosphate (PP $_{i}$) is formed. In a third step, PP $_{i}$ is released and in the final step DNA $_{HV}$ is released. The loop is closed, and the procedure can start again. Actually, in each cycle, the DNA $_{HV}$ molecule is not exactly increased by one link, but rather the two complementary strands of DNA are separated and each forms the template for synthesis of a complementary daughter strand.

From the results of their kinetic studies, Leinbach et al. (87) proposed the mechanism presented in Figure 10. In the presence of

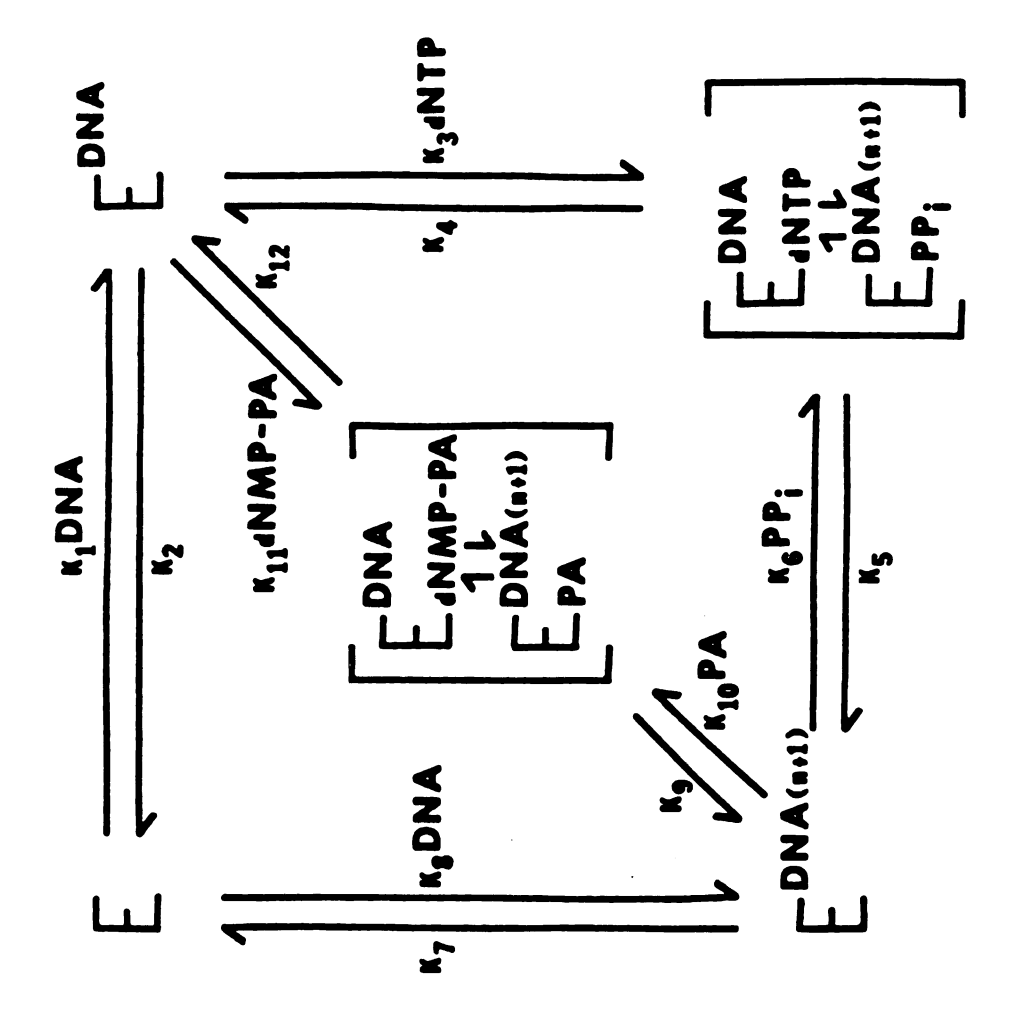


Figure 10. DNA Synthesis and Mode of Action of PAA.

PA, an alternate pathway exists in addition to the basic polymerization pathway. Phosphonoacetate binds to the polymerase at the PP_i binding site (believedly via complexation with magnesium ion) and is thus a competitive inhibitor of PP_i in the exchange reaction. Phosphonoacetate may simply dissociate from the $E_{PA}^{DNA(n+1)}$ complex or may undergo reaction with the nucleotide at the 3' end of the DNA primer chain to yield the postulated nucleotide, dNMP-PA, and E_{PA}^{DNA} (dNMP: deoxynucleoside monophosphate). Thus, PA inhibition occurs because the $E_{PA}^{DNA(n+1)}$ complex is diverted by PA from the main polymerization pathway into an alternate pathway.

The kinetics results are not consistent with the second scheme proposed - PA being a simple dead-end inhibitor in which it could only bind and dissociate from the $E^{DNA(n+1)}$ complex, but are consistent with the first scheme proposed.

To fully accept this scheme, however, the postulated nucleotide, dNMP-PA, must be identified in the reaction mixtures. Attempts to do so have not proved successful.

From the alternate pathway scheme it can be seen that PA and PP_i inhibit DNA_{HV} synthesis in an analogous manner. Studies performed by Leinbach <u>et al</u>. (87) confirmed this fact; the apparent inhibition constants for pyrophosphate, however, are two to three orders of magnitude greater than those for phosphonoacetate, that is, the amount of PP_i required to produce 50% inhibition is 100 to 1000 times larger than the amount of PA required for the same result.

1.7.5. <u>DRUGS AGAINST HERPESVIRUSES</u> - In the case of Herpesviruses, several drugs having an inhibitory power have been studied, although only one is currently used commercially in the U.S., and two or three outside the U.S. (see references 88 and 89 for a good review of most of them). These drugs are, however, usually specific for one or two types of viruses only, and may also be incorporated into host DNA. The potential for genetic damage, infertility or even carcinogenesis may not be negligible.

At least some of these compounds have been compared to PAA. Ara-A $(9-\beta-D$ -arabinofuranosyl adenosine) is about as effective as PAA against Herpes Simplex virus type 1 (90), while Ara-A was unsuccessful (91, 92) in clinical trials in humans with Herpes Genitalis. In rabbits, Ara-A and PA were equally effective in the treatment of Shope fibroma (93), while idoxuridine and PA had the same effect in treatment of Herpes Keratitis in rabbits (94, 95), however, idoxuridine has been shown to be carcinogenic and teratogenic. Tilorone hydrochloride (96) was found uneffective against Herpes Simplex virus type 1 in mice as opposed to PAA. Against Cytomegalovirus, Ara-A was also found less effective than PAA.

1.7.6. TOXICOLOGICAL EFFECTS OF PAA - Thus, all the drugs other than PAA that have been used against Herpesvirus are usually specific of one virus only, and may be or have been proved to be carcinogenic or teratogenic because of their mode of action. The best solution would be a compound that inhibits DNA synthesis by

a direct interaction with viral DNA polymerase. This solution is represented by PAA. However, PAA may have some toxic effects of its own, and its clinical drug usefulness is uncertain.

Meyer et al. (95) reported that intravenous PAA in a concentration of 300 mg/kg produced severe tetanic muscular spasms in rabbits, often resulting in death; the same dose given to mice orally or intraperitonally was well tolerated (97, 98).

Roboz et al. (99) developed an analytical technique for the determination of PAA in blood. The method is based on the monitoring of selected ions of PAA and phosphonopropionic acid (internal standard), formed in the chemical ionization (methane) source of a combined gas chromatography-mass spectrometer system. The drug is quantified in blood after removing proteins and lipids as the trimethylsilyllated derivative. The detection limit is 20 ng/ml when 0.2 ml of serum is analyzed. The technique is applicable to serum from mice, rabbit, monkey and man.

In the case of mice, oral administration of 500 mg/kg drug results in slow increase of blood levels (to 50 μ g/ml in one hour) followed by a drop to 2 μ g/ml by two hours. A dose of 500 mg/kg of PAA given subcutaneously kills monkeys in two days and results in blood levels in the 0.5-3.0 mg/ml range. A total dose of 100 mg/kg given subcutaneously in 25 mg/kg doses (every two hours, four times) is well tolerated and yields blood levels in the μ g/ml range. Owl monkeys with kidney disease develop higher blood levels than squirrel monkeys, but both yield levels down to 2 μ g/ml in 24 hours. A total dose of 1000 mg/kg a day is well tolerated when infused continuously resulting in a slow increasing blood level (from 155 to 400

 $\mu g/ml$) which decreases to about 55 $\mu g/ml$ 24 hours after terminating infusion.

For therapeutic trials, a minimum of 50 μ g/ml continuous blood level is recommended. This is achievable with a dose of approximately 230 mg/kg a day.

Bopp et al. (100), using PA-14C, determined the amount of PA retained by the different parts of the body.

Orally administered PA was poorly absorbed in rat (14%, 100 mg/kg), rabbit (2%, 20 mg/kg) and monkey (8%, 20 mg/kg) as determined from urinary excretion. Absorption averaged 60% in dogs given 1 mg/kg, but was quite variable. The total recoveries in seven days after i.v. administration of the compound (20 mg/kg) accounted for 104% in adult dog, but only 88% in rat and monkey, 66% in rabbit and 62% in puppy, suggesting that a substantial amount of ¹⁴C remained in the body.

Whole body autoradiography studies in rats demonstrated that the ^{14}C was retained in bone. Seven days after i.v. administration of the drug (20 mg/kg) the levels of radioactivity expressed as PAA in dry femur were 55, 62, 24, 4, and 57 µg/g in rat, rabbit, monkey, adult dog and puppy, respectively. During a 25-50 day period after i.v. administration (20 mg/kg), the elimination of ^{14}C was at least biphasic, with half-lives of 5.8 days in rat, 8.7 days in rabbit, and 13.9 days in both monkey and dog. The levels of PAA in dry femur on day 50 were 9.6 µg/g in rat, 24.6 µg/g in rabbit, 0.8 µg/g in monkey and 3.0 µg/g in dog. Long-term retention studies in rabbits demonstrated the persistence of ^{14}C in bone for over 200 days.

1.8. PHOSPHONOACETIC ACID DERIVATIVES

For the preceding reasons and to try to obtain a better antiviral agent as well as to determine the mode of action of PAA, derivatives of PAA have been tested.

Herrin et al. (101) and Lee et al. (102) have studied the effect of PAA derivatives on some Herpesviruses. Esters of the acetic function of PAA eventually proved to be inhibitors of Herpes Simplex virus-induced DNA polymerase, but always to a smaller extent than PAA.

Replacement of either the carboxylate or the phosphonate moiety resulted in a loss of effectiveness of the compound. An amino, methylamino or phosphono group cannot substitute for the carbonyl group, neither can a carboxyl or a sulfo group for the phosphono group.

The only two other phosphonates active against Herpesvirus besides PA are 2-phosphonopropionic acid (see Figure 9) which is about 50 times less active, and phosphonoformic acid (PFA, see Figure 9) which has approximately the same efficiency as PAA.

Since PFA decomposes in acidic medium (103, 104), it seems to have a better future than PAA. Phosphonoformic acid was first synthesized in 1924 by Nylen (105), who also reported the following salts: Zn, Mn, Cu, Pb and Ag.

Esters of PFA have been used in oil (106) because they provide extreme pressure lubricity in lubricating oils and are useful as hydraulic fluids.

According to Warren and Williams (104), the pK_a 's of PFA are 0.49, 7.27 and 3.41 for the phosphonic and carboxylic moieties, respectively. Nylen (103) reported 0.39 and 3.18 in 4 M NaCl.

The crystal structure of trisodium phosphonoformate (PF) hexahydrate has been determined (107), it consists of sodium ions surrounded octahedrally by six oxygen atoms, some from water molecules, some from the PF ions.

So far, very few studies have been performed on the antiviral action of PFA. Reno <u>et al</u>. (108) found that it was at least as effective as PAA against Herpes virus of turkey and Herpes Simplex virus, but PFA was not found to be an effective inhibitor of a PAA resistant mutant of the Herpesvirus of turkey, nor of its induced DNA polymerase.

These facts suggest that PFA and PAA have basically the same biochemical properties and mode of action against Herpesvirus incuded DNA polymerase, aside from the acidic decarboxylation reaction of PFA which makes it a very promising clinical drug.

1.9. CONCLUSION

It is seen from the above that the physicochemical properties of PAA are not well known and even its acidity constants have not been accurately determined. On the other hand, it is an interesting molecule from the point of view of its acid-base equilibria and its complexing abilities. In addition, it appears to have very important physiological and even therapeutic properties. It was of interest to us, therefore, to investigate in some detail the acid-base and the complexing behavior of PAA.

CHAPTER 2

MATERIALS AND METHODS

2.1. REAGENTS

Phosphonoacetic acid (PAA, from Richmond Organics) was dissolved in glacial acetic acid (22 g of PAA in 100 ml of glacial acetic acid) at a temperature close to its boiling point, and cooled down to room temperature. Crystals obtained after this recrystallization were rinsed with ethyl ether. The product was then dried at 60-70°C in the vacuum oven for at least 24 hours. The melting point is 142.5-143.5°C (stem correction included, heat rate: 2°C/minute), in agreement with the literature value (54): 142-143°C. Elemental analysis (Spang) gave the following figures: calculated/experimental: C: 17.15/17.16; H: 3.60/3.55; P: 22.12/22.13. A mass spectrum using the field desorption technique gave the following peaks: HO(0) P⁺(CH₂COOH); ⁺P(OH)₃ (CH₂COOH)₂ and [(0) P(OH)₂ CH₂COOH]₂ H⁺.

Tetramethylammonium bromide (TMAB, from Eastman organic chemicals, technical grade) was purified in the usual manner (109) by recrystallization from methanol (100 g in 1 to 1.5 l of boiling methanol, then cooled down with a dry ice acetone mixture), followed by two precipitations from methanol solution by the addition of ethyl ether (dissolution of the precipitate in 3 liters of methanol, filtration, addition of 4.5 lb of ether, filtration, drying of the precipitrate at room temperature under vacuum for 24 hours, and repetition). Tetramethylammonium bromide was then dried under vacuum at room temperature for 48 hours. The compound decomposes slowly with time and/or heat and had to be repurified every two to three months. The melting point is higher than 300°C [literature (110, 111): decomposition above 240°C].

The other chemicals used have already been described in Part I.2.1.

2.2 RESINS

The anion exchange resin was Dowex 1x2, 50-100; the cation one was Dowex, 100-200; 50-X-8. The anion transfer membrane used for the coulometric titrations was from Ionics, type 103-PZL-183, and was treated with KBr before use to convert it to the bromide form. The membrane should be always kept wet, otherwise, it becomes porous and useless.

2.3. SPECTROSCOPY

- 2.3.1. <u>VISIBLE SPECTROSCOPY</u> Absorbances in the UV visible range were measured with a Cary 17 double beam spectrometer, and the base line has been adjusted through the entire range.
- 2.3.2. NUCLEAR MAGNETIC RESONANCE SPECTROSCOPY The instruments used to observe the sodium-23, magnesium-25, phosphorous-31 and proton NMR spectra have been described previously (Part I.2.2.2.). For carbon-13, a Varian CFT-20 Fourier transform NMR spectrometer was used. The instrument is equipped with a computer controlled pulse generator and data collection. The field strength is 18.682 kG and carbon-13 resonates at 20 MHz. When an external reference is used, it is enclosed in a capillary tube coaxially centered in the 8 mm OD NMR tube containing the sample solution; otherwise, an internal reference (dioxane) is used. The chemical shifts are reported vs TMS. For carbon-13 and proton NMR, a positive chemical shift is downfield of the TMS.

2.4. CYCLIC VOLTAMMETRY

Cyclic voltammograms have been measured with a PAR model 174 polarographic analyzer and recorded with a Houston omnigraphic 2000 recorder. The solutions were contained in a cell consisting of two compartments separated by a frit. The solution on both sides was at the same ionic strength (0.4 M with TMAB). The solutions were degazed for 15 minutes with a stream of nitrogen.

The electrodes were as follows: reference electrode: thallium amalgam ($E_{calomel}$ - E_{ref} = 840 mV); counter electrode: platinum wire; working electrode: mercury dropping electrode. The sweeping rates were 50, 20 and 10 mV/s. Triplicate runs were made for each solution and for each sweep rate. Usually the average of the maximum and minimum (frontward and backward peaks) were the same, and were independent of the sweep rate. The half wave potential of the metal ion for a given solution was obtained by averaging all the maxima and minima of the different spectra.

2.5. POTENTIOMETRY

The potentiometric measurements were done with a line powered voltmeter (Analogic), #AN 2546 (\pm 2 V at \pm 0.1 mV). A high impedance buffer was built by the electronics shop to connect the electrode to the voltmeter. The following electrodes were used: Sargent Welch 300 72-15 (combination pH electrode, with a thallium amalgam reference, which is more stable at high temperature than the usual calomel reference), and Corning NAS 11-18 (sodium ion electrode)

used with a calomel reference electrode. The Sargent Welch electrode was replaced after 3 months, because its response became unstable.

Measurements made outside and inside of a Faraday cage showed that 60 cycle noise was up to 80 mV peak-to-peak outside and less than 1 mV inside the cage. Static noise was detected by random potential fluctuations, up to 40 mV outside and down to less than 0.1 mV inside the cage. Static noise is due to the operator and to charges building up on the instruments. Cyclic and static noise were picked up by the cables bringing the current from the coulometer to the electrodes, resulting in potential fluctuations of up to 0.8 mV. These fluctuations completely disappeared when shielded cables were used.

The titrations were performed in a thermostated cell, 3.5 cm I.D. and 9.0 cm in length. The temperature was maintained constant by a water bath. The cell is closed with a teflon top, with an inlet for a stream of nitrogen. Before reaching the cell, the nitrogen goes through two bubblers containing an aqueous solution of $Co(II)SO_4$ and a slightly basic solution of $BaCl_2$ to eliminate oxidizing impurities and CO_2 . Before each titration, the solutions were temperature equilibrated for at least 30 minutes. The solutions were stirred with an air driven magnetic stirrer. After the addition or generation of the titrant, the solution was stirred for 30 seconds, and the voltage was recorded after 1.5 minutes; therefore, it took two minutes to get one data point.

In the case of the pH measurements, extensive use was made of a coulometer described in the next section. The anode compartment

of the coulometer consists of a 12 mm OD glass tube, 15 cm in length, with a piece of anion transfer membrane at the end. The membrane is held tight with a teflon cap (16 mm OD, 20 mm long, with an 8 mm I.D. hole at the end), and an 0 ring. Care must be taken not to have an air bubble against the membrane when putting the compartment in solution, otherwise, the electric contact is not possible. When working at temperatures higher than 35°C, a slightly larger glass compartment was used, since teflon has a slightly larger expansion coefficient than glass.

The two electrodes connected to the coulometer consisted of a platinum rectangle (17 x 10 mm) and a platinum grid (30 mm in length, 32 mm in diameter). After each run, each electrode was cleaned by immersion in 6 \underline{M} HNO₃ and generation of current for 60 seconds using each electrode in turn as an anode and as a cathode.

2.6. COULOMETER

The base in the potentiometric experiments was generated via the use of a constant-current coulometer. A block diagram is shown in Figure 11. The scheme for the different parts of the coulometer was kindly furnished by Dr. C. G. Enke's group, Marty Rabb (electronic designer) and the electronic shop. The instrument itself was assembled with Dr. J. Hoogerheide.

The time base consists of a Crystek 1 MHz crystal oscillator and a Mostek MK 5009 counter time base circuit. The gate is formed of NAND gates (two SN 7400, Texas Instruments). The pulse generator contains a 555 timer chip (T.I.). Five of seven 7490 decade counters

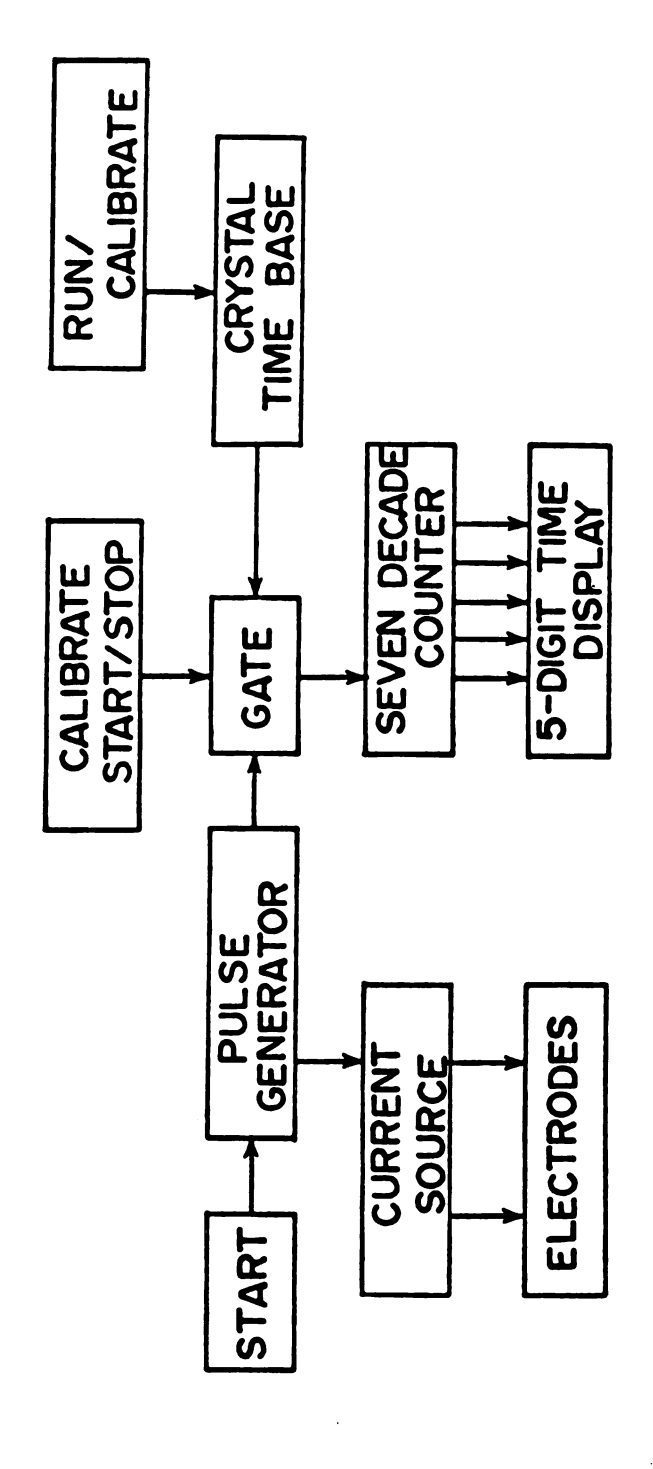


Figure 11. Block Diagram of the Constant Current Coulometer.

were multiplexed to provide a five-digit display. The current source consists of a 741 CP operational amplifier, with a temperature compensated Zener diode to provide an accurate and stable voltage reference. An Intersil DG 191 solid state switch was used to decrease the residual current between current generations. The power board converts 115 V, 60 Hz into \pm 15 & 5 V D.C.

The general mode of operation of the instrument is the following:

Operational mode: activation of start (by depressing the start switch) causes generation of a pulse (+5 V) by the pulse generator. This pulse turns on the current until the phase returns to a logical zero (0 V). The gate is simultaneously opened, allowing the time base oscillations to be counted, thus giving a measure of time which the current was on. In the operational mode, the time base frequency is 10^4 Hz.

Calibrate mode: manual opening and closing of gate allows 10^2 Hz time base to be counted. Readout is in seconds. The calibrate mode is used to count clock pulses up to 20,000 against a reference time source. The total of 20,000 seconds allows considerable error in the start and stop actions (1 ppt corresponds to 20 seconds).

The characteristics of the coulometer are as follows: current rise and fall time on the order of 1 μ s, residual current of approximately 2 nA, current stable to ± 1 ppt and time base accurate to better than 0.5 ppt. Further information can be obtained in the operating manual (133).

2.7. SAMPLE PREPARATION

- 2.7.1. CYCLIC VOLTAMMETRY In order to prevent the precipitation of $Cd(OH)_2$ for this experiment, a solution of $Cd(NO_3)_2$, TMAB and PAA was titrated by TMAH up to a pH of 11 (all the ligand was then in the phosphonoacetate form). The concentration of cadmium ion was 5.046 x 10^{-4} . The ionic strength of the solution was high (0.4), so that the solution with a ligand to metal mole ratio of 100 could be obtained without changing the ionic strength. Eleven solutions were run at mole ratios from 0 to 100 by increment of 10. The solutions were deoxygenated with a flow of nitrogen for 15 minutes prior to run.
- 2.7.2. <u>SODIUM ION ELECTRODE MEASUREMENTS</u> Sodium ion measurements have been performed by using a Corning NAS 11-18 electrode. The calibration was performed by titrating 10 ml of 1.0 <u>M</u> basic TMAB solution with 30 ml of a basic solution of 0.02 <u>M</u> NaCl-1.0 <u>M</u> TMAB. Tetramethylammonium hydroxide was used to obtain the basic pH. The above procedure gave a potential-sodium ion concentration calibration curve. Then 20 ml of the 0.015 <u>M</u> basic solution of NaCl were titrated with 20 ml of basic PA at an ionic strength of 1.0. In these conditions, the highest mole ratio of PA to sodium ion attained was 10. These titrations were performed in the Faraday cage.
- 2.7.3. <u>pH MEASUREMENTS</u> Since laboratory distilled water is contaminated with a small amount of morpholine (morpholine distills with water), tap water 2 x 10^{-2} <u>M</u> in KMnO₄ and 2 x 10^{-2} <u>M</u>

in KOH was distilled. This distilled water was boiled for at least 15 minutes to expell the carbon dioxide, and then cooled down and kept under nitrogen. The distilled water obtained had a conductance corresponding to 1 ppm of sodium ion equivalent, and had a neutral pH.

A purified stock solution of 6 \underline{M} HCl was prepared by the distillation of an approximately 6 \underline{M} HCl solution under atmospheric pressure. A 7 x 10^{-2} \underline{M} stock solution was prepared from the 6 \underline{M} solution, and titrated in the usual way against Na₂CO₃, with bromocresol green as indicator. A further dilution brought the concentration down to 7 x 10^{-4} \underline{M} . This last solution was used to calibrate the pH electrode. The amount of PAA required for each titration was weighed on a CAHN model 4100 microbalance.

The stock solution of citric acid had to be standardized against Na₂CO₃ with phenolphthalein as indicator, since a titration of a known amount of citric acid monohydrate gave an equivalent weight slightly smaller than the theoretical one. The magnesium bromide stock solution was standardized with EDTA in the usual manner.

When PAA alone or citric acid were titrated, 30 ml of $7 \times 10^{-4} \, \underline{\text{M}}$ HCl at the working ionic strength were used for the calibration of the electrode and 14 points were obtained at 30-second intervals with a current setting of 5 mA. The titration was stopped before the end point (at approximately 390 seconds) in order to remain in the acidic medium. This way a plot of potential vs proton concentration and not activity was obtained.

Then, without removing the electrode of the solution, 5 ml of 4.9×10^{-3} PAA was added, and the solution was titrated coulometrically. Data were collected at 25-second intervals. The equivalence points in this last titration were determined by the first derivative method. It has been found that taking the electrode out of solution to rinse it and putting it back in another solution can give rise to a change of up to 0.4 mV in potential reading.

It was often found that the experimental final end point corresponding to the titration of HCl and the weak acid was off compared to the calculated value. However, the experimental elapsed time between two equivalence points of the weak polyacid was always equal to the calculated value (determined from the number of equivalents measured with the microanalytical balance).

When the complexation of PAA with a metal ion was studied, the amount of metal ion necessary for the titration was present in the calibrating solution. The concentration of metal ion was 7×10^{-4} M except for sodium ion which was 2.8×10^{-2} M.

When work was done at different temperatures, the volumes of solution used were corrected by using the values given in the CRC Handbook (112). The temperature of the solution was measured and kept constant to \pm 0.1°C.

2.8. DATA HANDLING

Extensive use was made of the CDC 6500 computer, with several programs: MINIQUAD 76A for the PAA titrations, and KINFIT4 for the calibration of the electrode and the sodium-23 NMR measurements with 12-crown-4 (see Appendices B and C).

CHAPTER 3

RESULTS AND DISCUSSION

3.1. ACIDITY STUDIES OF PAA

- 3.1.1. SPECTROSCOPIC STUDIES OF PAA It has been reported in the literature (74) that in the deprotonation of PAA, the first proton results from the dissociation of the acetic acid group, while the last two protons come off the phosphoric acid moiety. The pK's of phosphoric and acetic acid are 2.15, 7.20, 12.40 and 4.75, respectively, while the ones of PAA are approximately 1.5, 5 and 8 (see p 97). Therefore, intuitively one would correlate the second pK of PAA to the acetic acid function.
- 3.1.1.1. <u>Phosphorus-31 and Proton NMR</u> The proton NMR spectrum of the free acid in D_2O consists of a doublet at 2.964 and 3.082 ppm, with a coupling constant of 21.2 Hz. The signal is split due to a J_{P-H} coupling. No signal was observed for the acidic protons, due to the fast exchange between the deuterium of the solvent and the protons.

A phosphorus-31 NMR spectrum of 0.3 $\underline{\text{M}}$ PAA consists of three peaks because of the coupling between P and the two protons on the neighboring carbon. The coupling constant has a value of 21.0 \pm 0.5 Hz, in good agreement with the value obtained from proton NMR measurements. The chemical shift of the middle peak, referenced to 85% H₃PO₄ is -16.0 ppm at pH 1.0. Since it has been found that PA forms a weak complex with the sodium ion, in the study of the change in phosphorus-31 chemical shift $\underline{\text{vs}}$ pH, the latter was adjusted with tetramethylammonium hydroxide.

The result of this study is shown in Figure 12. An upfield shift (to -13.2 ppm at pH 3.2) is followed by a downfield one (to -16.5 ppm at pH 6.5) and a final upfield shift (to -13.3 ppm for pH 10.5). At pH above 10.5, the phosphorus-31 chemical shift does not change. These results are in good agreement with the results of Riess et al. (67), who reported a chemical shift of -13.3 ppm for a PAA solution at pH 14.

A comparison of the change in chemical shift to the distribution of PAA species at different pH values (see Figure 13) shows that the chemical shift change seems to be related to the removal of the different protons. It seems quite reasonable to relate an upfield shift to the removal of a proton closely related to the phosphorus.

Crutchfield et al. (113), however, found a downfield shift of 0.5, 3.0 and 2.5 ppm, respectively, for each deprotonation step of H_3PO_4 . Jones and Katritzky (114) observed the same results and stated that it was not clear whether shielding of the phosphorus in the species H_3PO_4 , $H_2PO_4^-$, HPO_4^{2-} and PO_4^{3-} would increase with the ionization (because of the increasing charge) or decrease (because of distribution of the same number of electrons over a larger volume as a consequence of expansion).

It has been found that phosphorus-31 chemical shift is related to \underline{p} or \underline{s} electrons in 90% of the cases and to \underline{d} electrons in the remaining 10%.

In a series of papers and books (115-118), Letcher and van Watzer formulated a quantum mechanical derivation of the phosphorus-31 chemical shifts using \underline{s} , \underline{p} and \underline{d} orbitals and allowing full latitude in the π bonding. This has been accomplished by using an

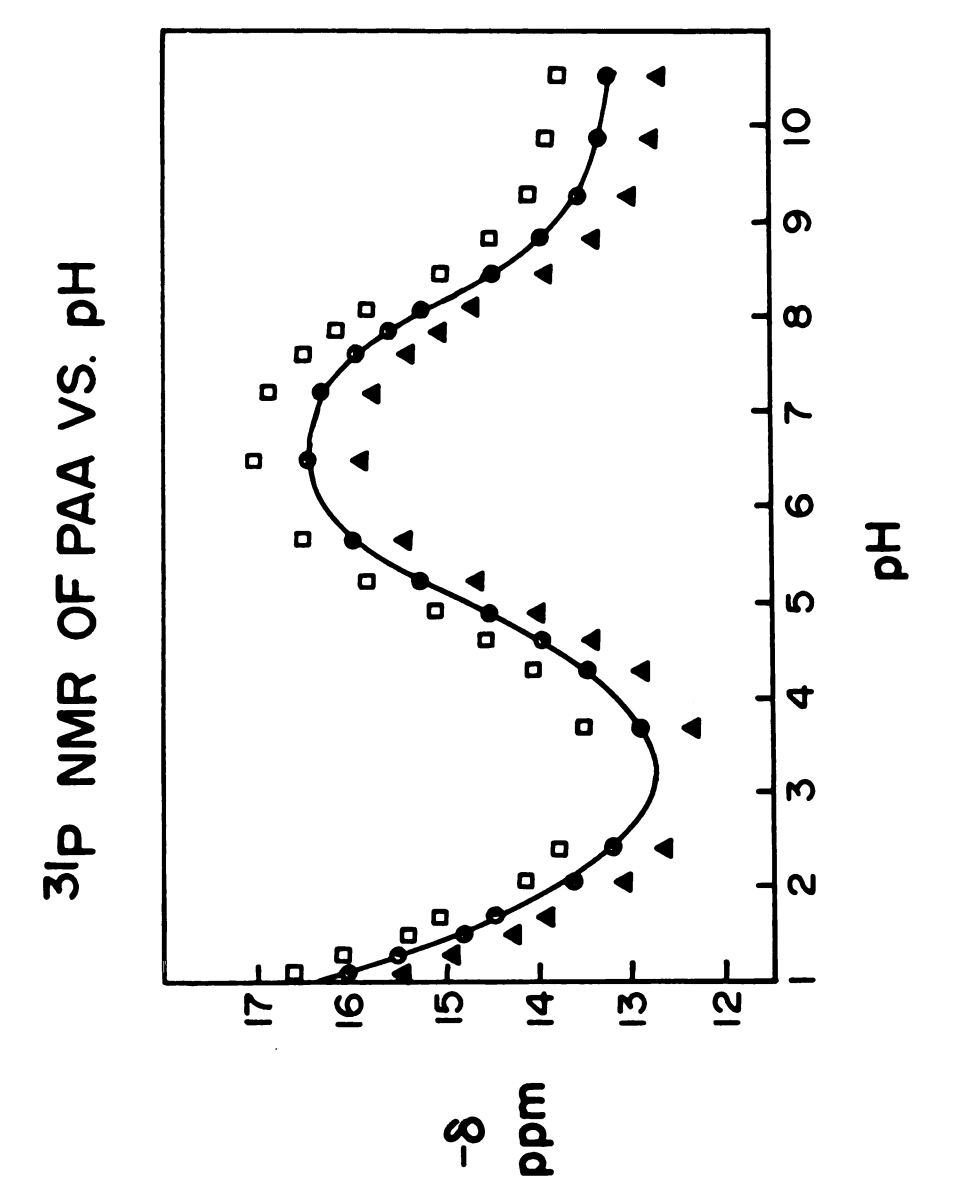


Figure 12. Phosphorus-31 Chemical Shift of 0.3 M PAA vs pH.

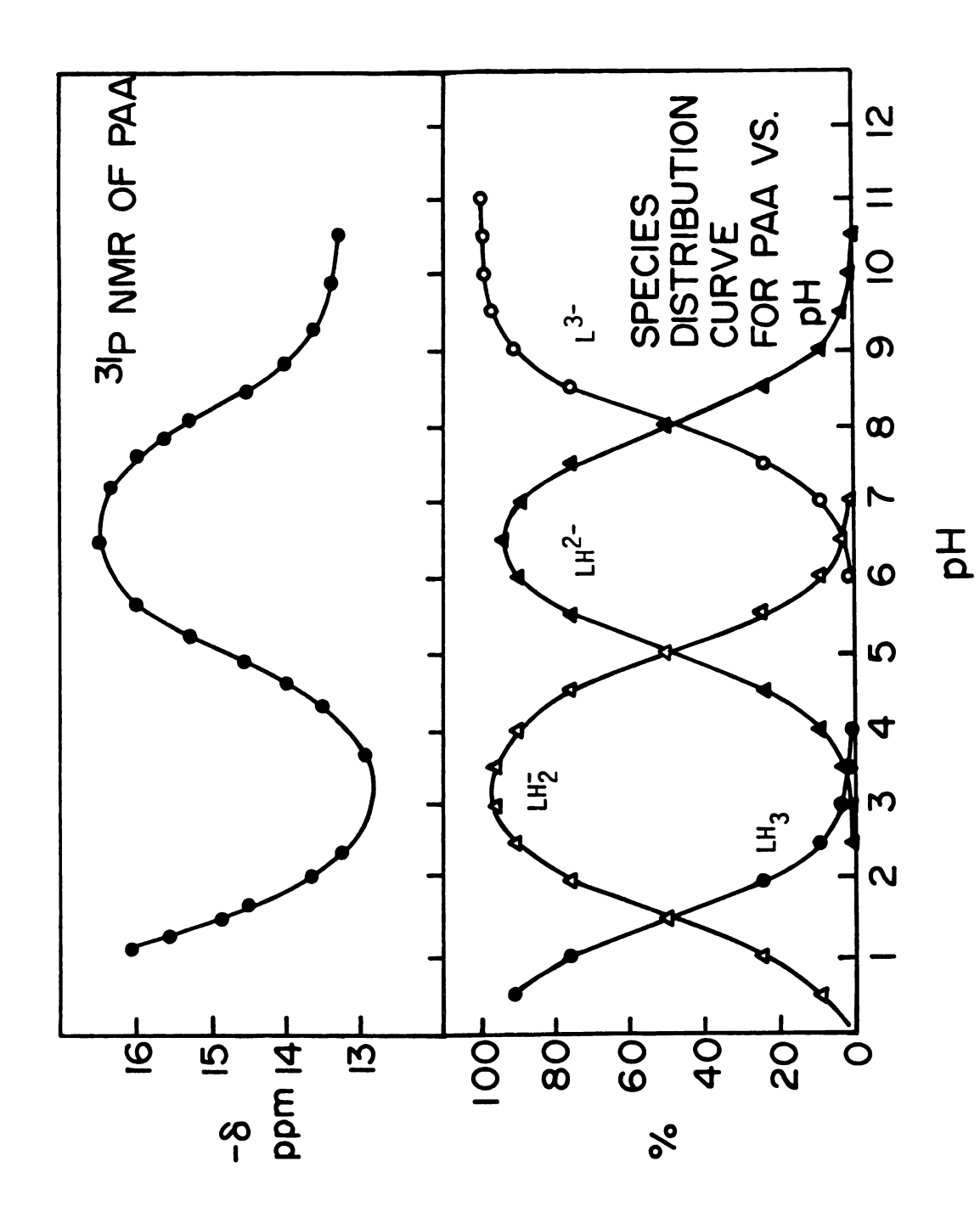


Figure 13. Comparison of the Phosphorus-31 Chemical Shifts and the Species Distribution of PAA vs pH.

artificially chosen coordinate notation which allows the chemical shift expression to be stated in a particularly simple functional form, using a minimum number of hybridization parameters. This derivation has been applied to several forms of molecules, including molecules of the MPZ₂T type.

According to this derivation, the chemical shift may be treated as the summation of σ -bond and π -bond contributions. The distinction made between σ and π bonding is that σ molecular orbitals involve only \underline{s} and \underline{p} orbitals while \underline{d} orbitals alone are involved in the π bonding. Moedritzer (119) further developed the quantum derivation of Letcher and van Watzer, and applied it to the case of the chemical shift change of a series of oxyacids of phosphorus \underline{vs} pH.

Thus, for molecules in which the phosphorus has a coordination number of 4, the phosphorus-31 chemical shift is comprised of a σ -bond contribution determined solely by the <u>p</u>-orbital occupation and a π -bond contribution corresponding to <u>d</u> orbitals only. The chemical shift can be expressed as:

$$\delta = \delta_0 + \delta_\sigma + \delta_\pi \tag{9}$$

where δ is the chemical shift referenced to 85% H_3PO_4 , δ_0 is the absolute chemical shift of the reference standard and δ_σ and δ_π are the σ and π contributions, respectively.

The theory showed that δ_π is negative and is proportional to the increase in total occupation of the d_π orbitals of the phosphorous, being independent of the distribution of this total character among the various bond. For P atoms having 4 neighbors, δ_π = -147n $_\pi$, where n $_\pi$ is the total number of electrons in the d $_\pi$ orbitals of

the phosphorous atom being viewed by phosphorus-31 NMR. On the other hand, the \underline{p} -orbital occupation was treated in terms of several parameters: the angular geometry, consisting of the molecular symmetry and bond angles, and the polarity of the bonds.

Moedritzer then proposed that the change in phosphorus-31 chemical shift could be expressed as the sum of small variations in: 1) the effective electronegativity of the neighboring oxygens due to association of hydrogen, 2) the bond angles and 3) the total occupation of the \underline{d} orbitals. Therefore, according to Moedritzer, equation (9) becomes:

$$\Delta \delta = C \Delta \chi_0 - 147 \Delta n_{\pi} - A \Delta \theta \tag{10}$$

where $\Delta\chi_0$ is the change in the effective electronegativity of the oxygens caused by their association with the hydrogen(s), n_π is the change in the total number of electrons in the d_π orbitals of the phosphorous induced by variations in the character of the P-O bond brought about by hydrogen association, $\Delta\theta$ is the increase in OPO bond angle caused by association of the hydrogen, and A and C are numbers which may vary from one oxyacid to another.

In the case of PAA we can write equation (10) slightly differently:

$$\Delta \delta = C \Delta \chi_0 + B \Delta \chi_R - 147 \Delta n_{\pi} - D \Delta n_{\pi}^R - A \Delta \theta$$
 (11)

where B and D are constants, $\Delta\chi_R$ reflects the change in electronegativity of the organic group (acetic acid group presently), Δn_π^R corresponds to the change in P-O π bond from rearrangement of π electrons, and the other terms have been defined previously.

Upon protonation of the phosphoric acid moieties, we have an increase in electronegativity of the corresponding oxygen atom, corresponding to a positive contribution to the chemical shift. On the other hand, we also have feedback of π electrons from the P-O bond onto the phosphorus resulting in an increase in π electrons and a negative contribution to the chemical shift. The change in bond angle has not been considered here and is probably not completely negligible although of minor contribution.

According to the theory developed by Moedritzer, in the case of phosphonic acids, we must have a larger contribution to the chemical shift from the feedback mechanism than from the change in polarity (while the opposite is true for the $\rm H_3PO_4$ case). No quantitative evaluation of each term has been done so far, and the above argumentation explains why the above theory of phosphorus-31 NMR chemical shift has been referred to as a "tug of war" (118), but the theory fits our experimental results.

Studies performed by Riess et al. (67) showed that although the terms involving changes in n_{π}^R or θ are not negligible, they are much smaller than the contribution of the electronegativity of the carboxyl group. Furthermore, no π bonding is involved in the P-CH₂ bond, and the effect of the rearrangement of the π electrons around the P-O π bonds due to change in electron distribution of the CH₂ group is most probably negligible. We can also assume that the change in $\Delta\theta$ (0-P-O angle) upon protonation of the acetic acid moiety which is at the other end of the molecule is negligible.

By bonding a proton to the carboxylic group, the electronegativity of the related oxygen increases, thus increasing the electronegativity of the two carbons [corresponding to a decrease in p-electrons, as shown by ¹³C NMR (see below)] which corresponds to a positive contribution to the chemical shift as shown in equation (11). This formalism also applies to the replacement of the acetic acid moiety by the formic acid moiety as shown in Part II.3.3.1.

No conclusion can be drawn from the change of the coupling constant J_{P-H} vs pH because of the precision of the measurements when J_{P-H} is determined from ^{31}P NMR spectra. Whatever is the change, it will be small anyway since J_{P-H} changes between 19.5 and 21.5 Hz with a precision of ± 0.5 Hz. The value is as expected (118) for the P-H coupling through an intermediate nucleus, i.e., between 15 and 25 Hz. On the other hand, the line-width of the central peak changes from 3 Hz at pH 1.0 to 8 Hz at pH 6.0 and back down to 3 Hz at pH 9.0.

A study of the chemical shift of phosphorus-31 in the free acid \underline{vs} concentration shows an upfield shift from -16.4 ppm at 1.0 \underline{M} to -13.3 ppm at 10^{-2} \underline{M} . If we again take a pK₁ of 1.5, a simple calculation shows that a 1.0 \underline{M} solution of PAA contains 84% of triprotonated acid, while a 10^{-2} \underline{M} solution contains 80% of diprotonated acid. According to Figure 13, the chemical shift should then be below -16 ppm, and at -13.3 ppm for the 1 \underline{M} and 10^{-2} \underline{M} solutions, respectively, in good agreement with the experimental results.

3.1.1.2. Carbon-13 NMR - Of more interest for the pK-acidity function correlation is the study of the change in

carbon-13 NMR chemical shift and J_{p-C} coupling constant \underline{vs} pH. Generally speaking, an upfield shift for any NMR measurement can be related to an increase in \underline{s} (diamagnetic) electron density or a decrease in \underline{p} (paramagnetic) electron density. As a rule, shifts in carbon-13 NMR are mostly related to \underline{s} electron density. However, the PAA case is slightly different, and resembles the studies performed on the deprotonation of carboxylic acids.

Upon deprotonation, the carbon-13 NMR chemical shift of the carboxylic carbon moves downfield by approximately 5 ppm, due to a decrease of the electronegativity of the oxygen, which corresponds to an increase in \underline{p} electron density around the oxygen atom and, therefore, around the carbon. The decoupled carbon-13 NMR spectrum of 0.4 \underline{M} aqueous PAA shows two doublets, corresponding to the $\underline{C}00H$ and the $\underline{C}H_2$ carbons (at 172.8 and 173.1 ppm, and 34.4 and 40.7 ppm, respectively at pH 1.0). The doublets correspond to the P-C coupling, with a larger coupling constant for the carbon closer to the phosphorus. Figure 14 shows the change in chemical shift \underline{v} s pH for one of the peaks of the $\underline{C}H_2$ carbon signal, and the values for the four peaks are listed in Table V.

As expected, we have a downfield chemical shift. When the pH is increased, however, the change starts with the removal of the phosphoric acid proton, and the overall change corresponding to the removal of the three protons is 7.5 ppm for the $\underline{\text{C}00\text{H}}$ carbon signals, and 6.2 and 5.5 ppm for the $\underline{\text{CH}}_2$ carbon peaks. In this case, again, the pH was adjusted with tetramethylammonium hydroxide.

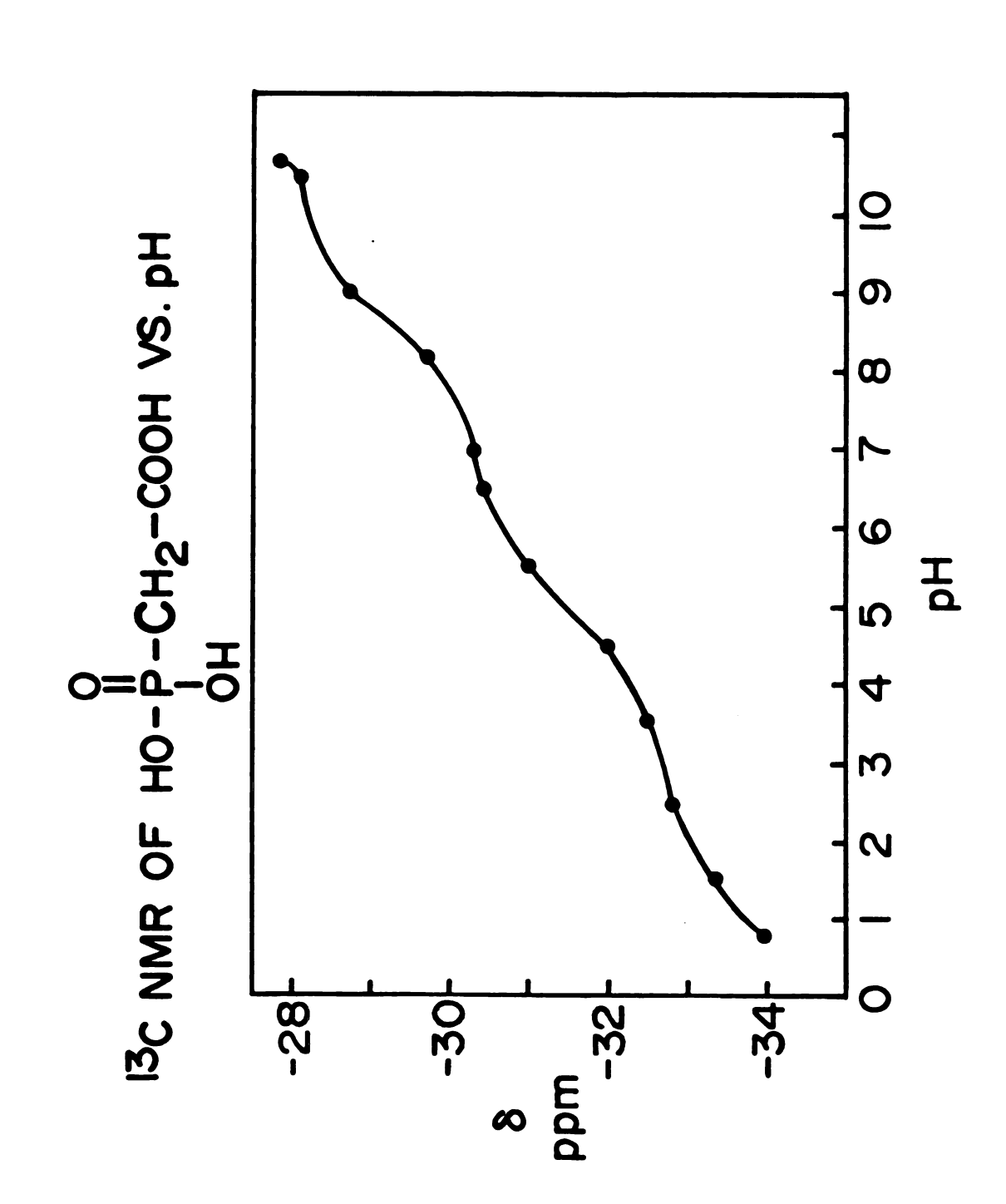


Figure 14. Carbon-13 Chemical Shift (Referenced to Dioxane, Which is 68.1 ppm Downfield of TMS) of the $\underline{\text{CH}}_2$ Carbon of 0.7 $\underline{\text{M}}$ PAA $\underline{\text{vs}}$ pH.

84

Table V. Carbon-13 Chemical Shift of 0.7 \underline{M} PAA \underline{vs} pH

рН 0.76	<u>с</u> оон		<u>C</u> H ₂	
	173.0	172.7	40.4	34.2
1.48	173.7	173.4	40.9	34.8
2.44	174.4	174.0	41.3	35.4
3.51	174.7	174.5	41.6	35.7
4.46	175.4	175.1	42.1	36.2
5.47	176.8	176.5	43.1	37.2
6.45	177.6	177.3	43.7	37.7
6.93	177.7	177.4	43.8	37.9
8.11	178.3	178.1	44.3	38.4
8.95	179.4	179.1	45.2	39.4

On the other hand, if we consider the J_{C-P} coupling constant for the $\underline{C}H_2$ carbon (see Figure 15), we have a decrease in J_{C-P} from 125.5 to 118.3 Hz for a change in pH from 0.8 to 4.0 followed by a slight increase from 118.3 to 119.5 Hz (pH changes from 4.0 to 6.5) and a final decrease from 119.5 to 112.2 Hz when the pH is brought to 10.6.

The J_{C-H} coupling constant has been related by quantum mechanical calculation to the <u>s</u> electron density around the carbon and the hydrogen (120), an increase in the electronic density corresponding to an increase in J_{C-H} . From this assumption, several authors (121, 122) related the J_{P-C} value to the <u>s</u> electron density around the carbon. On the other hand, Tebby (123) reported that the effects of electronegative substituents on coupling are different for phosphorous and carbon. Either they do not increase the <u>s</u>-character of the remaining bonds, or another factor such as π -bonding is introduced.

Because of the numerous variables and unknowns concerning the chemical shift and specially the J_{C-P} coupling constant (very little work has been published on that matter and the theory is still missing at the present time, presumably because of the lack of data), it seems unrealistic to try to explain the shape of the J_{P-C} vs pH curve quantitatively. Qualitatively, it seems reasonable to relate the two decreases in the J_{P-C} coupling constant to the deprotonation of the phosphoric acid moieties.

In conclusion, we have correlated the second pK of PAA to the acetic acid moiety in the molecule. The change in direction of the phosphorus-31 NMR signal shift has been explained in terms of changes in the \underline{d} electron density around the phosphorus and of changes in electronegativity of the different substituents.

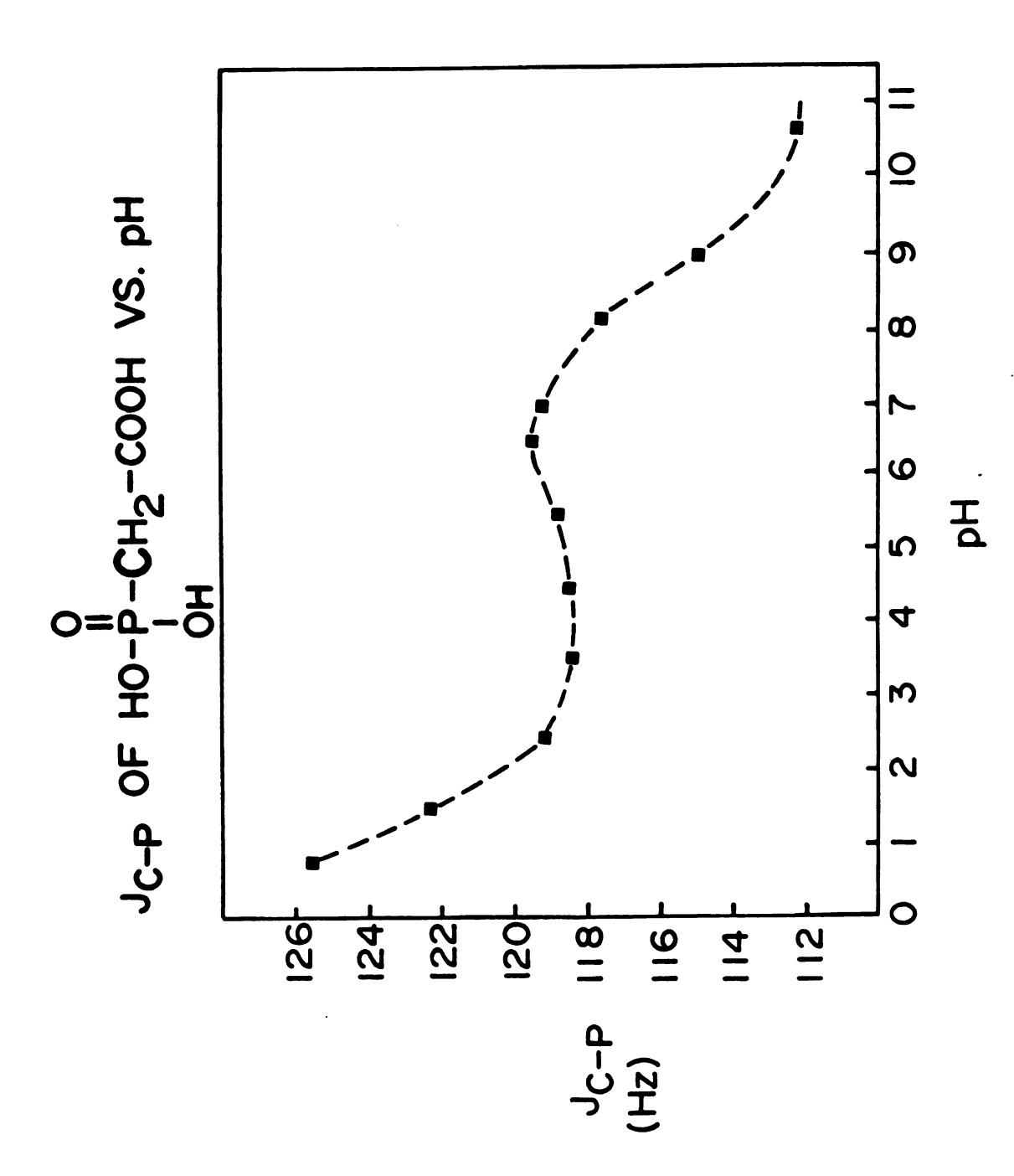


Figure 15. Change in J_{C-p} Coupling Constant of the \underline{CH}_2 Carbon of PAA vs pH.

3.1.2. <u>POTENTIOMETRIC STUDIES OF THE pK'S OF PAA</u> - Once the pK's of PAA assigned to the different acidity functions, it was of interest to determine precisely the pK's of PAA at low ionic strength and to get the thermodynamic values by extrapolation to zero ionic strength.

It was decided to determine these values from measurements performed with a pH electrode, however, because of the reported complexation (72, 73) between phosphate ions of various types and the sodium ions, it was decided to use a much bulkier cation for the base and the supporting electrolyte, i.e., the tetramethylammonium ion. Some titrations have been performed with tetramethylammonium hydroxide as a base, but since the tetramethylammonium hydroxide commercially available is an approximately $1 \, \underline{M}$ solution, problems occurred due to the presence of carbonate ions in the base which interfered with the determination of the pK's of PAA (CO_2 cannot be removed in a solution with a pH above 7.5 by degassing). Moreover, the commercial product from Eastman contained a precipitate soluble in acid.

Attempts to synthesize the base in the laboratory by ion exchange resins were not successful. The use of a cation exchange resin resulted in incomplete exchange of the sodium ion, while the use of an anion exchange resin resulted in only partial exchange of the bromide ion. For these reasons, it was decided to generate the base electrically with a home-built coulometer.

3.1.2.1. <u>Coulometric Titrations</u> - The advantages of that method are the elimination of the preparation and handling

of a multiplicity of standard solutions, the increase in the precision in the amount of titrant used, and in the purity of the titrant since the solvent is used to generate it.

The reactions involved in the electrode processes are:

$$2 H_3 0^+ + 2 e^- \qquad \stackrel{?}{\leftarrow} H_2 + 2 H_2 0$$
 (12)

2
$$H_30^+ + 2 e^ \stackrel{?}{\leftarrow}$$
 $H_2 + 2 H_20$ (12)
2 $H_20 + 2 e^ \stackrel{?}{\leftarrow}$ $H_2 + 2 OH^-$ cathodic reactions (13)
4 $OH^ \stackrel{?}{\leftarrow}$ $O_2 + 2 H_2O + 4 e^-$ (14)

$$^{+}$$
 $^{+}$ $^{-}$ $^{+}$ $^{-}$ $^{-}$ $^{+}$ $^{-}$ $^{-}$ $^{-}$ $^{-}$ (14)

6 H₂0
$$\stackrel{?}{\downarrow}$$
 0₂ + 4 H₃0⁺ + 4 e reactions (15)

$$0_2 + 2 H_3 0^+ + 2 e^- + H_2 0_2 + 2 H_2 0$$
 (16)

$$0_2 + 2 H_2 0 + 2 e^{-} + H_2 0_2 + 2 OH^{-}$$
 (17)

$$H_2O_2 + 2H_3O^+ + 2e^- + 4H_2O$$
 (18)

$$H_2^0_2 + 2 e^- \qquad \stackrel{\rightarrow}{\leftarrow} 2 OH^-$$
 (19)

As can be seen from the last four equations, oxygen must be removed from the solutions to prevent formation of $\mathrm{H}_2\mathrm{O}_2$ and unwanted cathodic reactions. In order to keep the solutions free from oxygen, they were kept under nitrogen atmosphere as explained in the experimental part. In nonbasic conditions, the anodic reaction will generate protons.

Since the mobility of proton through the membrane separating the anodic and cathodic compartments is much larger than the mobility of the tetramethylammonium ion, this would result in pollution of the solution by an acidic impurity. To remedy that problem as well as to decrease the ohmic resistance of the system, concentrated (0.2 to 0.5 M) solutions of the supporting electrolyte tetramethylammonium bromide were used in the anodic compartment. The anodic reactions then become:

$$Br^{-} \neq 1/2 Br_{2} + e^{-}$$
 (20)

In these conditions, the increase in negative charges due to the formation of base in the cathodic compartment is counterbalanced by a flow of tetramethylammonium ions through the membrane (the membrane is impermeable to the solvent).

As mentioned previously (see Part II.2.2.7.3.), a titration of 7 x 10^{-4} M HCl at the working ionic strength is first performed. The EMF of the cell:

Glass electrode//Acid solution, 7 x 10^{-4} \underline{M} at/Thallium amalgam constant ionic strength reference electrode

is:
$$E = E^{\circ} + \frac{RT}{F} \ln [H^{+}] + E_{i} + E_{asym} + \frac{RT}{F} \ln \gamma_{H}^{+}$$
 (21)

where E° is the standard potential referred to the thallium amalgam reference, R, T and F have their usual meaning, E_{j} is the junction potential, E_{asym} is the asymmetry potential and $\gamma_{H}+$ and $[H^{+}]$ are the activity coefficient and the concentration of the hydrogen ion. At a constant ionic strength, the E_{j} and E_{asym} potentials as well as the activity coefficient of the hydrogen ion are assumed to be constant. Therefore, the EMF of the cell can be expressed as:

$$E = E^{\circ}' + \frac{RT}{F} \times 2.303 \log [H^{+}]$$
 (22)

Using the computer program PHCALIB-KINFIT4 (see Appendix B), the experimental points are fitted to the equation:

E = intercept + slope x log ([H⁺]₀ -
$$\frac{t \times i_0}{F \times v_0}$$
 + residual) (23)

where $[H^+]_0$ is the initial concentration of HC1 (7 x 10⁻⁴ M), i_0 is the intensity of the current used to generate the base in mA, t is the time during which the base is generated in seconds, and v_0 is the volume of acid in ml. Residual is a concentration

of acid or base impurity that could be present in the solution. Initially, the three terms intercept, slope and residual were refined, but it was found that the last two terms are coupled. Since the temperature of the solution is constant to 0.1°C, and pH glass electrodes are known to have nernstian response, the slope term was calculated from the solution temperature and kept constant, and only the two other terms were refined.

Once the calibration of the electrode is performed, and in order to keep the junction and asymmetry potentials as constant as possible, the acid to be titrated is added without removing the electrode from the solution.

Using this procedure, citric acid was titrated at an ionic strength of 0.1 by tetramethylammonium bromide (TMAB). The pK's obtained are shown in Table VI and compared to literature values. As can be seen the agreement is quite good when compared to the tetramethylammonium chloride supporting electrolyte case (the largest difference between the two sets of values is 0.11 pK units and the smallest 0.01).

3.1.2.2. pK's of PAA - The pK's of PAA were then determined at different ionic strength. The data reduction was performed by using the computer program MINIQUAD 76A (see Appendix C for an explanation of the data handling) and the three following expressions of the K's:

$$K_1 = [LH_2^-] [H^+]/[LH_3]$$
 (24)

$$K_2 = [LH^-][H^+]/[LH^-]$$
 (25)

Table VI. Acidity Functions of Citric Acid at Ionic Strength 0.1.

Temperature (°C)	Medium	рК	pK ₂	pK ₃	Reference
20	KC1	2.96	4.39	5.67	a
20	KC1	3.08	4.39	5.49	b
25	KNO ₃	2.79	4.30	5.65	С
25	KNO3	2.92	4.39	5.72	d
25	KNO3	3.04	4.47	5.80	d
20	NaClO ₄	2.87	4.35	5.68	е
20	NaClO ₄	2.96	4.38	5.68	f
30	NaNO ₃	2.94	4.44	5.82	g
25	(Me) ₄ NC1	2.88	4.36	5.84	h
25	(Me) ₄ NBr	2.89	4.32	5.78	this work

^aA. Okac and Z. Kolarik, Collect. Czech. Chem. Commun., 24,1 (1959)

bK. K. Tripathy and R. K. Patnaik, J. Indian Chem. Soc., 43, 772 (1966)

^CK. S. Rajan and A. E. Martell, Inorg. Chem., 4, 462 (1965)

dT. N. Briggs and J. E. Stuehr, Anal. Chem., 47, 1916 (1975)

^eE. Campi, G. Ostacoli, M. Meirone, and G. Saini, J. Inorg. Nuclear Chem., 26, 553 (1964)

fc. F. Timberlake, J. Chem. Soc., 5078 (1964)

^gR. C. Warner and I. Weber, J. Am. Chem. Soc., 75, 5086 (1953)

hS. S. Tate, A. K. Grzybowski, and S. P. Datta, J. Chem. Soc., 3905 (1965)

$$K_3 = [L^{3-}][H^+]/[LH^-]$$
 (26)

The relationship between the concentration and thermodynamic

formation constant is for K_3 :

$$K_3^{t} = K_3^{c} \frac{\gamma_L^{3-\gamma_H^{+}}}{\gamma_{IH}^{2-}}$$
 (27)

by using the Guntelberg modification of the Debye-Huckel equation:

$$\log \gamma_n = - A Z_n^2 \sqrt{I}/(1 + \sqrt{I})$$
 (28)

with

$$A = \frac{1.823 \times 10^6}{(\varepsilon T)^{3/2}}$$
 (29)

we can rewrite equation (28) as

$$pK_{3}^{c} = pK_{3}^{t} - A \left(Z_{L}^{2} + Z_{H}^{2} - Z_{LH}^{2}\right) \sqrt{T}/(1 + \sqrt{T})$$

$$pK_{3}^{c} = pK_{3}^{t} - 6A \sqrt{T}/(1 + \sqrt{T})$$
(30)

Similarly we have:

$$pK_{2}^{c} = pK_{2}^{t} - 4A \sqrt{I}/(1 + \sqrt{I})$$
 (31)

$$pK_1^C = pK_1^{t} - A \sqrt{T}/(1 + \sqrt{T})$$
(32)

Half-way between the second and third equivalence points we have:

$$[TMA_{b}^{\dagger}] = 2.5 [PAA]$$
 (33)

with $[TMA_b^+]$: concentration of tetramethylammonium ion corresponding to the formation of the equivalent amount of base, on the other hand:

$$[LH^{-}] = [L^{3-}] = 1/2[PAA]$$
 (34)

therefore, we have:

$$I = [S.E.] + 1/2 ([LH_2^-] + 2^2 [LH^-] + 3^2 [L^{3-}])$$

or $I \simeq [S.E.] + 4.5 [PAA]$ (35)

where [S.E.] is the concentration of supporting electrolyte. Similarly, at half-way between the first and second equivalence points:

$$I = [S.E.] + 2 [PAA]$$
 (36)

With a concentration of PAA: 7×10^{-4} M and a concentration of supporting electrolyte of 0.02, the change in ionic strength during the titration of the third acidity function corresponds to an increase of the ionic strength of 15%. This fact explains why the lowest ionic strength used was 0.02. On the other hand, at an ionic strength of 0.1, a 1 ppt acid or base impurity in the supporting electrolyte represents an error of 1.5% when referred to PAA. This factor itself limited the acid molarity to 7×10^{-4} minimum.

Several comments can be made about the use of equation (31). First, it has been shown that the validity domain of the Guntelberg equation extends to an ionic strength of approximately 0.1, and, therefore, the pK's of PAA were determined at ionic strength lower than that value. Second, when the Guntelberg equation is used, it is equivalent to the Debye-Huckel equation with a diameter of the solvated ion of 3.05 Å (at 25°C). Bates (124) proposed to use a value of 9 Å for the proton, but we have different ions which sizes are not directly available, and, therefore, the use of the Guntelberg equation seems to be a reasonable approach to the problem.

The computer program MINIQUAD 76A reduces the data by calculating the overall formation constants of the equilibria involved, and first starts by refining the pK_3 value, then the pK_2K_3 and finally the $pK_1K_2K_3$, therefore, the error in the value of this last term

is a cumulation of the error on each term. For this reason and because the first acidity of PAA is fairly strong (pK₁ \simeq 1.5), the extrapolation of the concentration values of pK₁ to zero ionic strength was not possible. The thermodynamic values of pK₂ and pK₃ are 5.11 \pm 0.04 and 8.69 \pm 0.05, respectively. The slope of the ionic strength plot is -0.942 and -2.98, respectively, while the theoretical values are -2.04 and -3.05 at 25°C. The thermodynamic plots and the corresponding values are shown in Figures 16 and 17, and Table VII.

A non-negligible factor in these potentiometric measurements is the fact that the glass electrode aged. At the end of a twomonth utilization period, pK values at different ionic strengths started to fall consistently below the straight lines of Figures 17 and 18 by 0.05 pK units. At the same time, the readings were becoming less stable (precision of \pm 0.2 or 0.3 mV instead of 0.1 mV). Upon replacement of the combined glass electrode by a new one, the pK values fell back on the line, and no more unstability problems were encountered. The EMF's recorded in two different buffers (acidic and basic) were 165.1/181.4 and -174.6/-155.6 mV for the new/old electrode. The calibration of the electrode is done in the acidic medium and the difference between the two electrode potentials increases from 16.3 to 19.0 mV from acidic to basic pH, or a change of 2.7 mV or 0.046 pK units, which corresponds to the pK difference experimentally observed between the two sets of data.

A species distribution plot at ionic strength 0.05 and 25°C is shown in Figure 18.

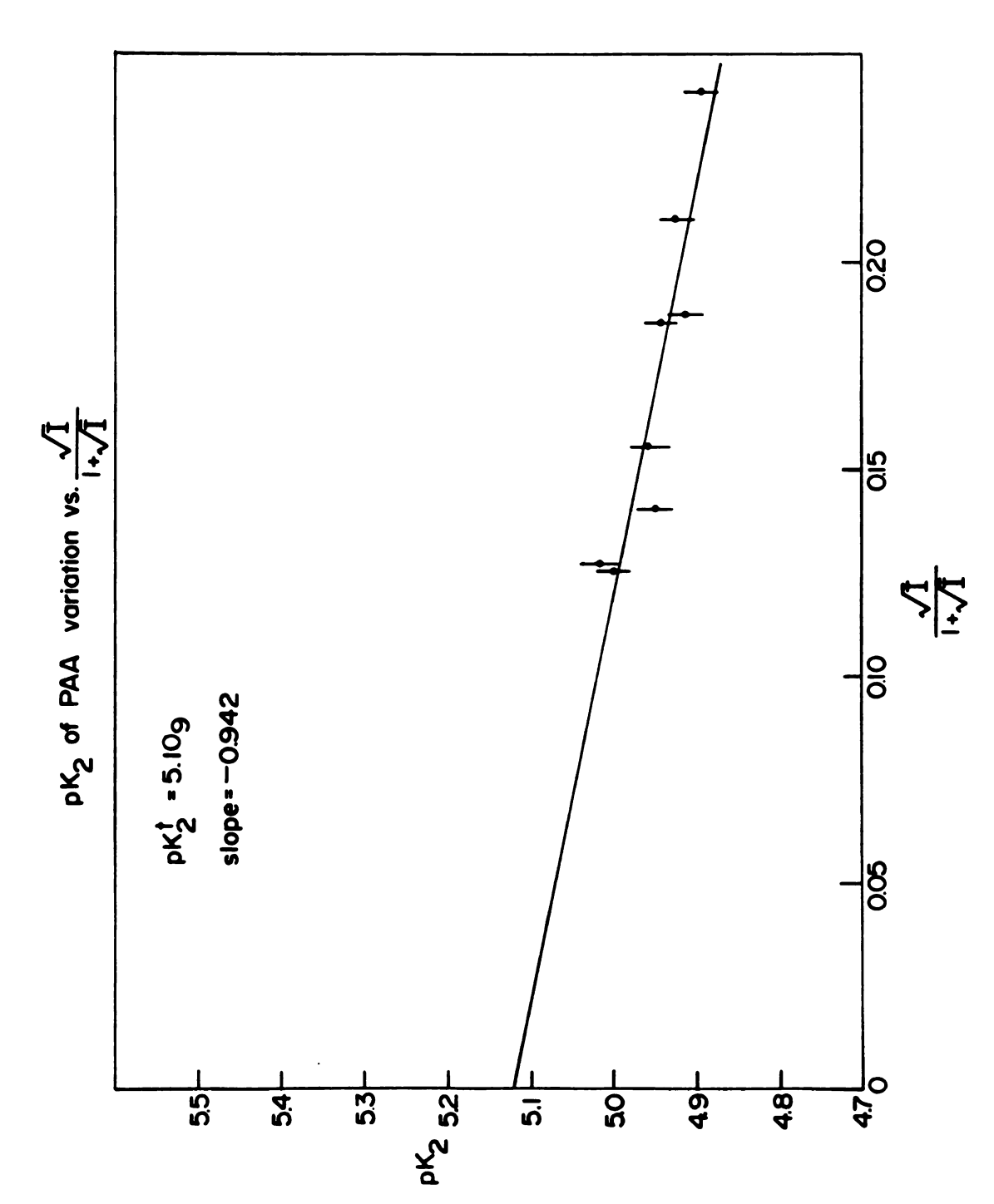


Figure 16. Plot of the pK2 of PAA vs Ionic Strength, the Line is a Linear Least Squares Fit.

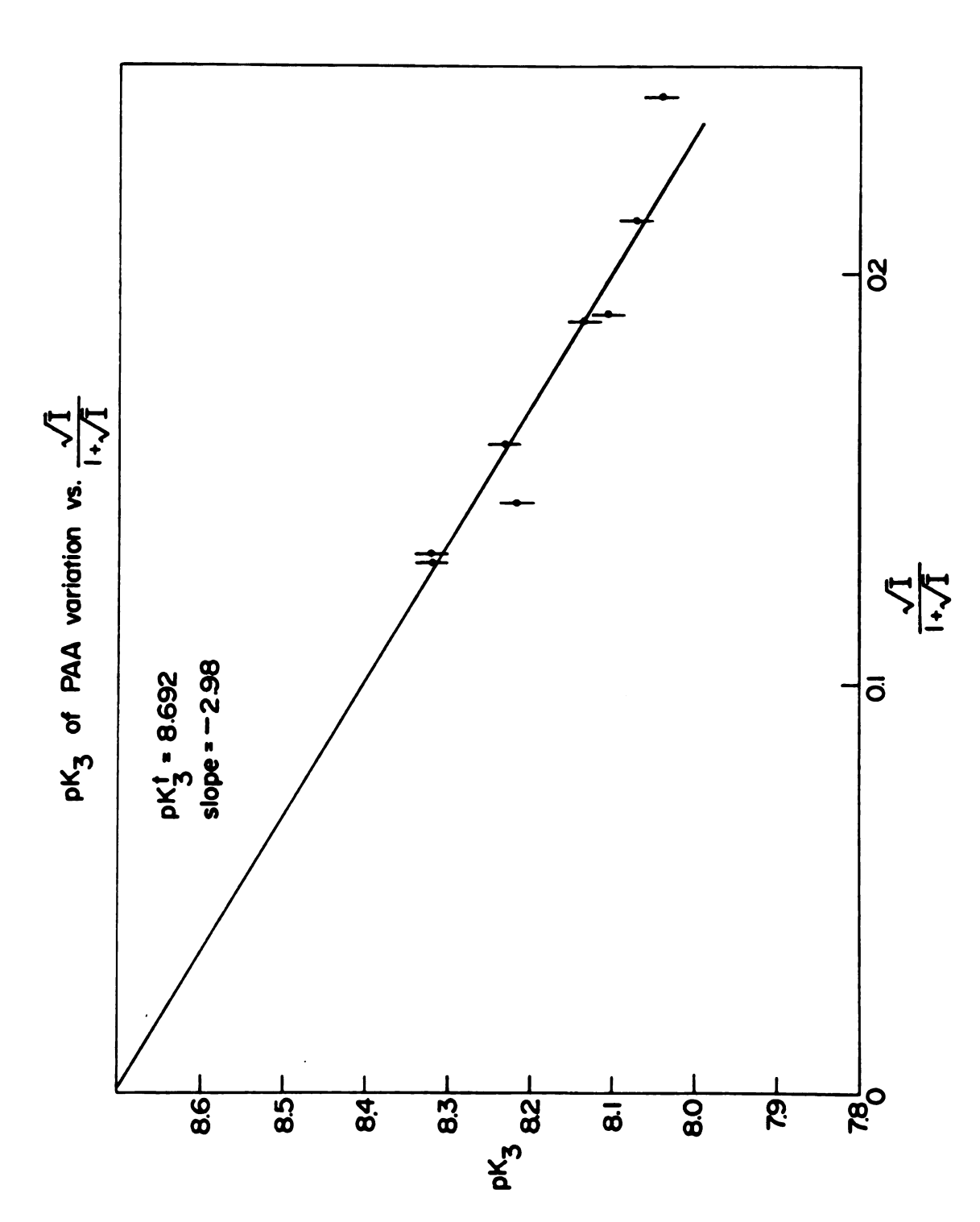


Figure 17. Plot of the pK $_3$ of PAA <u>vs</u> Ionic Strength, the Line is a Linear Least Squares Fit.

Table VII. Acidity Functions of PAA at Various Ionic Strengths at $25\,^{\circ}\text{C}$.

Ionic Strength x 10 ²	рКլ	pK ₂	pK3
9.95	2.26 ± 0.04	4.90 ± 0.02	8.04 ± 0.02
6.954	2.22 ± 0.04	4.93 ± 0.02	8.07 ± 0.02
5.144	1.97 ± 0.04	4.91 ± 0.02	8.11 ± 0.02
5.104	2.18 ± 0.04	4.94 ± 0.02	8.14 ± 0.02
3.224	2.01 ± 0.04	4.96 ± 0.02	8.23 ± 0.02
2.492	1.91 ± 0.04	4.95 ± 0.02	8.22 ± 0.02
1.963	2.13 ± 0.04	5.02 ± 0.02	8.32 ± 0.02
1.876	1.93 ± 0.05	4.99 ± 0.02	8.32 ± 0.02
0.00	≃ 2.0	5.11 ± 0.04	8.69 ± 0.05

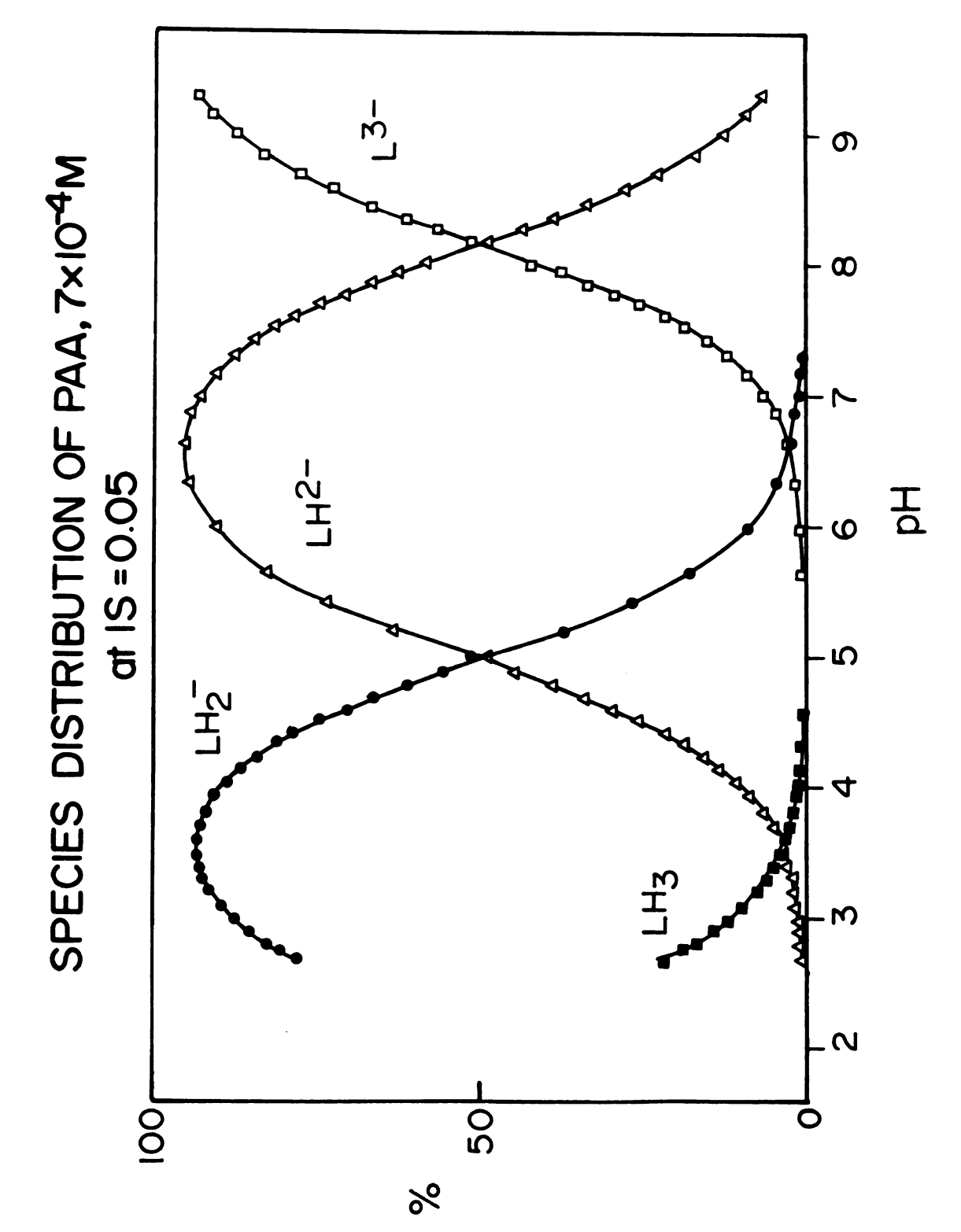


Figure 18. Species Distribution Plot of PAA at 0.05 Ionic Strength.

3.1.2.3. <u>Thermodynamics of Protonation</u> - The thermodynamic equilibrium constant K is related to the appropriate thermodynamic functions ΔG° , ΔH° and ΔS° by the relation:

$$-RT \ lnK = \Delta G^{\circ} = \Delta H^{\circ} - T\Delta S^{\circ}$$
 (37)

or:

$$1nK = -\frac{\Delta H^{\circ}}{RT} + \frac{\Delta S^{\circ}}{R}$$
 (38)

Thus, the slope and intercept of a plot of lnK \underline{vs} 1/T will provide us with the values of ΔH° and ΔS° , provided this plot is a straight line.

The values of the pK's were determined at an ionic strength of 0.05 at different temperatures, and the thermodynamic values at a given temperature were determined by using the Guntelberg equation. When the temperature changes, several parameters must be changed: the volume of solution used, measured at 22°C must be corrected for the expansion (contraction) of the solution with temperature, and, therefore, the ionic strength of the solution is also affected. It can be seen from equation (30) that ε and T are involved in the calculation of the activity coefficient, and since the change in temperature also involves a change in dielectric constant, corrections must be made.

The values of A at different temperatures were modified in the following way: the value for A at temperature T was extrapolated from the values given by Harned and Owen (125) and multiplied by the ratio of the experimental value of A obtained at 25°C (see Part II. 3.1.2.2.) over the theoretical value at that temperature. For the same reason as previously, ΔH° and ΔS° could only be determined for the second and third acidity functions. These determinations are shown in Figure 19 and the corresponding values are listed in Table VIII together with the corresponding values for acetic

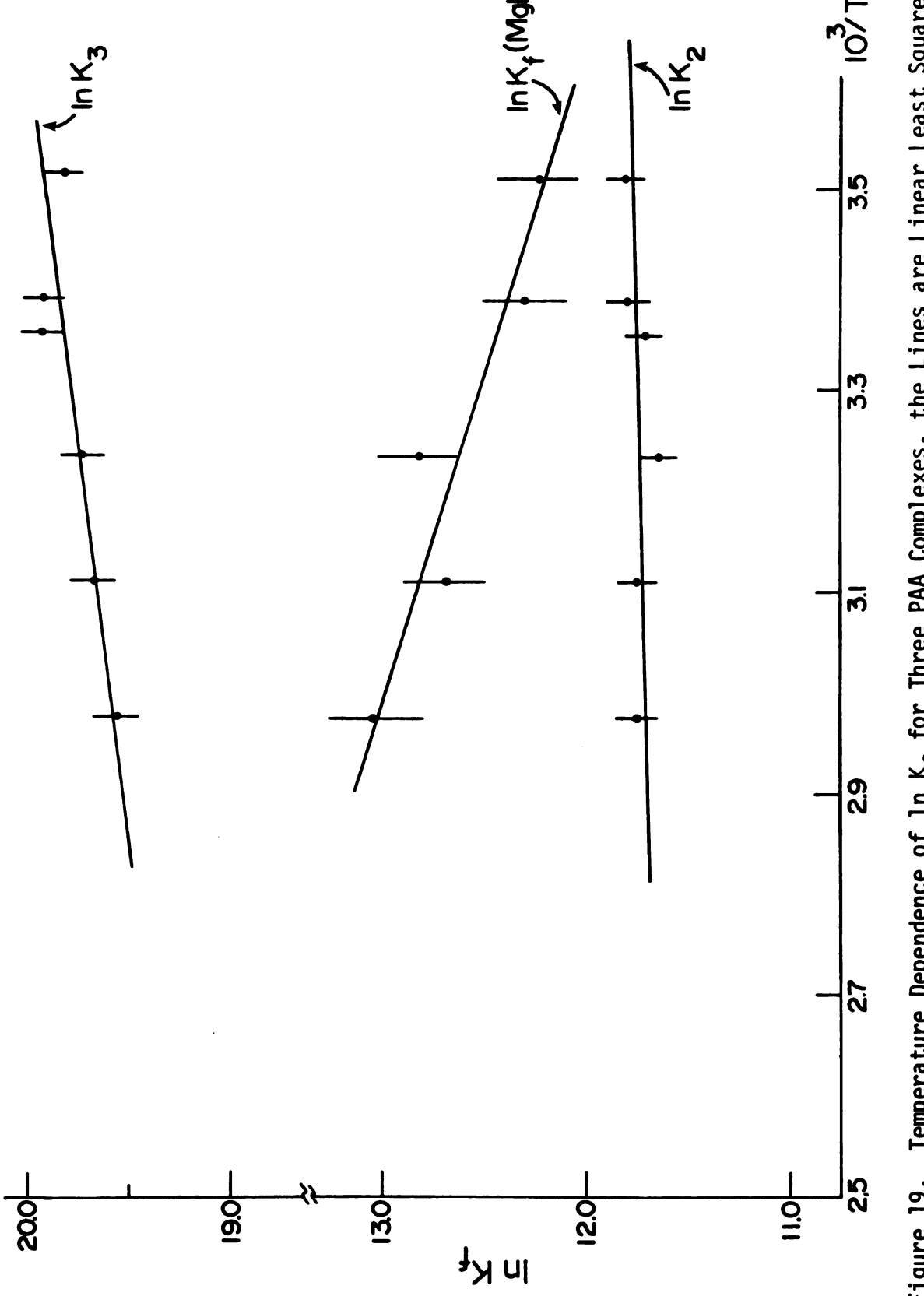


Figure 19. Temperature Dependence of ln $K_{\rm f}$ for Three PAA Complexes, the Lines are Linear Least Squares Fits.

Table VIII. Thermodynamic Quantities for Acid Association and for the Mg-PA Complex.

Complex	ΔH° (Kcal, mole ⁻¹)	ΔS° (cal, mole ⁻¹ , °K ⁻¹)	ΔG° at 22°C (Kcal, mole ⁻¹)	log K _f at 22°C (I = 0)
K _f of Mg-PA	3.0 ± 0.7	35 ± 2	-7.2 ± 0.7	5.35 ± 0.09
K ₂ of PAA	-0.2 ± 0.3	22.6 ± 0.9	-6.9 ± 0.3	5.13 ± 0.04
K ₃ of PAA	-1.3 ± 0.4	35 ± 1	-11.7 ± 0.4	8.66 ± 0.05
K of HOAc ^a	90.0-	21.6	-6.42	4.757
K ₂ of H ₃ PO ₄ ^a	-0.09	29.9	-9.72	7.200

^aMeites, Handbook of Analytical Chemistry, p 1-21, McGraw-Hill Book Co., 1st ed., 1963

acid and ${\rm H_3PO_4}$ (126). The protonation reactions are entropy stabilized. This is expectable since we are replacing two species of opposite charges by one species with a smaller overall charge.

3.2. COMPLEXATION STUDIES OF PAA

3.2.1. SPECTROSCOPIC STUDIES

3.2.1.1. <u>Visible Spectra</u> - Aqueous solutions of manganese chloride are yellow-green. Upon the addition of PAA, the solution turns pink. A possible explanation for this color change is given by Cotton and Wilkinson (127). The majority of manganese complexes are high spin, in octahedral field this configuration gives spin forbidden as well as parity forbidden transitions, thus accounting for the extremely pale color of such compounds. In tetrahedral environments, the transitions are still spin forbidden, but no longer parity forbidden, the energy of the transitions is about 10 times stronger, and the compounds have a noticeable pale yellow-green color.

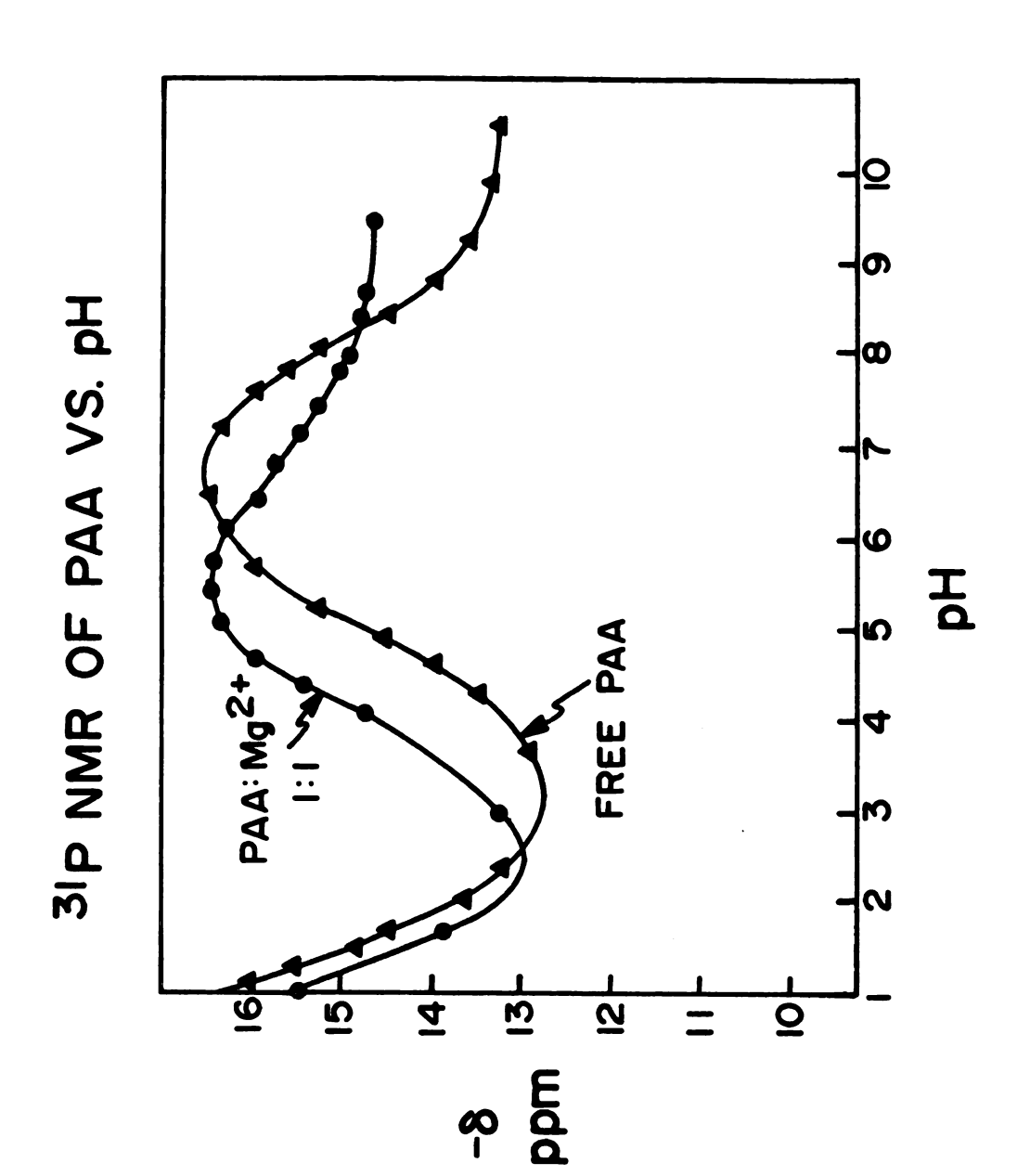
These results show that there is complexation between the metal ion and PAA.

Interaction of PA with copper ion was indicated by changes in the absorbances of copper ion solutions upon addition of PA. The molar absorptivity at λ_{max} of 780 \pm 5 nm is 10. When PAA is present at a mole ratio PA/Cu of 1.8, in basic medium (pH higher than 9), λ_{max} is at 765 \pm 3 nm with a molar absorptivity of 30.

- 3.2.1.2. Sodium-23 NMR When enough PA was added to a 2 x 10^{-2} M solution of NaCl at pH above 9, to make the PA/Na⁺ ion mole ratio equal to 8, the sodium-23 resonance shifted slightly downfield from 0.36 to -0.05 ppm. At the same time, the line-width increased from 11.2 to 21.2 Hz. While those changes are small, they indicate unambiguously the formation of a weak sodium complex.
- 3.2.1.3. <u>Phosphorus-31 NMR</u> Results similar to the sodium-23 NMR ones were observed. The phosphorus-31 resonance shifts slightly downfield from -13.3 to -14.9 ppm for a sodium:PA mole ratio change from 0 to 10.

The change in chemical shift of a 0.3 M PAA - 0.3 M MgCl₂ solution vs pH is shown in Figure 20 and compared to the results previously obtained for PAA alone. The plot presents several interesting points. At pH above 9, when the potentiometric results indicate quantitative complexation of magnesium ions, the chemical shift is -14.7 ppm compared to -13.3 ppm for the free PA. We have seen that protonation of the acetic acid moiety results in an upfield shift of the phosphorus-31 NMR signal, while protonation of the phosphoric acid moieties causes a downfield shift. At a pH of 9, PAA is completely deprotonated and, therefore, becomes a tridentate ligand. Formation of the Mg²⁺ complex affects all three sites and the result is a downfield phosphorus-31 shift.

Secondly, at pH between 3 and 6, the NMR signal of a PAA solution moves downfield when $MgBr_2$ is added, indicating evidence of complexation with the LH^{2-} ion (i.e., formation of a monoprotonated complex).



Phosphorus-31 Chemical Shift of 0.3 M PAA and of a 1:1 Mg:PAA Solution vs pH. Figure 20.

Thirdly, at pH below 3, the chemical shift of the PAA and PAA-magnesium ion solutions are different, showing evidence of the formation of diprotonated complex. Lowering of the pH of a free PAA solution upon addition of magnesium reinforces this hypothesis.

At pH above 8, a mole ratio plot at the concentrations required by our phosphorus-31 NMR spectrometer $(0.3 \, \underline{\text{M}})$ is limited to an Mg:PA mole ratio of approximately 1 because of the precipitation of Mg(OH)₂. As can be seen in Figure 21, the chemical shift goes downfield when the mole ratio increases, but the change in chemical shift is too small (1 to 1.5 ppm) to allow us to determine the stoichiometry of the complexes.

At the same time, the J_{P-H} coupling constant changes from 20.6 to 18.6 Hz.

3.2.2. CYCLIC VOLTAMMETRY - The stoichiometry of the complexes between divalent cations and PA ions was determined by cyclic voltammetry. Since the magnesium ion is not reducible in water, the Ni(II)/Ni and Zn(II)/Zn systems were first tried, because of the similarity in the size of the ions (crystallographic radii of 0.65 and 0.74 Å, respectively, and of 0.65 Å for the magnesium ion). However, the Ni(II)/Ni couple does not show a reversible behavior at the dropping mercury electrode (DME). The free Zn(II)/Zn couple is reversible, but shows an irreversible behavior when ligand is added to the solution.

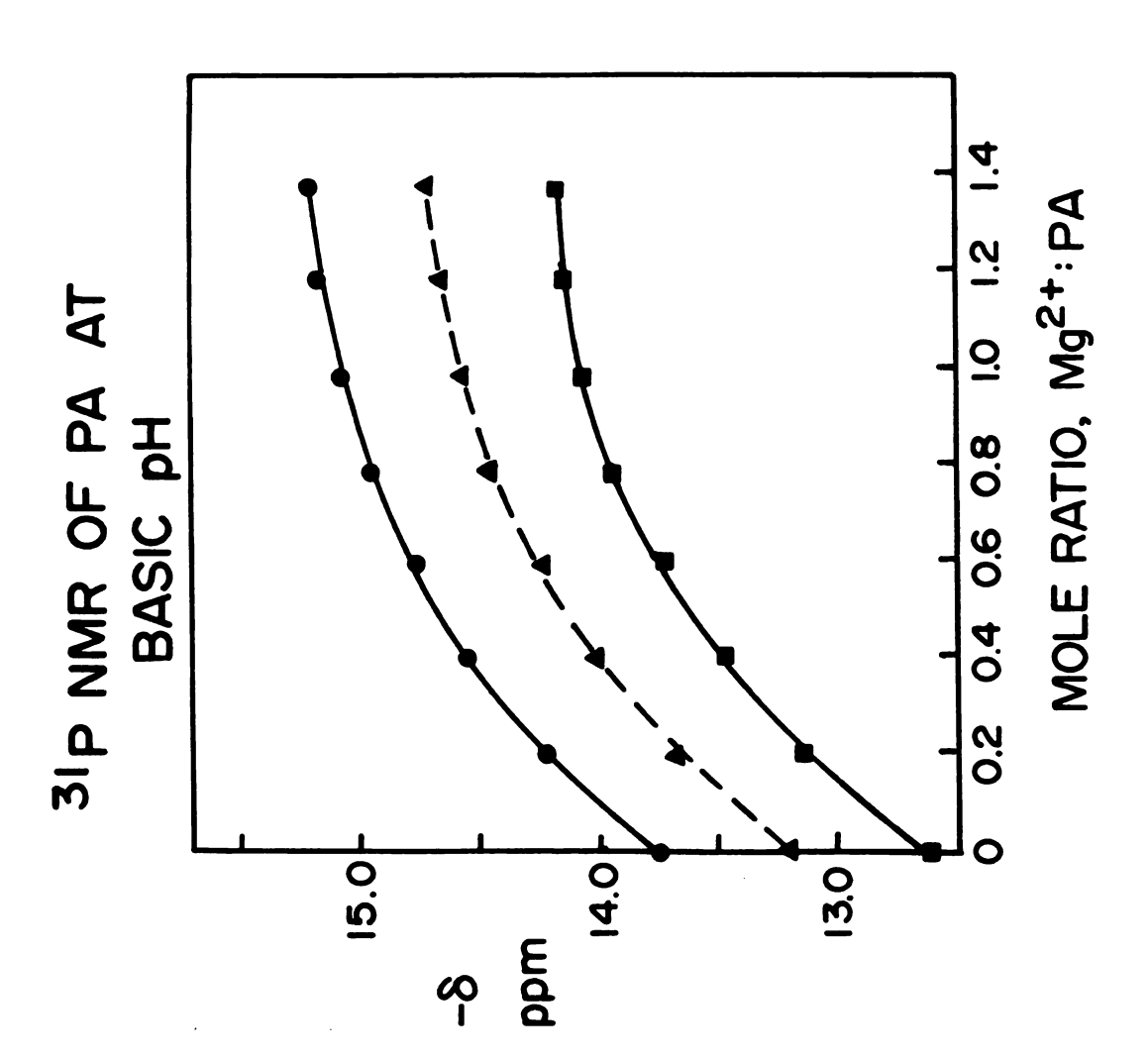


Figure 21. Phosphorus-31 Chemical Shift of 0.3 M PAA vs Mole Ratio of Magnesium at pH Above 9.

Finally, the Cd(II)/Cd couple was tested (the radius of the Cd^{2+} ion is 0.97 Å) and the rate of exchange of the electron at the DME for the free or complexed metal ion is fast enough to have a reversible diffusion controlled behavior in the different experimental conditions.

Lingane and De Ford and Hume equations (128, 129) are well known and their derivations are out of the scope of this study. To be able to use these equations several requirements have to be met. The electrode reaction must be reversible, this is ascertained by the difference in mV between the forward and backward peak extrema. It was found to be 35 mV at sweep rates of 20 mV or less [for the Cd(II)/Cd couple the theoretical value is 30 mV]. The ligand to metal concentration ratio must be high. This way the change in free ligand concentration upon complexation is small compared to its analytical concentration, and free and analytical concentrations can be equated. The diffusion current constants of the free and complexed metal ions must be approximately equal. Finally, the experiment was run at a constant ionic strength to alleviate the activity coefficient problem.

We can then express the Lingane equation for the following equilibrium:

$$M + jL \stackrel{?}{\leftarrow} ML_{j}$$
 (39)

with

$$\beta_{\text{ML}_{j}} = \frac{[\text{ML}_{j}]}{[\text{M}][\text{L}]^{j}} \tag{40}$$

as:

$$\Delta E_{1/2} = (E_{1/2})_{\text{free}} - (E_{1/2})_{\text{complex}} = \frac{2.303\text{RT}}{\text{nF}} \log \beta_{\text{ML}_{i}} C_{L}^{j}$$
 (41)

 C_L : analytical concentration of ligand in solution, j: stoichiometric coefficient, $(E_{1/2})_{free}$, $(E_{1/2})_{complex}$: 1/2 wave potentials of the free and complexed metal ions, respectively. This equation applies to only one type of complexes in solution.

De Ford and Hume (129), using the same assumptions derived an equation for stepwise reactions:

$$\Delta E_{1/2} = \frac{2.303RT}{nF} \log \beta_{ML_{j}} C_{L}^{j}$$

$$\Delta E_{1/2} = 29.58 \log (\beta_{ML} C_{L} + \beta_{ML_{2}} C_{L}^{2} +)$$
(42)

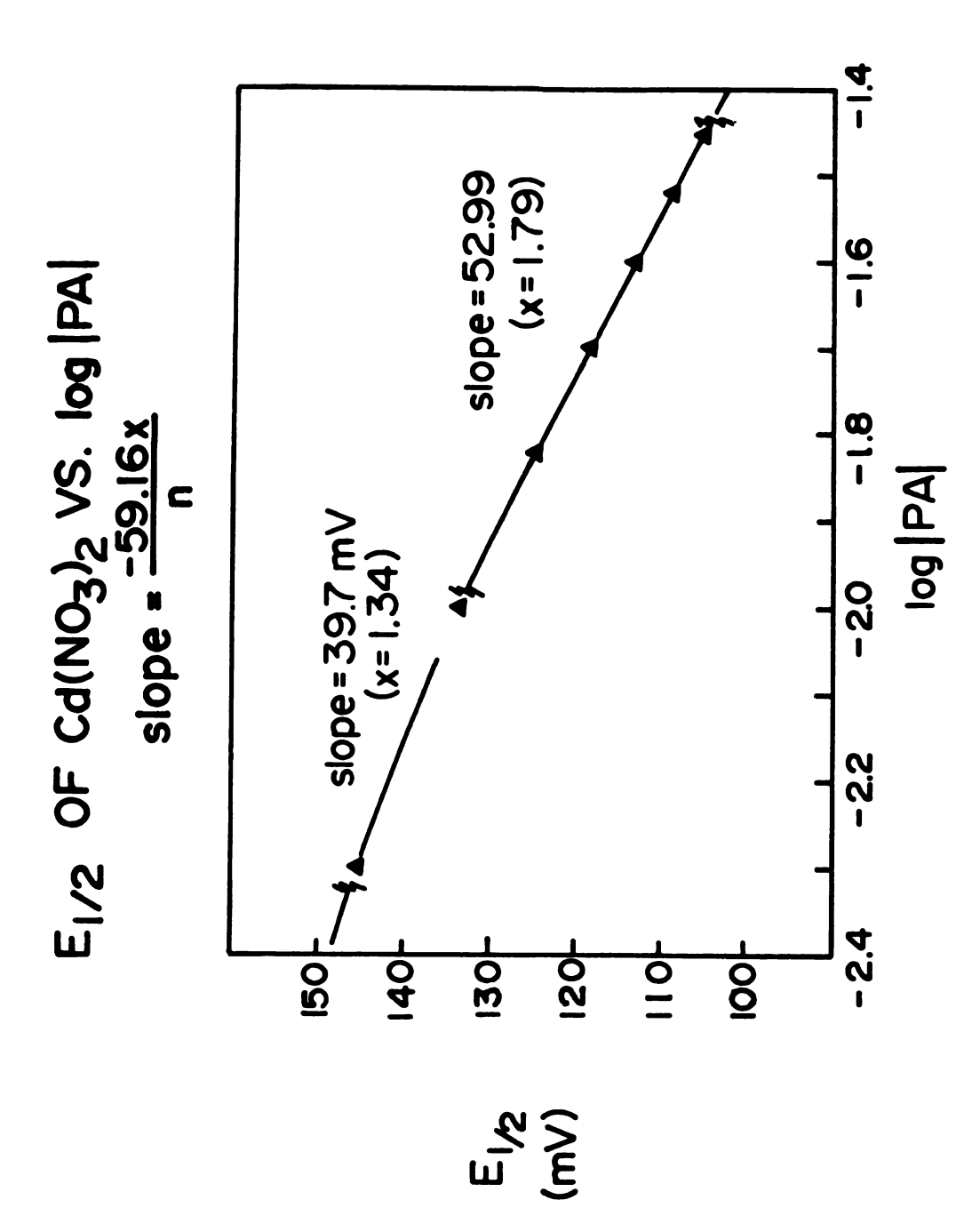
This equation predicts that the half-wave potential of the cadmium couple should shift towards more negative values when PA is added to the solution, which is actually observed.

In the case of step equilibria, a plot of $\Delta E_{1/2}$ <u>vs</u> log C_L will give [equation (42)] a curve with a variable slope. At low ligand concentration, the major term is $\beta_{ML}C_L$ and successively becomes $\beta_{ML_2}C_L^2$, $\beta_{ML_3}C_L^3$, etc... when C_L increases, corresponding to a change in slope from 30 mV to multiples of this value. As can be seen from Figure 22 and Table IX, the slope of such a plot changes from slightly above 1 to slightly below 2 when the ligand concentration increases, showing evidence of a CdL and a CdL₂ complex in solution.

De Ford and Hume extended their derivation to allow for calculation of the overall formation constants. A series of Fronaeous equations (130) can be defined as:

$$F_0(L) = 1 + \beta_1[L] + \beta_2[L]^2 = \exp(\Delta E_{1/2} \text{ nF/RT})$$
 (43)

$$F_1(L) = \frac{F_0(L) - 1}{[L]} = \beta_1 + \beta_2[L]$$
 (44)



Plot of E $_{1/2}$ as a Function of Log [PA] for the Cd $^{2+}$ -PA System (Reference: Thallium Amalgam). Figure 22.

Table IX. Half-wave Potential of the Cd(II)/Cd Couple in the Presence of PA \underline{vs} Thallium Amalgam.

[PA] x 10-3 (mole/1)	log [PA]	E _{1/2} (mV)	
0.00		194.2	
5.022	-2.299	145.3	
10.06	-1.997	133.3	
15.09	-1.821	124.8	
20.13	-1.696	118.5	
25.16	-1.599	113.3	
30.20	-1.520	109.0	
35.23	-1.453	105.3	
40.27	-1.395	100.5	
45.30	-1.344	98.0	
50.34	-1.298	94.3	

$$F_2(L) = \frac{F_1(L) - \beta_1}{[L]} = \beta_2$$
 (45)

assuming we only have a 1:1 and a 2:1 complex.

A plot of F_0 (L) \underline{vs} [L] will be a steeply rising curve, however, as [L] approaches zero, the graph will have a limiting slope of β_1 , and an intercept on the F_0 (L) axis of 1. A preliminary value of β_1 is obtained. A plot of F_1 (L) \underline{vs} [L], on the other hand, will have a limiting slope as [L] tends to zero, of β_2 and an intercept on the F_1 (L) axis of β_1 . A confirmative estimation of β_1 is possible and, in addition, a preliminary value of β_2 is obtained. The values of β_1 and β_2 found are given in Table X.

The precision in the determination of β_1 and hence of β_2 is limited by the previously mentioned assumption that we have a high ligand to metal mole ratio.

3.2.3. POTENTIOMETRIC STUDIES OF COMPLEXATION

- 3.2.3.1. Sodium Ion Electrode Study Due to the low stability of the sodium-PA complex and the high charge of the PA ions, the experiment was performed at 1.0 ionic strength. It has been shown (131) that at high ionic strength, the activity coefficient is much less sensitive to the variations of the ionic strength. Thus, in our experimental conditions, the change in ionic strength was small enough during the course of the titration to be neglected in a first approximation. The value of the formation constant is 3.3 (Table X).
- 3.2.3.2. <u>Glass Electrode Study</u> Figure 23 represents a coulometric titration of PAA and PAA with MgBr₂. In the latter

Table X. PAA Complexes With Metal Ions.

	Na	Мg ^b	Ca ^b	Srb	Ba ^b
log K _f (ML)	1.43 ± 0.02	4.50 ± 0.02	3.85 ± 0.02	3.67 ± 0.02	3.67 ± 0.02
log K _f (MLH)	0.79 ± 0.05	2.56 ± 0.05	2.32 ± 0.06	2.56 ± 0.06	2.50 ± 0.06
	Nad	ာဗ			
log Kf(ML)	0.52	3.9 ± 0.1			
log K _f (ML ₂)		1.9 ± 0.1			

 $a_{I} = 0.078$ $b_{I} = 0.05$ $c_{I} = 0.4$ $d_{I} = 1.0$

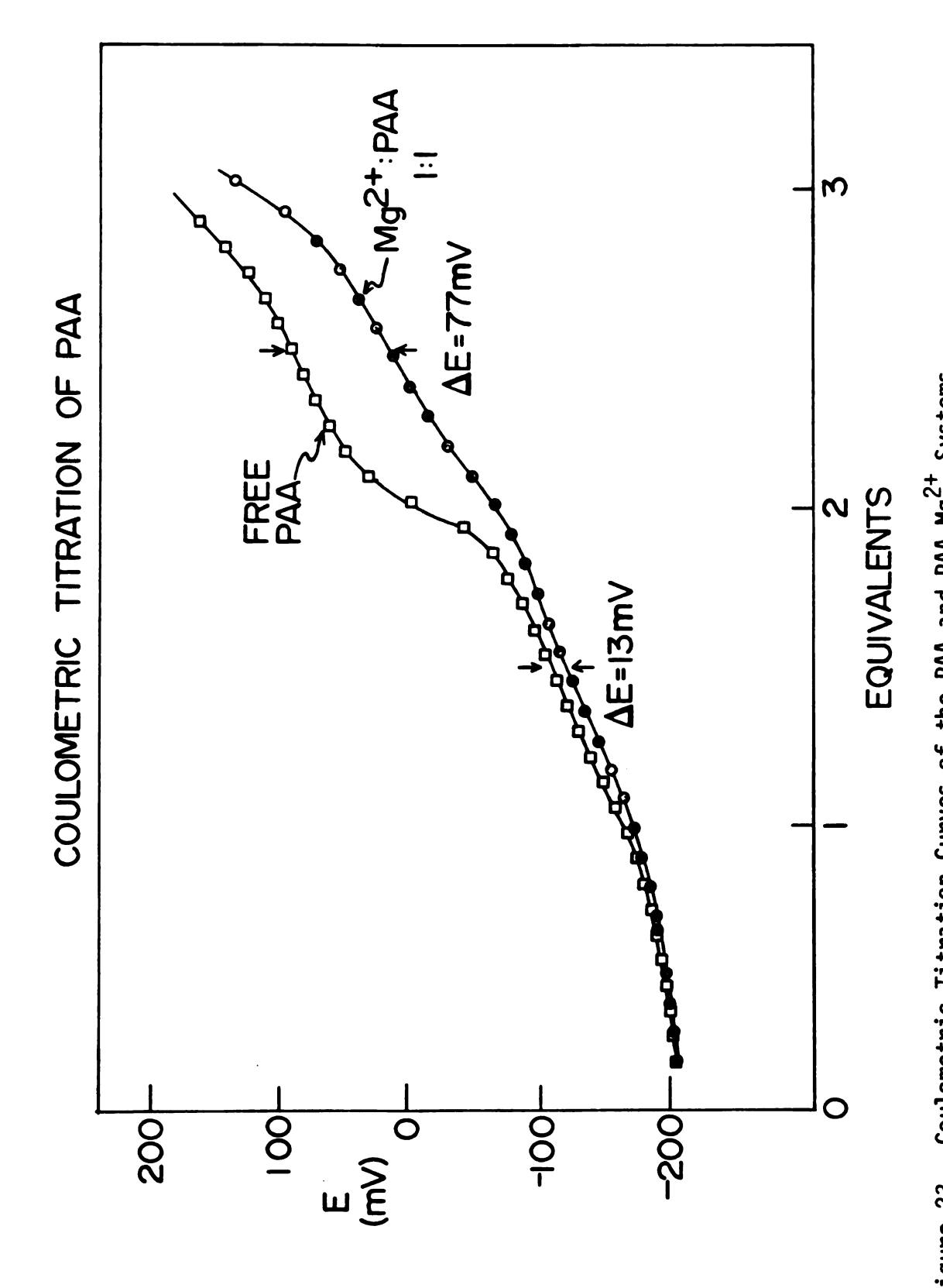


Figure 23. Coulometric Titration Curves of the PAA and PAA-Mg $^{2\pm}$ Systems.

case, the following equilibria are taking place in solution:

$$Mg^{2+} + LH_2^- \stackrel{\rightarrow}{\leftarrow} MgLH + H^+$$
 (46)

$$Mg^{2+} + LH^{2-} \stackrel{?}{\leftarrow} MgL^{-} + H^{+}$$
 (47)

Experimental results showed that the latter complex was more stable than the former one. Phosphorus-31 NMR results showed evidence of a diprotonated complex, however, in our experimental conditions (7 x 10^{-4} M PAA and 7 x 10^{-4} M MgBr₂) the amount of magnesium ions complexed and the corresponding release of protons are small, and the resulting change in pH is not detectable.

The formation constants of the magnesium-PAA complexes were determined at different ionic strengths. The data are listed in Table XI and plotted in Figures 24 and 25.

The Guntelberg modification of the Debye-Huckel equation allows us to express the thermodynamic values of the complexes of equations (46) and (47) as follows:

$$K_{f}^{t}(MgL) = \frac{[MgL]}{[Mg][L]} \times \frac{\gamma_{MgL}}{\gamma_{Mq}\gamma_{L}} = K_{f}^{c}(MgL) \times \frac{\gamma_{MgL}}{\gamma_{Mq}\gamma_{L}}$$
(48)

$$\log K_f^{\mathsf{C}}(\mathsf{MgL}) = \log K_f^{\mathsf{t}}(\mathsf{MgL}) - \frac{12A\sqrt{I}}{(1+\sqrt{I})}$$
 (49)

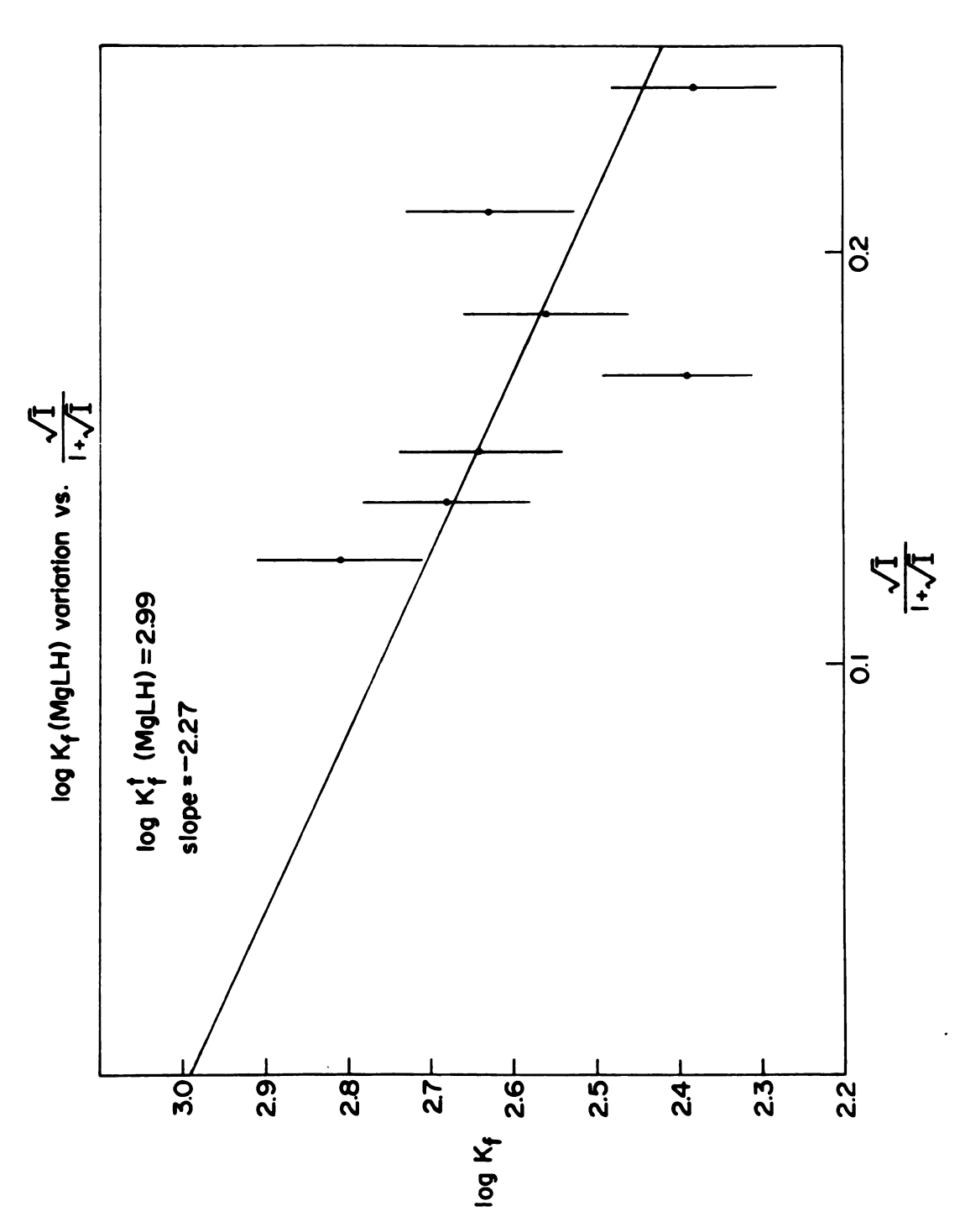
and similarly:

$$\log K_{f}^{c}(MgLH) = \log K_{f}^{t}(MgLH) - \frac{8A\sqrt{I}}{(1+\sqrt{I})}$$
 (50)

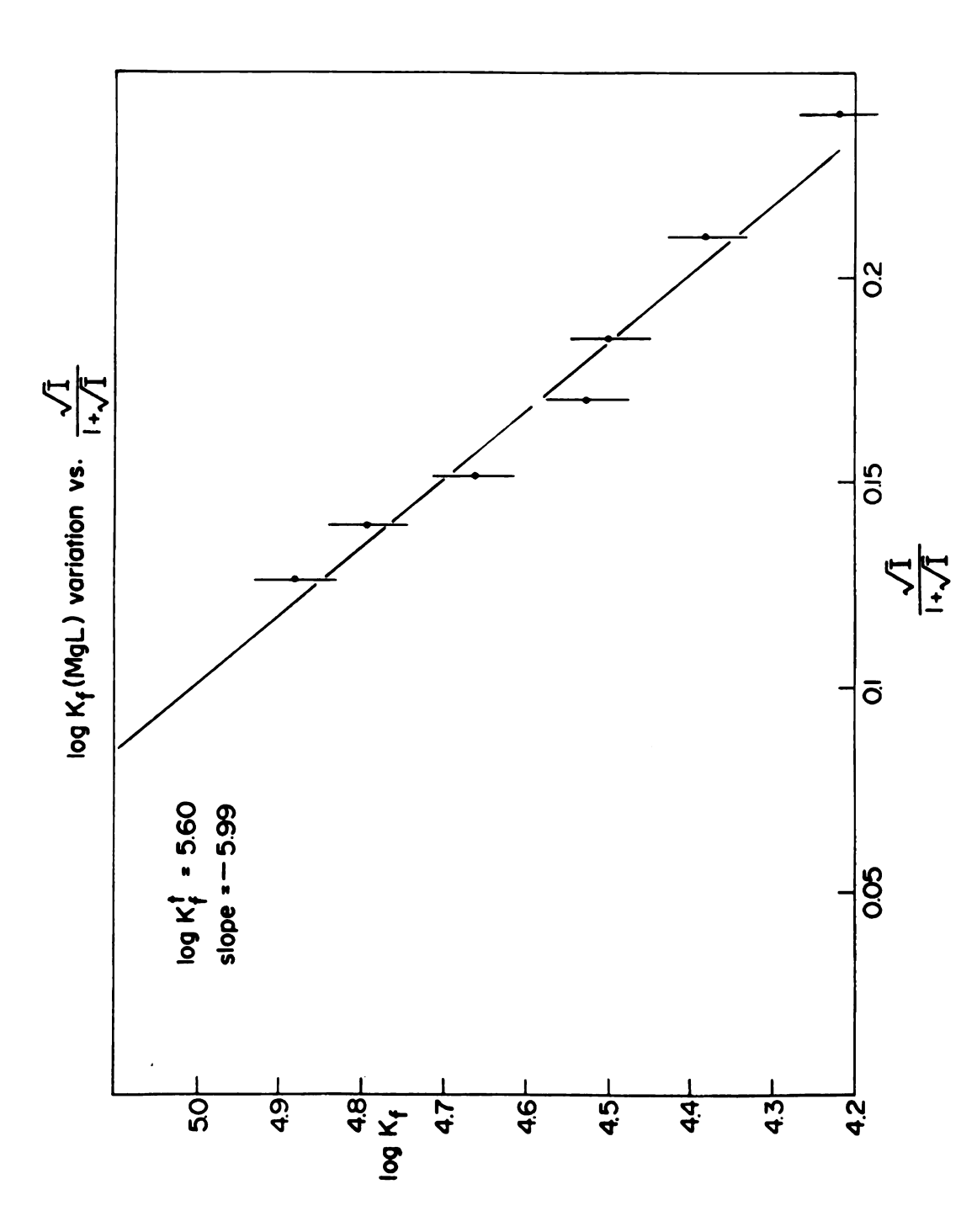
The theoretical slopes for the deprotonated and protonated complexes at 25°C are -6.11 and -4.07, respectively. The experimental values are -5.99 and -2.27. As in the case of the protonation of PAA, the completely deprotonated form follows the theory quite well, while the value for the monoprotonated form is off by a factor of 2. In these conditions the thermodynamic values of the formation

Table XI. Formation Constants for PAA-Magnesium Complexes at Various Ionic Strengths at 25°C.

Ionic Strength x 10 ⁺²	log K _f (MgLH)	log K _f (MgL)
X 10 -	TOG KT (FIGER)	TOG KT(FIGE)
9.94	2.4 ± 0.1	4.22 ± 0.05
7.04	2.6 ± 0.1	4.38 ± 0.05
5.112	2.6 ± 0.1	4.50 ± 0.05
4.185	2.4 ± 0.1	4.53 ± 0.05
3.176	2.6 ± 0.1	4.66 ± 0.05
2.425	2.7 ± 0.1	4.80 ± 0.05
2.047	2.8 ± 0.1	4.88 ± 0.05
0.00	3.0 ± 0.3	5.58 ± 0.09



Plot of Log K $_{\rm f}$ of the Monoprotonated PAA-Mg $^{2+}$ Complex vs Ionic Strength, the Line is a Linear Least Squares Fit. Figure 24.



Plot of the Log K $_{\rm f}$ of the Completely Deprotonated PAA-Mg $^{2+}$ Complex vs Ionic Strength, the Line is a Linear Least Squares Fit. Figure 25.

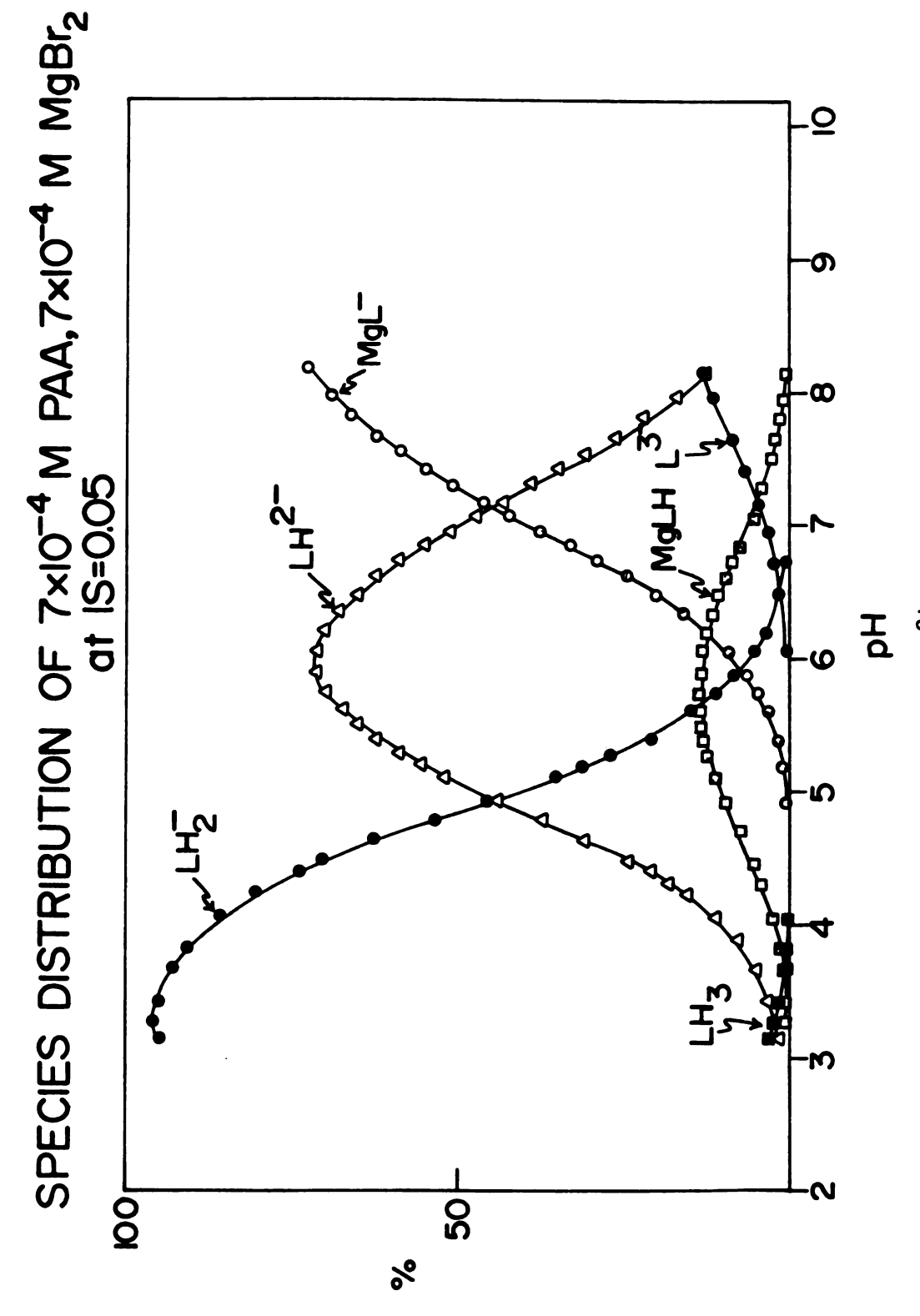
constants of the mono- and deprotonated complexes are 1.0×10^3 and 4.0×10^5 , respectively.

By analogy with the cadmium-PAA system, similar complexes were assumed in the magnesium-PAA case. However, our potentiometric results disagree with this hypothesis and show that the magnesium-PAA complexes are different from the cadmium-PAA ones. These results show evidence of completely deprotonated and monoprotonated magnesium-PAA complexes.

These complexes have one or no charge. In these conditions the change in ionic strength during the titration is negligible, and the value of the ionic strength can be equated to the concentration of supporting electrolyte. A species distribution plot at an ionic strength of 0.05 is shown in Figure 26. It can be seen that for a 1:1 mole ratio of PA:magnesium, approximately 50% of the magnesium (or PAA) is complexed at pH = 7, which is the physiological pH.

The formation constants of the PAA-calcium ion complexes were determined at 25°C at an ionic strength of 0.05, and compared to the values of the magnesium ion complexes. A similar study was performed with strontium and barium ions. The stability of the complexes decreases with increasing radius of the metal (see Table X).

The complexation of sodium ion has been studied by the same method (Table X). At 0.078 ionic strength, the sodium-PA complex has a formation constant of 27. Owing to the low ionic strength, this value is compatible with the formation constant of 3.3 found by sodium ion electrode measurement at 1.0 ionic strength.



Species Distribution Plot of the PAA-Mg²⁺ System at 0.05 Ionic Strength. Figure 26.

These results definitely show that sodium salts cannot be used as supporting electrolytes.

3.2.3.3. Thermodynamics of Magnesium Complexation -Measurements of the formation constants of the magnesium complexes at different temperatures lead to the determination of the ΔG° , ΔH° and ΔS° of the reaction. The precision in the determination of the monoprotonated complex formation constant was low and prevented the calculation of the thermodynamic quantities for that reaction. These quantities were determined for the deprotonated complex only. A Van't Hoff plot of these formation constants is shown in Figure 19. The thermodynamic quantities are listed in Table VII. As can be seen, the complexation reaction is entropy stabilized and enthalpy destabilized. For EDTA, the changes in entropy and in enthalpy at 0.1 ionic strength have been reported to be 50.5 to 52 cal/mole, °K and -3.14 to 2.9 kcal/mole (132). The entropy stabilization effect of complexation is readily explained by the fact that we go from two ions with high charge to size ratios to a larger entity with a single negative charge.

3.3. PHOSPHONOACETIC ACID ANALOGS

In order to determine why PAA is an inhibitor of the replication of Herpesviruses, biochemists have conducted studies with analogs or derivatives of PAA. As mentioned earlier, it has been found that phosphonoformic acid (PFA) is the only compound found so far which shows a biological activity similar to that of PAA.

On the other hand, 2-phosphonopropionic acid (2-PPA) has an activity 50 times smaller, while 3-phosphonopropionic acid (3-PPA) does not show any activity at all. The complexes between magnesium and these compounds have been studied in an attempt to correlate activity and complexing power of these ligands.

3.3.1. <u>SPECTROSCOPIC STUDIES OF PFA</u> - A phosphorus-31 NMR spectrum of the trisodium salt of phosphonoformic acid (PFA) consists of one peak with a chemical shift of -0.34 ppm <u>vs</u> 85% H₃PO₄. If we consider the differences between the PAA and PFA molecules, we can rewrite equation (10) as:

$$\Delta \delta = B \Delta \chi_{R} - A \Delta \theta_{OPO} - 147 \Delta n_{\pi}$$
 (51)

Again, the change in electronegativity of the R group between the two molecules is the major factor influencing the chemical shift [see Riess et al. (67)]. The formic acid carbon has a larger electronegativity than the CH₂ carbon of the acetic acid group, and in going from PAA to PFA, a positive chemical shift is expected, which is indeed experimentally observed.

3.3.2. <u>DETERMINATION OF THE pK'S</u> - The determination has been done at 0.05 ionic strength to allow for eventual use of the Guntelberg equation (28) to determine the thermodynamic values. Since PFA undergoes a decarboxylation reaction in acidic medium, its trisodium salt was used instead. Complexation between sodium and PF ions is suspected, however, owing to the low concentration of sodium ion, calculations showed that the

influence of the sodium ion on the values of the pK's and the formation constants of the complexes is negligible.

The values obtained for the pK's of PFA, 2-PPA, 3-PPA are compared to the PAA values in Table XII.

3.3.3. <u>COMPLEXATION</u> - Once the pK's of the above-mentioned acids had been determined, it was possible to study the complexation of magnesium ion by these different ligands. The formation constants determined by potentiometric measurements are listed in Table XII.

Experimental results show that less stable complexes are formed when the length of the PAA molecule is modified. Loss of stability is also observed when a hydrogen of the $\underline{\text{CH}}_2$ group of PAA is substituted by a methyl group.

These results are only partly satisfactory since biochemical studies have shown that PFA has about the same biochemical activity as PAA. However, if we compare the species distribution plots of the two acids when magnesium ions are present in the solution (see Figures 26 and 27), we see that at pH 7.0 approximately 60% of the magnesium ions are involved in a complex with PFA, while less than 50% are with PAA. Similar calculations show that at a pH of 7.0, 5% of the magnesium ions are complexed by 3-PPA, and 30% by 2-PPA. These results confirm the hypothesis that the mode of action of PAA involves complexation with magnesium ions.

Table XII. Complexation Formation Constants of PAA and PAA Analogs at 25°C and 0.05 Ionic Strength

	PAA	PFA	2-PPA	3-PPA
рК ₁	2.18 ± 0.04	1.7 ± 0.1	1.8 ± 0.1	2.26 ± 0.04
pK2	4.94 ± 0.02	3.59 ± 0.02	5.15 ± 0.02	4.63 ± 0.02
pK ₃	8.14 ± 0.02	7.56 ± 0.02	8.54 ± 0.02	7.75 ± 0.02
log K _f (MgLH)	2.6 ± 0.1	1.7 ± 0.3	1.4 ± 0.6	1.7 ± 0.1
log K _f (MgL)	4.50 ± 0.05	3.59 ± 0.05	4.38 ± 0.05	2.28 ± 0.05

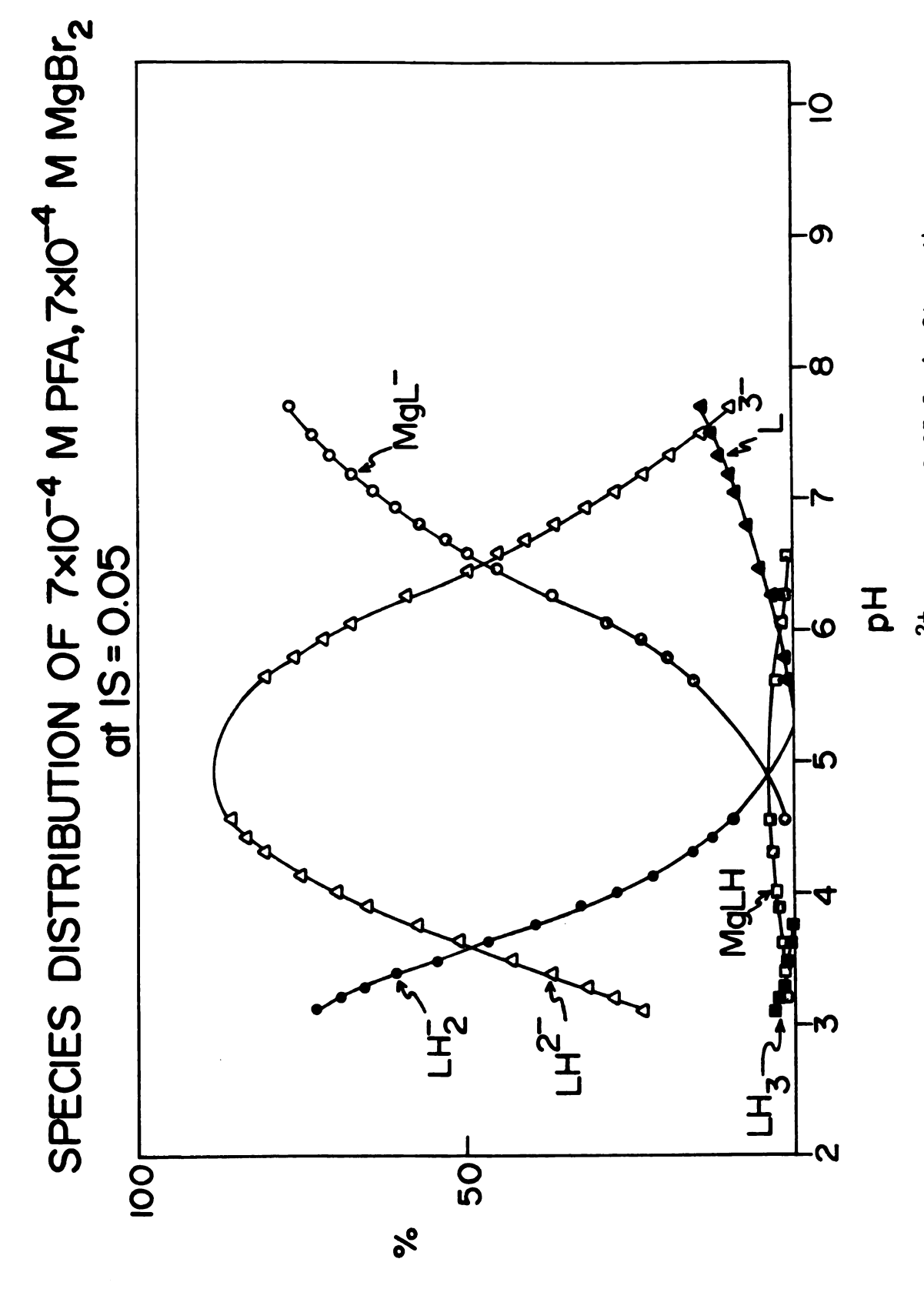
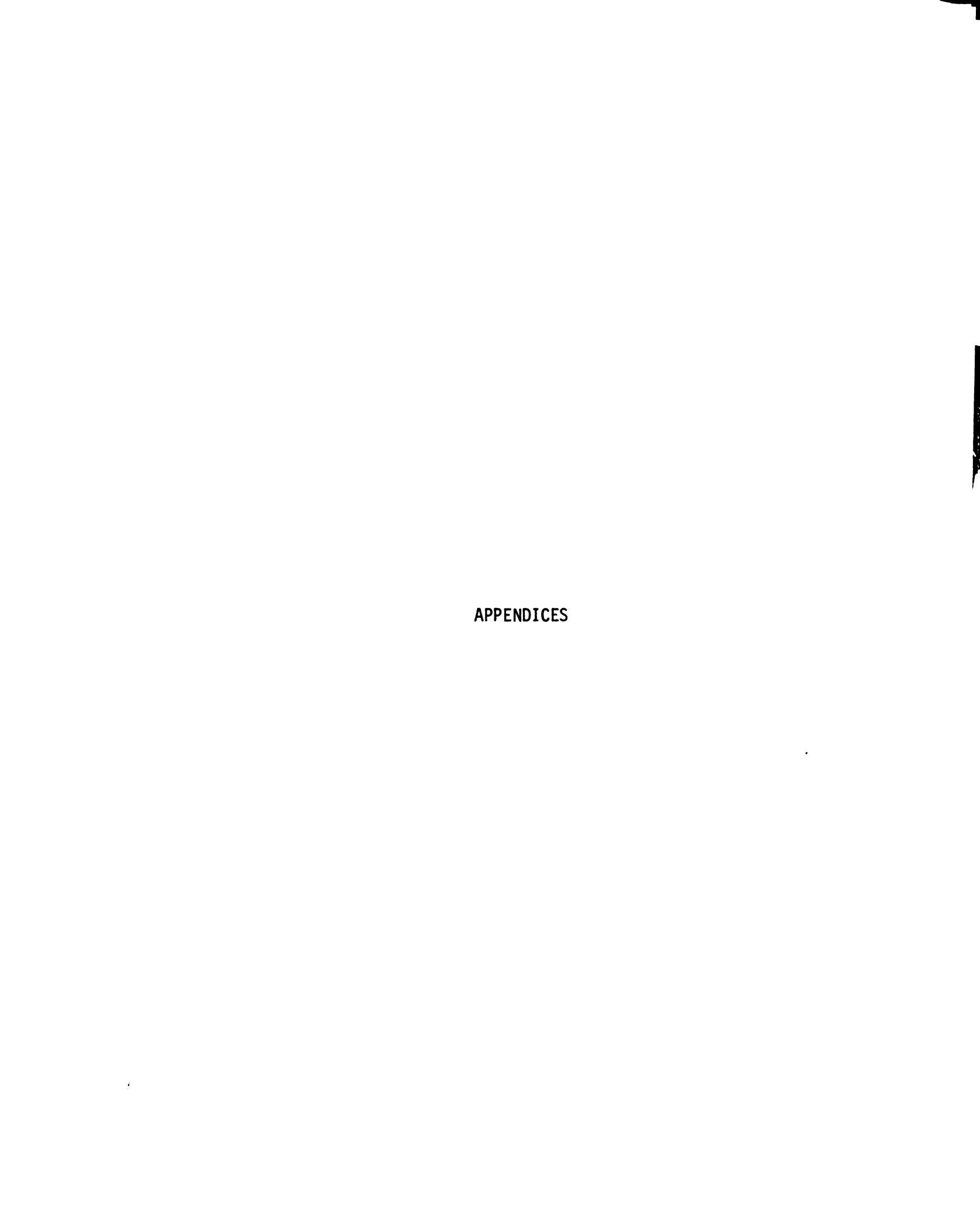


Figure 27. Species Distribution Plot of the PFA-Mg $^{2+}$ System at 0.05 Ionic Strength.

3.4. CONCLUSION

A relationship between the pK's of PAA and its acidity functions has been established by phosphorus-31 and carbon-13 NMR. The chemical shift changes have been explained in terms of changes in electronegativity of the substituents, π -bonding feedback, and \underline{s} and \underline{p} electron shielding. Spectroscopic studies (UV, NMR) showed evidence of complexation of sodium and magnesium ions by PAA. The stoichiometry of the PA-Cd²⁺ ion complexes has been studied by cyclic voltammetry. The acid dissociation constants of PAA and the stability of the complexes of PAA with metal ions have been determined by potentiometric measurements. The pK's and log K_f of magnesium ion complexes with several phosphonic acids have been determined, and related to the biochemical activity of these ligands.



APPENDIX A

SODIUM-23 NMR

A.1. INTRODUCTION

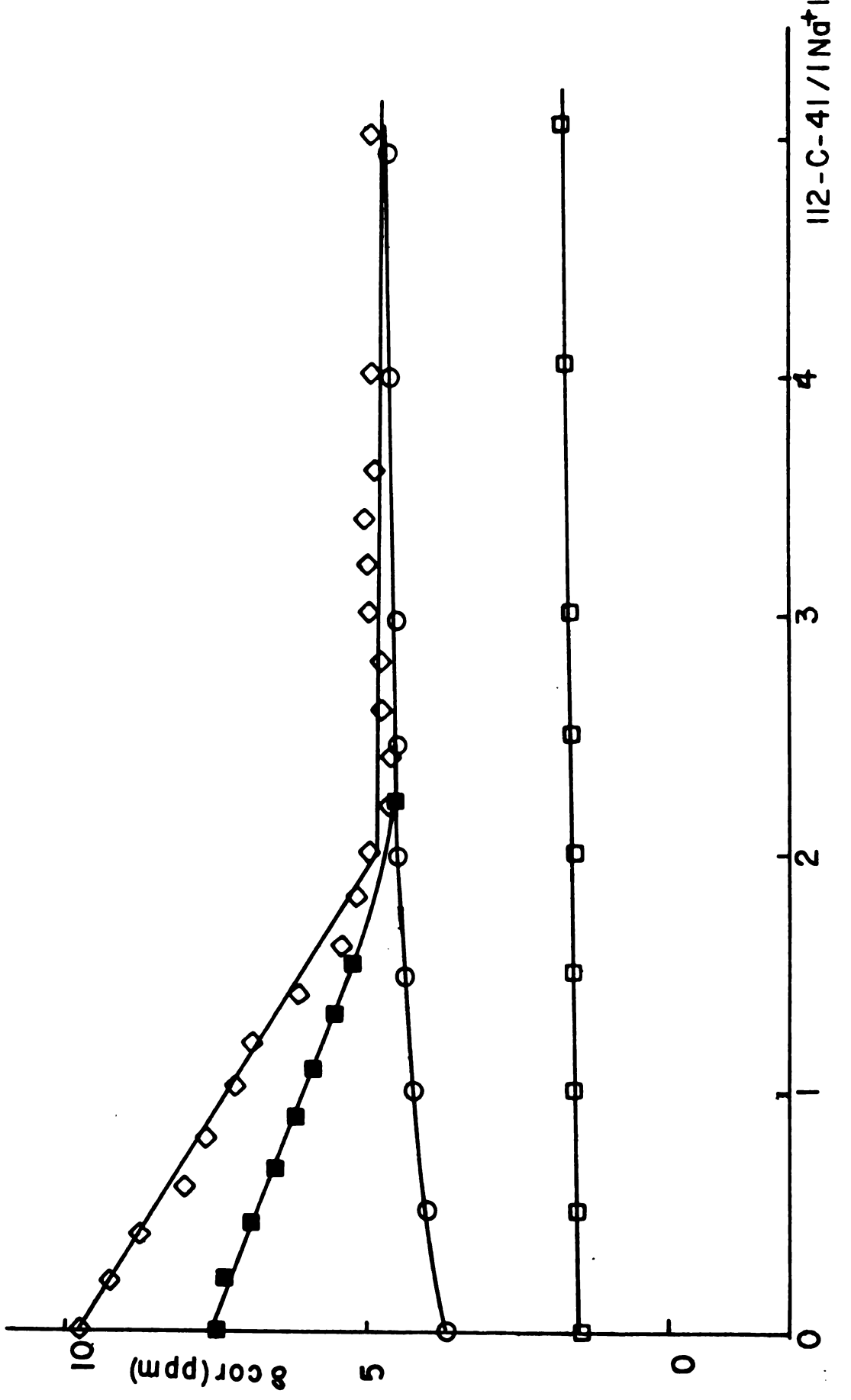
Complexation of sodium ions by the crown ether 12-crown-4 (12-C-4) was studied in different solvents. In order to minimize the number of equilibria taking place in solution, sodium salts which do not exhibit chemical shift dependence on concentration were chosen. In this case, it is reasonable to assume that the ion pairing for these salts in the solvent considered is negligible. All the studies reported in this appendix have been done at a constant concentration of salt. Since there is no ion pairing, and the crown ether bears no charge, the activity correction is small at best and $K_{\mathbf{f}}$'s obtained can be taken as thermodynamic values.

A.2. RESULTS AND DISCUSSION

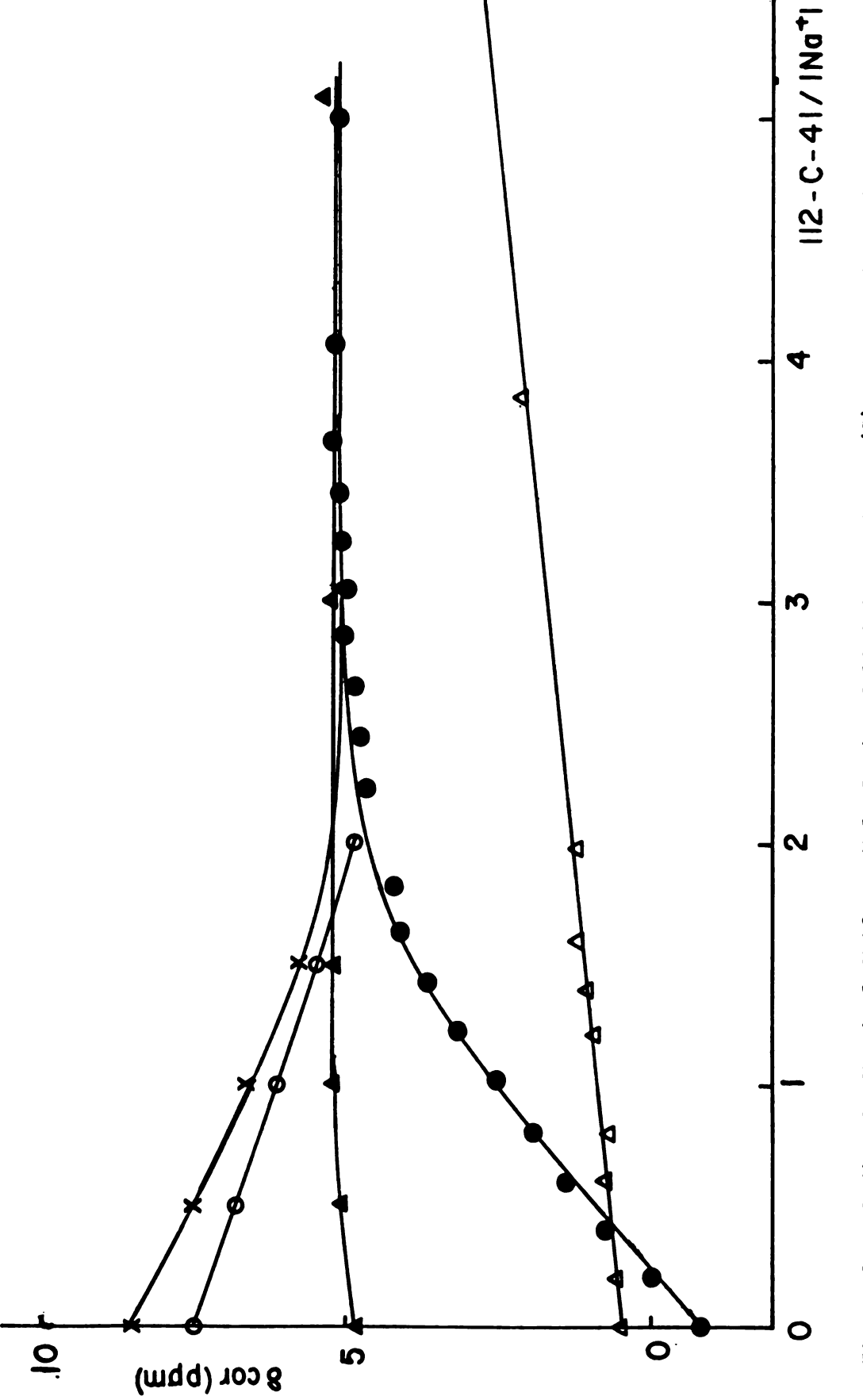
The stability of the crown complex is largely determined by the size relationship between the inner diameter of the crown and the diameter of the desolvated ion, and by the solvating ability of the solvent. If the rate of exchange of the sodium ion between the two sites (free and complexed ion) is greater than $\Delta\nu\pi/2$, where $\Delta\nu$ is the difference between the characteristic resonances (in Herz) of each site, only one population resonance is observed. This is the case with 12-C-4 and sodium ion. The ligand 12-C-4 has a cavity size of 1.2 to 1.5 Å while sodium ion has a diameter of 1.9 Å (from crystallographic measurements), therefore, in the cases where the solvent does not have too strong of a solvating ability, the

formation of 2:1 sandwich complexes is expected (2 crowns for 1 sodium ion). This is the case for acetone, acetonitrile, propylene carbonate (PC), pyridine, and THF. As can be seen from the graphs (Figures 28 and 29), there is a break in the chemical shift change for the various solvents at a mole ratio of 2. In several cases [acetone, acetonitrile, tetrahydrofuran (THF)], the complex precipitated out of solution for a mole ratio above 2. In the case of methanol or water, a precipitate appeared as soon as the ligand was added to a solution of sodium tetraphenyl borate (water, methanol) or sodium perchlorate (methanol). In the former case, an elemental analysis showed that we had a 2:1 complex: NaBPh4(12-C-4)2 calculated/experimental: C: 69.16/69.30, H: 7.55/7.42. The melting point of the tetraphenyl borate complex was found to be 248.5-249.5°C.

In the case of dimethylsulfoxide (DMSO), methanol or aqueous solutions, the solvent molecules compete quite successfully with the ligand, consequently, only a weak complex is formed, and a large excess of ligand is necessary to produce a variation of the chemical shift from the position characteristic of the solvated sodium ion in the given solvent. It is quite interesting to note that for all solvents except water, methanol and DMSO, the chemical shift above a mole ratio of 2 is the same, showing that once complexed, the sodium ion is not affected by the solvent: the two crowns around the sodium ion shield it effectively from the solvent. Figures 28 and 29 show that in the case of the three other solvents (DMSO, water, methanol), the chemical shift of the sodium ion tends to the same limiting value of 5.0 ± 0.5 ppm when the ligand



Sodium-23 Chemical Shift vs Mole Ratio of 12-C-4. NaBPh₄: (\diamondsuit) : 0.1 M in PC, (\blacksquare) : 0.034 M in THF; (\bigcirc) : 0.04 M NaI in Methanol; (\bigcirc) : 0.04 M NaCl04 in Water. Figure 28.



Sodium-23 Chemical Shift vs Mole Ratio of 12-C-4. NaBPh₄: (\blacksquare): 0.04 \underline{M} in Pyridine, 0.1 \underline{M} in DMS0 (Δ), Acetone (X), \overline{DMF} (\triangle), Acetonitrile (O). Figure 29.

concentration increases. In the case of dimethylformamide (DMF), no chemical shift change is observed, and, therefore, no conclusions can be drawn as far as the strength of the complex is concerned, since it is obvious from the preceding remarks that the solvated and complexed sodium ions have the same chemical shift.

We assume that in all solutions containing the crown ether and the sodium ion, the latter is found in three environments: free solvated sodium ion, 1:1 12-C-4:sodium ion complex and 2:1 12-C-4:sodium ion complex. The exchange between the three sites is fast compared to the sodium-23 NMR time scale, therefore, only the mass average chemical shift is observed:

$$\delta_{\text{obs}} = \delta_{\text{M}} \times_{\text{M}} + \delta_{\text{ML}} \times_{\text{ML}} + \delta_{\text{ML}_2} \times_{\text{ML}_2}$$
 (52)

where δ_{obs} is the observed chemical shift, x_M , x_{ML} , x_{ML} , x_{ML} are the respective mole fractions of the free, 1:1 and 2:1 complexed metal ions, while δ_M , δ_{ML} and δ_{ML_2} are the respective chemical shifts of the three species. Assuming the following equilibria:

$$M + L \stackrel{?}{\leftarrow} ML \tag{53}$$

$$M + 2L \stackrel{\Rightarrow}{\leftarrow} ML_2 \tag{54}$$

where L is the ligand, the formation constants of the complexes in concentration units are:

$$K_{1} = \beta_{1} = \frac{[ML]}{[M][L]}$$
 (55)

$$\kappa_2 = \frac{[ML_2]}{[ML][L]} \tag{56}$$

$$\beta_2 = \frac{[ML_2]}{[M][L]^2} \tag{57}$$

where [L], [M], [ML] and $[ML_2]$ represent the equilibrium concentrations of free ligand, free metal, 1:1 and 2:1 complexes, respectively. By using the ligand and metal mass balance equations:

$$C_{M}^{T} = [M] + [ML] + [ML_{2}]$$
 (58)

$$C_1^T = [L] + [ML] + [ML_2]$$
 (59)

where C_M^T and C_L^T represent the total concentrations of metal and ligand, respectively, we can express the concentration of free metal as:

$$[M]^{3} + p[M]^{2} + q[M] + r = 0$$
 (60)

with:

$$p = \frac{(c_{M}^{T} \kappa_{1}^{2} - 8c_{M}^{T} \kappa_{2} \kappa_{1} + 4c_{L}^{T} \kappa_{2} \kappa_{1} - \kappa_{1}^{2} c_{L}^{T})}{(4\kappa_{2}\kappa_{1} - \kappa_{1}^{2})}$$
(61)

$$q = \frac{(1 + K_1 C_L^T + K_1 K_2 C_L^{T2} + 4K_1 K_2 C_M^{T2} - 4C_L^T C_M^T K_1 K_2)}{(4K_2 K_1 - K_1^2)}$$
(62)

$$r = \frac{-c_{M}^{T}}{(4K_{1}K_{2} - K_{1}^{2})} \tag{63}$$

This cubic equation has three real roots for a mole ratio of ligand to metal less than 2, and one real root after. Once the concentration of free metal is known, equation (52) can be written as a function of the two formation constants of the 1:1 and 2:1 complexes, and the chemical shifts previously defined. Since $\delta_{\rm M}$ can be easily determined from measurements of solutions of sodium salt without the ligand, equation (52) contains 4 unknowns. For a fairly strong 2:1 complex, $\delta_{\rm ML_2}$ can be determined experimentally by the addition

of such excess of L that essentially all of the metal ion is in the 2:1 complexed form. For weak complexes, however, either the limiting chemical shift value is unobtainable, or such large excess of L is needed that the solution loses even a semblance of ideality.

The procedure we used to solve equation (52) was to substitute the experimental parameters δ_{ODS} , C_{M}^{T} , C_{L}^{T} and δ_{M} and vary K_{1} , K_{2} , δ_{ML} , and $\delta_{\text{ML}_{2}}$ until the calculated chemical shifts would correspond to the experimental values within the error limits on concentration (1%) and shift (0.05 ppm). The data were analyzed on a CDC-6500 computer using the Fortran IV program KINFIT4 (135). A description of the subroutine EQN used is given in appendix B. Actually, before the data could be processed, the correct root of the cubic equation (60) to be used had to be determined. We had the choice between three roots, all mathematically valid, but for a given mole ratio, only one has a physical significance.

In order to determine which root to use, the best solution was to simulate data by using KINFIT4 (see appendix B) with the expected values of the chemical shifts of the complexes, and their formation constants. From these results, it readily appeared in which region of ligand to metal mole ratio each of the roots could be reasonably used. Once the domain of validity of each root was determined, the experimental data were processed, and as a check, the refined values of the chemical shifts and formation constants were used to generate data for each root.

Following this procedure, the chemical shifts and formation constants were determined for the following systems: NaBPh $_{\Delta}$ -(12-C-4)

Table XIII. Formation Constants of Sodium-(12-C-4) Complexes and Their Chemical Shifts

Solvent	1:1 Complex		2:1 Complex	
	K _f	δ(ppm)	Kf	δ(ppm)
Pyridine	200 ±10	3.9 ± 0.1	150 ± 40	5.4 ± 0.1
Methano1	60 ± 10	4.7 ± 0.1	20 ± 25	4.9 ± 0.1

in pyridine, and NaI-(12-C-4) in methanol [NaBPh₄-(12-C-4)₂ and NaClO₄-(12-C-4)₂ complexes are not soluble enough in methanol for NMR purposes with our instrument]. The formation constants and chemical shifts are listed in Table XIII. As can be seen, it is doubtful that we have a 2:1 complex in methanol. In the case of PC, the formation constant K_2 is larger than 10^4 , and for the other solvents, precipitation of the complex at a mole ratio near 2 prevented the determination of the formation constants. However, it can be seen from Figures 28 and 29 that δ_{ML_2} is 5.0 ± 0.5 ppm for all the solvents studied, except water and DMSO. In these last two cases, the complexes are too weak, due to the good solvating ability of water and DMSO, and the formation constants could not be determined.

A comparison of the IR spectra of 12-C-4 alone and of the $NaBPh_4(12-C-4)_2$ complex between 700 and 4000 cm⁻¹ did not show any new band which could be attributed to the complex. This result correlates well with the literature result for lithium ion and 12-C-4 complex (135). The complex bands are in the far IR region.

Thus, it has been shown that sodium ion and 12-C-4 form
2:1 complexes in most of the solvents studied and that the crowns shield the nucleus from the solvent.

APPENDIX B

APPLICATIONS OF THE COMPUTER PROGRAM KINFIT4

B.1. CALIBRATION OF A pH GLASS ELECTRODE

B.1.1. <u>PROGRAM FUNCTION</u> - The program KINFIT4 is a general curve-fitting routine (134). The subroutine EQN of this program was modified to allow for calibration of the electrode. The electrode calibration equation is:

E = intercept + slope x log (
$$[H^+]_0 - \frac{t \times i_0}{F \times v_0}$$
 + residual) (23)

where intercept and residual are the unknowns [labelled as U(1) and U(2) in the computer program], E (experimental potential) and t (time) are the variables [XX(1) and XX(2), respectively] and i_0 (coulometric current in mA), v_0 (initial volume of acid), $[H^+]_0$ (initial proton concentration) and slope are the constants [CONST(1) to CONST(4)]. The subroutine EQN used in the present case is listed in B.1.2., and a sample of data input in B.1.3.

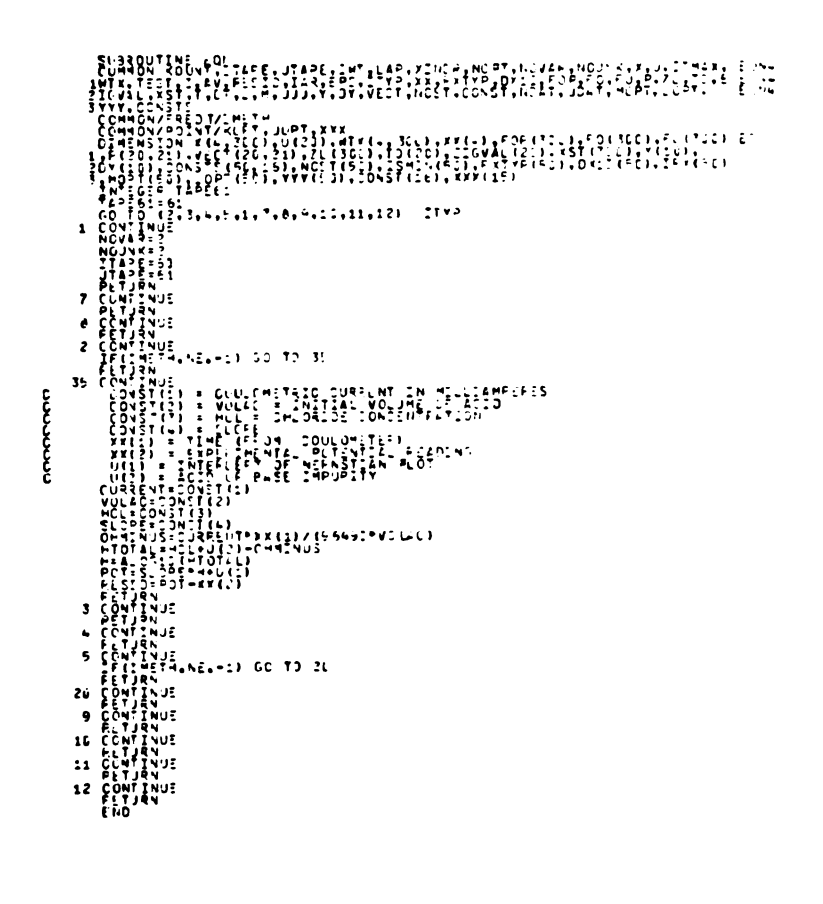
The data input is as follows: the first card contains the number of data points, the maximum number of iterations to be performed, the number of constants and the convergence tolerance. After the second card (title card) comes a card containing the values of the constants (if any), and then the card containing initial estimates of the unknowns. The cards following are data cards. In the present case, the input is observed potential as a function of the time during which base was generated. Each datum is followed by its estimated variance.

PLEASE NOTE:

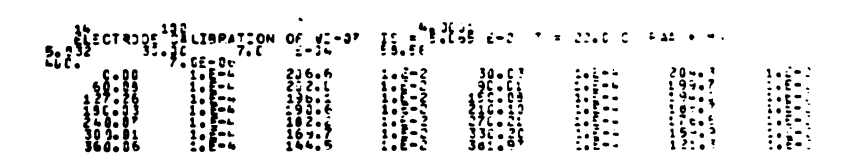
Dissertation contains small and indistinct print. Filmed as received.

UNIVERSITY MICROFILMS.

B.1.2. SUBROUTINE EQN



B.1.3. DATA SAMPLE



B.2. DETERMINATION OF THE FORMATION CONSTANTS OF 1:1 AND 2:1 COMPLEXES FROM NMR DATA

B.2.1. PROGRAM FUNCTION - The data of the plot chemical shift \underline{vs} mole ratio of ligand were fitted to equation (52)

$$\delta_{\text{obs}} = \delta_{\text{M}} \times_{\text{M}} + \delta_{\text{ML}} \times_{\text{ML}} + \delta_{\text{ML}_2} \times_{\text{ML}_2}$$
 (52)

which was rewritten as:

$$\delta_{\text{obs}} = \frac{c_{\text{M}}}{c_{\text{M}}^{\text{tot}}} \left(\delta_{\text{M}} - \delta_{\text{ML}_2}\right) + \frac{c_{\text{ML}}}{c_{\text{M}}^{\text{tot}}} \left(\delta_{\text{ML}} - \delta_{\text{ML}_2}\right) + \delta_{\text{ML}_2}$$
(64)

The constants are: C_M^{tot} , total concentration of metal ion [CONST(1) or CMT in subroutine EQN], δ_M , chemical shift of the free metal [CONST(2) or DELO]. The variables are C_L^{tot} , total concentration of ligand [XX(1) or CLT] and the experimental chemical shift [XX(2)]. The unknowns are: K_{ML} , the 1:1 complex formation constant [K_1 or U(1)], and its chemical shift δ_{ML} [DEL1 or U(2)], and K_{ML_2} , the 2:1 complex formation constant [K2 or U(3)] and its chemical shift δ_{ML_2} [DEL2 or U(4)].

The concentration of free metal in solution is obtained by solving the cubic equation (60). Before a mole ratio of 2 (ligand to metal), there are three real roots, and only one after. The root used before a mole ratio of 2 was determined by choosing the value of the angle θ (θ = $\phi/3$, $\phi/3$ + $2\pi/3$, $\phi/3$ + $4\pi/4$). In order to find the domain of validity of each root, the program KINFTI4 was used to simulate data with approximate—values of the unknowns for each root (see B.2.2.1. for a listing of EQN in these conditions). Once this step accomplished, the experimental data were refined with the proper roots. The subroutine EQN used is listed in B.2.2.2. and a sample of data input in B.2.3.

The order of the cards in the data deck has been given in B.1.1. The only change is in the data input: we now have the ligand concentration in solution as a function of the chemical shift, with their respective estimated variances.

B.2.2. SUBROUTINES

B.2.2.1. Subroutine EQN for Data Simulation

```
FIRACS(CCSFT)

PIE ACCS(CCSFT)

PIE ACCS(CCSFT)

THE ACCS
                                                                                                                                                                                          201 44
                                       301 C.VY.N.D.

102 T.S. 103 T. SOFT (D.T.)

103 T.S. 103 T. SOFT (D.T.)

104 T. SOFT (D.T.)

105 T. SOFT (D.T.)

105 T. SOFT (D.T.)

106 T. SOFT (D.T.)

107 T. SOFT (D.T.)

108 T. SOFT (D.T.)

108 T. SOFT (D.T.)

108 T. SOFT (D.T.)

108 T. SOFT (D.T.)

109 T.
NSETPHO

TE2 CLUTINUE

SCOI YMHAHABBS S/3-

VMHAHABBS S/3-

CMLKCLY-Z-CMY-Z-(M)/(1-K1-CM)

CMLKCLY-Z-CMY-Z-(M)/(1-K1-CM)

CMLKCLY-Z-CMY-Z-(M)/(1-K1-CM)

CMLKCLY-Z-CMY-Z-(M)/(1-K1-CM)

OF TO THE COMPANY OF THE COMPANY
```

B.2.2.2. Subroutine EQN

```
ETT::1
- (TEST1: NE. 1) 70 TO 3L:
```

B.2.3. DATA SAMPLE

APPENDIX C

APPLICATION OF THE

COMPUTER PROGRAM MINIQUAD 76A TO THE

DETERMINATION OF EQUILIBRIUM CONSTANTS

FROM POTENTIOMETRIC DATA

APPLICATION OF THE COMPUTER PROGRAM MINIQUAD 76A TO THE DETERMINATION
OF EQUILIBRIUM CONSTANTS FROM POTENTIOMETRIC DATA

C.1. PROGRAM MINIQUAD 76A

This program (136) determines the formation constants from potentiometric data. Up to 20 equations involving 5 reactants can be considered at the same time, and up to 3 electrodes can be used to determine the concentration of free species.

The equation constants are calculated for the reaction

$$aA + bB + cC \stackrel{?}{\leftarrow} A_a B_b C_c$$
 (65)

with the formation constant

$$K_{f} = \frac{[A_{a}B_{b}C_{c}]}{[A]^{a}[B]^{b}[C]^{c}}$$
(66)

In such a case the reaction

$$LH^{2-} + Mg^{2+} \stackrel{?}{\leftarrow} MgLH \tag{67}$$

with the formation constant

$$K_{f}(MgLH) = \frac{[MgLH]}{[Mg][LH]}$$
(68)

becomes

$$L^{3-} + H^{+} + Mg^{2+} \stackrel{\rightarrow}{\leftarrow} MgLH$$
 (69)

with

$$K_{f}' (MgLH) = \frac{[MgLH]}{[Mg][L][H]}$$
(70)

or

$$K_{f}^{l} (MgLH) = \frac{K_{f}(MgLH)}{K_{3}(PAA)}$$
 (71)

With the computer program MINIQUAD 76A, the formation constants can be either held constant or refined in the calculations. The coulometric (volumetric) titration data consist of the measured electrode potential as a function of the time during which the titrant was generated (the volume of titrant added). In these acid base titrations, one of the mass balance equations describes the concentration of species involving dissociable hydrogen ions. The hydroxide ion is considered as a "negative proton", and the proton concentration in a basic titrant is equal to the negative value of the hydroxide ion concentration.

C.2. DATA INPUT INSTRUCTIONS FOR MINIQUAD 76A

- C.2.1. 1 card /20A4/ : descriptive title
- C.2.2. 1 card /815/: LARS, NK, N, MAXIT, IPRIN, NMBEO, NCO, ICOM.

LARS is an indicator for the data points to be considered in the refinement: with LARS=1 all the data points are used, with LARS=2 alternate points, with LARS=3 every third point, etc. (last points on all titration curves are always used).

NK is the total number of formation constants.

N is the number of formation constants to be refined.

MAXIT is the maximum number of iteration cycles to be performed: with MAXIT=0 and according to the values of JPRIN and JP (see below) the residuals on mass balance equations and/or the species distribution are evaluated for the given formation constants and conditions.

IPRIN=O is normal; IPRIN=l monitors the progress of the refinement at each cycle; IPRIN=2 produces an additional listing of the experimental data at each titration point.

NMBEO is the total number of reactants (mass balance equations) in the system under consideration.

NCO is the maximum number of unknown concentrations of free reactants; if NCO=0 the whole job is abandoned before refinement.

ICOM=0 is normal; with ICOM=1 data points are eliminated before the refinement if the corresponding block of the normal equation matrix is found to be not positive-definite.

C.2.3. 1 card /3F10.6, 8X,I2/: TEMP, ADDTEMP, ALPHA, NOTAPE

TEMP is the reaction temperature in °C.

ADDTEMP is the titrant temperature in °C.

ALPHA is the coefficient of cubical expansion for the solvent used, ${}^{\circ}C^{-1}$.

NOTAPE=0 is normal; NOTAPE=1 reads values for EZERO and SLOPE (see below) from device TAPE3. This allows calibration curve data to be calculated and used in the same computer run.

C.2.4. NK cards /F10.6,715/: BETA(I), JPOT(I), JQRO(J,I) (NMBEO values), KEY(I)

The formation constants are expressed in exponential notation $\beta_1 = BETA(I) \cdot 10^{JPOT(I)}.$

JQRO(J,I) (J=1, NMBEO) are the NMBEO stoichiometric coefficients of the <u>i</u>th species with formation constant β_i . The order of coefficients is arbitrary, except that those referring to reactants

of which the free concentration is determined potentiometrically must come last. Such a choice implies that a progressive integer number (from 1 to NMBEO) is assigned to each reactant.

KEY(I) is the refinement key of the \underline{i} th formation constant: with KEY=0 the formation constant is not refined and with KEY=1 the formation constant is refined.

NMBE is the number of reactants (mass balance equations) involved in the titration curve.

JNMB holds the integer numbers previously assigned to the NMBE reactants involved.

NC is the number of unknown free concentrations at each point of the titration curve; the number of concentrations experimentally determined ($\underline{\text{i.e.}}$, the number of electrodes) is NEMF=NMBE-NC.

JP contains integer numbers corresponding to selected reactants: in the subroutine STATS the formation percentages relative to these reactants will be calculated, depending on the value of JPRIN.

1 card /5A10/ : REACT(I) (NMBE values)

REACT contains the names of the reactants, listed in the same order as JNMB.

1 card /4I5/ : JEL(I) (NEMF values), JCOUL

JEL holds the number of electrons transferred at each electrode. If the decimal cologarithm of concentration (e.g. pH) is to be read in, put JEL(I)=0.

JCOUL=0 is normal; JCOUL=1 if the total volume of the solution does not change during the titration ($\underline{e.g.}$, coulometric experiments).

TOTC contains the initial number of millimoles of reactants in solution; the order of reactants is the same as in JNMB.

EZERO(I) holds the standard potential of the <u>i</u>th electrode (mV); the value is ignored if JEL(I)=0.

ADDC contains the molar concentrations of titrant solutions (there is one for each reactant); the order of the reactants is the same as in JNMB.

VINIT is the initial volume of the solutions (cm^3) , and should correspond to the volume expected at the temperature of the TITRANT.

1 card /8F10.6/ : SLOPE (NEMF values).

SLOPE contains the slopes of the calibration curves for the species measured, in units of mV per decade of concentration, the value is ignored if JEL(I)=0.

LUIGI=0 is normal, LUIGI=1 indicates the end of a titration cruve, LUIGI<0 indicates the end of all titration curves, LUIGI=2 indicates that, for coulometric titration, current (mA) and fractional current efficiency are read instead of a data point.

TITRE contains the volumes of titrant solutions (cm^3) added in volumetric titrations or time of current passage (sec) in coulometric experiments.

EMF contains the potentials (mV) measured on each electrode with non-zero JEL value (otherwise the decimal cologarithms of concentration).

C.2.6. 1 card /I5/ : JPRIN

JPRIN controls the amount and type of output produced by STATS:

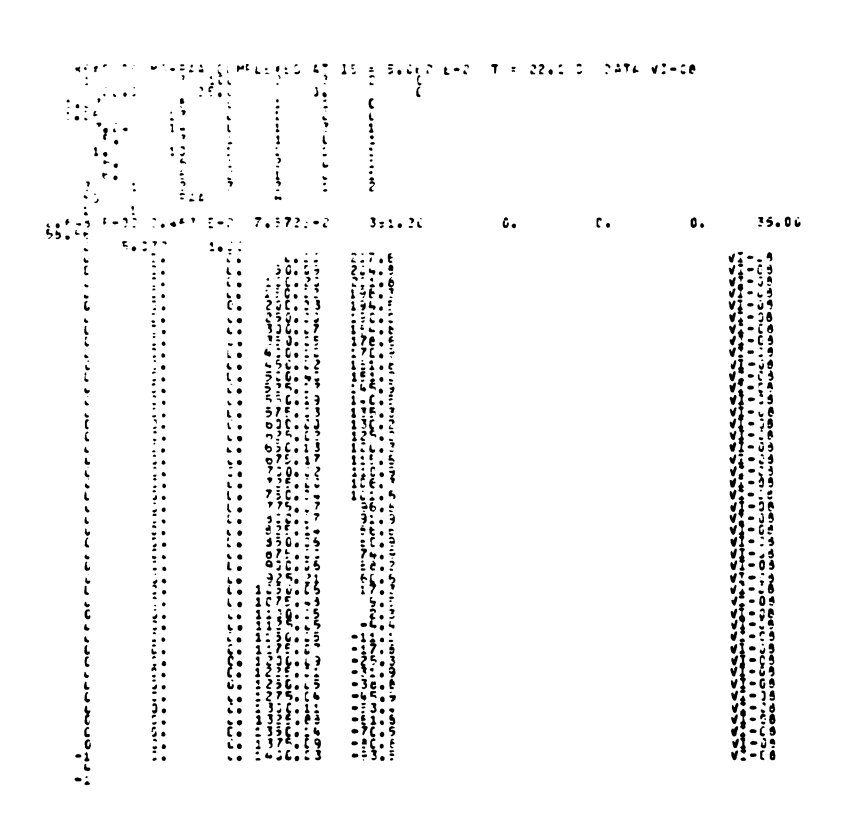
<u>JPRIN</u>	Statistical Analysis	<u>Tables</u>	Graphs
0	no	no	no
1	yes	no	no
2	yes	yes	no
3	yes	no	yes
4	yes	yes	yes

If JPRIN>1, the amount and type of tables and/or graphs is determined by the values contained in JP for each titration curve.

C.2.7. 1 card I5/: NSET

NSET=1 for another set of formation constants - items C.2.1. - C.2.4., C.2.6. and C.2.7. only -; NSET=0 for another complete set of data, NSET=-1 for the termination of the run.

C.3. DATA SAMPLE



BIBLIOGRAPHY

BIBLIOGRAPHY

- 1. (a) A. I. Popov, Pure and Applied Chem. <u>41</u>, 3 (1975).
 - (b) W. J. DeWitte, R. C. Schoening and A. I. Popov, Inorg. Nucl. Chem. Lett., 12, 251 (1976).
 - (c) J. S. Shih and A. I. Popov, Inorg. Nucl. Chem. Letters, 13, 105, (1977).
- 2. F. Alder and F. C. Yu, Phys. Rev., 82, 105, (1951).
- 3. M. Ellenberger and M. Villemin, C. R. Acad. Sci. Paris, Serie B, 266, 1430 (1968).
- 4. P. D. Dougan, S. N. Sharma, and D. Llewelyn Williams, Can. J. Phys., 47, 1047 (1969).
- 5. E. M. Dickson and E. F. W. Seymour, J. Phys. Chem., <u>3</u>, 666, (1970).
- 6. R. G. Bryant, J. Magn. Reson., 6, 159 (1972).
- 7. J. A. Magnusson and A. A. Bothner-By in "Magnetic Resonance in Biological Research," A. Franconi, Ed. Gordon and Breach, London, 1969, p. 135.
- 8. L. Simeral and G. E. Maciel, J. Phys. Chem. 80, 552, (1976).
- 9. J. H. Swinehart and H. Taube, J. Chem. Phys. 37, 1579, (1962).
- 10. N. A. Matwiyoff and H. Taube, J. Am. Chem. Soc., <u>90</u>, 2796, (1968).
- 11. R. D. Green and N. Sheppard, J. Chem. Soc. Faraday Trans. II 68, 821, (1972).
- 12. F. Toma, M. Villemin, and J. M. Thiery, J. Phys. Chem., <u>77</u>, 1294, (1973).
- 13. A. D. Covington and A. K. Covington, J. Chem. Soc. Faraday Trans. I, 71, 831, (1975).
- 14. R. N. Butler, J. Davies, M. C. Symons, Trans. Faraday Soc., 66, 2426, (1970).
- 15. B. N. Chernyshov, V. V. Kon'shin, Koord. Khim. 2, 365, (1976).
- 16. E. C. Ashby and R. C. Arnott, J. Organometal. Chem., <u>14</u>, 1, (1968).

- 17. (a) Nouveau traite de chimie minerale, Pascal, Masson et Cie Editeurs, 1958, tome IV, p. 170, and references therein.
 - (b) Handbuch der anorganische chemie, Gmelin, Berlin, Verlag Chemie GMBH, 1939, 27, teil B, p. 140 and references therein.
 - (c) Ikeuchi and Krohn, Acta Chem. Scand. 23, 2232, (1969).
 - (d) D. Bryce-Smith, Inorg. Synthesis, Vol. 6, p. 9.
 - (e) H. J. Abendroth, A. Peters, W. Fischer, Rev. Chim. Min., 11, 556, (1974).
 - (f) L. V. Gorbunov, V. N. Deciatnik, S. R. Raspopin, K. I. Trifonov, Zh. Neorg. Khim., 19, 3093, (1974).
 - (g) W. D. Treadwell and Th. Zurrer, Helv. Chim. Acta, <u>15</u>, 1271, (1932).
- 18. H. F. Halliwell and S. C. Nyberg, Trans. Faraday Soc., <u>59</u>, 1126, (1963).
- 19. F. L. Cook, T. C. Caruso, M. P. Byrne, C. W. Bowers, D. H. Speck, and C. L. Liotta, Tetrahedron Lett., 46, 4029, (1974).
- 20. M. A. Neuman, E. C. Steiner, F. P. van Remoortere, and F. P. Boer, Inorg. Chem., 14, 734, (1975).
- 21. R.D. McLachlan and V. B. Carter, Spectrochim. Acta, Part A, <u>30</u>, 1171, (1974).
- 22. A. Pullman, C. Giessner-Prettre, and Y. V. Kruglyak, Chem. Phys. Lett., <u>35</u>, 156, (1975).
- 23. F. A. L. Anet, J. Krane, J. Dale, K. Daasvatn, and P. O. Kristiansen, Acta Chem. Scand., 27, 3395, (1973).
- 24. B. K. Leong, T. O. Ts'o and M. Chenoweth, Toxicol. Appl. Pharmacol., 27, 342, (1974).
- 25. P. B. Chock, Proc. Nat. Acad. Sci. US, 69, 1939, (1972).
- 26. B. K. Leong, Chem. Eng. News, 4, 5, (1975).
- 27. B. Dietrich, J. M. Lehn and J. P. Sauvage, and J. Blanzat, Tetrahedron Lett., 2885 and 2889, (1969).
- 28. B. Dietrich, J. M. Lehn and J. P. Sauvage, and J. Blanzat, Tetrahedron, 29 1629, (1973).
- 29. J. M. Lehn and J. P. Sauvage, J. Amer. Chem. Soc., <u>97</u>, 6700, (1975).

- 30. W. E. Morf and W. Simon, Helv. Chim. Acta, 54, 2683 (1973).
- 31. J. M. Lehn, Structure and Bonding, 16, 2 (1973).
- 32. J. J. Christensen, D. J. Eatough, and R. M. Izatt, Chem. Rev., 74, 351 (1974).
- 33. J. D. Lamb, R. M. Izatt, J. J. Christensen, and D. J. Eatough, "Thermodynamics and Kinetics of Cation Macrocycle Interaction," Chapter in Chemistry of Macrocyclic Compounds, G. A. Melson, ed., Plenum, N.Y. in press.
- 34. D. N. Bhattacharyya, C. L. Lee, J. Smid, and M. Szwarc, J. Phys. Chem., 69, 608 (1965).
- 35. J. S. Shih, Ph.D. Thesis 1978, Michigan State University.
- 36. J. G. Hoogerheide, Ph.D. Thesis 1978, Michigan State University.
- 37. G. J. Templeman and A. L. Van Geet, J. Am. Chem. Soc., <u>94</u>, 5578 (1972).
- 38. D. H. Live, S. I. Chan, Analytical Chemistry, 42, 791 (1970).
- 39. M. S. Greenberg, R. L. Bodner and A. I. Popov, J. Phys. Chem., 77, 2449 (1973).
- 40. U. Mayer and V. Gutmann, Structure and Bonding, 12, 113 (1972).
- 41. (a) V. Gutmann and E. Wychera, Inorg. Nucl. Chem. Lett., $\underline{2}$, 257 (1966).
 - (b) V. Gutmann, "Coordination Chemistry in Nonaqueous Solvents" Springer-Verlag, Vienna (1968).
- 42. M. S. Greenberg, D. M. Wied and A. I. Popov, Spectrochim. Acta, 29A, 1927 (1973).
- 43. Y. Cahen, Ph.D. Thesis 1975, Michigan State University, East Lansing, Michigan.
- 44. A. I. Popov, Pure and Applied Chem., 41, 3 (1975).
- 45. A. I. Popov, "Polyhalogen Complex Ions" in Halogen Chemistry, vol. 1 V. Gutmann, ed., Academic Press, London and N.Y. (1967), p. 253.
- 46. R. H. Erlich and A. I. Popov, J. Amer. Chem. Soc., 93, 5620 (1971).
- 47. M. Greenberg, Ph.D. Thesis 1975, Michigan State University, East Lansing, Michigan
- 48. Y. M. Cahen, P. R. Handy, E. T. Roach, and A. I. Popov, J. Phys. Chem., <u>79</u>, 80, (1975).

- 49. T. C. Farrar and E. D. Becker, Pulse and Fourier Transform NMR, Academic Press, N.Y. and London, (1971), p. 65.
- 50. R. H. Erlich and A. I. Popov, J. Amer. Chem. Soc., <u>93</u>, 5620 (1971).
- 51. J. S. Shih and A. I. Popov, Inorg. Nucl. Chem. Letters, <u>13</u>, 105 (1977).
- 52. E. Kauffmann, personal communication.
- 53. K. Balasubrahmanyam and G. J. Janz, J. Am. Chem. Soc., $\underline{92}$, 4189 (1970).
- 54. P. Nylen, Ber., <u>57B</u>, 1032 (1924).
- 55. M. I. Kabachnik and T. A. Mastryukova, Izvest. Akad. Nauk., S.S.S.R., 163 (1953).
- 56. A. A. Shvets, O. A. Osipov, and A. M. Shakirova, J. Gen. Chem., USSR, 37, 2588 (1967).
- 57. E. M. Popov, M. I. Kabachnik, and L. S. Mayants, Russian Chem. Rev., 30, 362 (1961).
- 58. L. J. Bellamy and L. Beecher, J. Chem. Soc., 475 (1952).
- 59. L. J. Bellamy and L. Beecher, J. Chem. Soc., 729 (1953).
- 60. D. J. Harvey and M. G. Horning, J. Chromatogr., <u>79</u>, 65 (1973).
- 61. R. J. Maile, Jr., G. J. Fischesser and M. M. Anderson, J. Chromatogr., 132, 366 (1977).
- 62. H. Sohr, J. Electroanal. Chem. Interfacial Electrochem., 11, 188 (1966).
- 63. D. Balzer and H. Lange, Colloid Polym. Sci., <u>253</u>, 643 (1975).
- 64. D. Balzer and H. Lange, Colloid Polym. Sci., <u>255</u>, 140 (1977).
- 65. W. Althoff, M. Fild and H. P. Rieck, Z. Naturforsch. B. Anorg. Chem. Org. Chem., 31B, 153 (1976).
- 66. G. A. Gray, J. Am. Chem. Soc., <u>93</u>, 2132 (1971).
- 67. J. G. Riess, J. R. Van Wazer, and J. H. Letcher, J. Phys. Chem. <u>71</u>, 1925 (1967).
- 68. T. Bottin-Strzalko and J. Seyden-Penne, J. Chem. Soc., Chem. Commun., <u>22</u>, 905 (1976).
- 69. L. L. Burger, J. Phys. Chem., <u>62</u>, 590, (1958).

- 70. A. A. Elesin, A. A. Zaitsev, S. S. Kazakova, and G. N. Yakovlev, Radiokhimiya, 14, 541 (1972).
- 71. A. A. Elesin, A. A. Zaitsev, S. S. Kazakova, and G. N. Yakovlev, Nucl. Sci. Abstr., <u>28</u>, 18030 (1973).
- 72. S. M. Lambert and J. I. Watters, J. Am. Chem. Soc., 79, 4262 (1957).
- 73. J. I. Watters, S. M. Lambert and E. D. Loughran, J. Am. Chem. Soc., 79, 3651, (1957).
- 74. J. Mao, E. Robishaw, Biochemistry, <u>14</u>, 5475 (1975).
- 75. J. F. Cannelongo, U.S. Patent #3,370,029.
- 76. Th. Auel, Ger. Offen. #2,505,435.
- 77. Anonymous, Neth. Appl. #6,508,180.
- 78. G. T. Bottger and A. P. Yerington, U.S. Dept. Agr., Bur. Entomol. Plant Quarantine E-863, (1953).
- 79. E. F. Rogers, A. A. Patchett, Ger. Offen. #2,318,254.
- 80. E. F. Rogers, A. A. Patchett, Ger. Offen. #2,318,254.
- 81. L. L. Clark, U.S. Patent #4,016,264.
- 82. T. R. Herrin, J. S. Fairgrieve, U.S. Patent #4,052,439.
- 83. J. B. Schleicher, W. R. Roderick, Ger. Offen. #2,208,787.
- 84. L. R. Overby, R. G. Duff, J. C. Mao, Ann. N.Y. Acad. Sci., 284, 310 (1977).
- 85. J. A. Boezi, in press.
- 86. J. Hay, S. M. Brown, A. T. Jamieson, F. J. Rixon, H. Moss, D. A. Dargan and J. H. Subak-Sharpe, J. Antimicrob. Chemother., 3, Suppl. A, 63 (1977).
- 87. S. S. Leinbach, J. M. Reno, L. F. Lee, A. F. Isbell, and J. A. Boezi, Biochemistry, <u>15</u>, 426 (1976).
- 88. B. W. Fox, J. Antimicrob. Chemother. 3, Suppl. A, 23, (1977).
- 89. T. H. Maugh II, Science, <u>192</u>, 128.
- 90. R. J. Klein and A. E. Friedman-Kien, Antimicrob. Agents Chemother., 7, 289 (1975).
- 91. H. G. Adams, E. A. Benson, E. R. Alexander, L. A. Vontver, M. A. Remington, K. K. Holmes, J. Infect. Dis. <u>133</u> (Suppl.): A151-A159 (1976).

- 92. E. L. Goodman, J. P. Luby, M. T. Johnson, Antimicrob. Agents Chemother. 8, 693 (1975).
- 93. A. E. Friedman-Kien, A. A. Fondak, and R. J. Klein, J. Invest. Dermatol., 66, 99 (1976).
- 94. D. D. Gerstein, C. R. Dawson, and J. O. Oh, Antimicrob. Agents Chemother., 7, 285 (1975).
- 95. R. F. Meyer, E. D. Varnell, and H. E. Kaufman, Antimicrob. Agents Chemother., 9, 308 (1976).
- 96. J. F. Fitzwilliam and J. F. Griffith, J. Infect. Dis., 133, Suppl. A221, (1976).
- 97. N. L. Shipkowitz, R. R. Bower, R. N. Appell, C. W. Nordeen, L. R. Overby, W. R. Roderick, J. B. Schleicher, and A. M. von Esch, Appl. Microbiology, 26, 264 (1973).
- 98. R. J. Klein and A. E. Friedman-Kien, Antimicrob. Agents Chemother., 7, 289 (1975).
- 99. J. Roboz, R. Suzuki and G. Bekesi, and R. Hunt, Biomed. Mass. Spectrom., 4, 291 (1977).
- 100. B. A. Bopp, Ch. B. Estep, D. J. Anderson, Fed. Proc., <u>36</u>, 939 (1977).
- 101. T. R. Herrin, J. S. Fairgrieve, R. R. Bower, N. L. Shipkowitz, J. Mao, J. Med. Chem., 20, 660 (1977).
- 102. L. F. Lee, K. Nazerian, S. S. Leinbach, J. M. Reno, J.A. Boezi, J. Natl. Cancer Inst., 56, 823 (1976).
- 103. P. Nylen, Z. Anorg. Allg. Chem., 235, 33 (1937).
- 104. S. Warren and M. R. Williams, J. Chem. Soc., (B), 618 (1971).
- 105. P. Nylen, Ber., 57B, 1036 (1924).
- 106. H. Denham, U.S. Patent #2,629,731.
- 107. R. R. Naqvi and P. J. Wheatley, and E. Foresti-Serantoni, J. Chem. Soc. A, <u>17</u>, 2751 (1971).
- 108. J. M. Reno, L. F. Lee, J. A. Boezi, Antimicrob. Agents Chemother., 13, 188 (1978).
- 109. A. Unni, L. Elias, and H. Schiff, J. Phys. Chem., 67, 1216 (1963).
- 110. D. Duvillier, Ann. Chim. Phys. <u>23</u>, 327 (1881).
- 111. B. Schmidt, Ann., <u>267</u>, 265 (1892).

- 112. Handbook of Chemistry and Physics, Chemical Rubber Company, ed., (1967-8) p. F-4.
- 113. M. M. Crutchfield, C. F. Callis, R. R. Irani and G. C. Roth, Inorg. Chem., 1, 813 (1963).
- 114. R. Jones and A. Katritzky, J. Inorg. Nucl. Chem., 15, 193 (1960).
- 115. J. H. Letcher and J. R. Van Wazer, J. Chem. Phys., 44, 815 (1966).
- 116. J. H. Letcher and J. R. Van Wazer, J. Chem. Phys., 45, 2916 (1966).
- 117. J. H. Letcher and J. R. Van Wazer, J. Chem. Phys., 45, 2926 (1966).
- 118. J. H. Letcher and J. R. Van Wazer, Chapters 2 and 3 in Phosphorus 31 Nuclear Magnetic Resonance, M. Grayson, E. J. Griffith, ed., Interscience Publishers, N.Y. and London, (1967).
- 119. K. Moedritzer, Inorg. Chem., 6, 936 (1967).
- 120. Carbon-13 NMR for Organic Chemists, Levy Nelson, ed., Interscience (1972), p. 23.
- 121. J. C. Tebby, Organophosphorus Chemistry, vol. 1, Specialist Periodical Reports, The Chemical Society, ed., London (1970), p. 294.
- 122. G. Mavel and M. J. Green, Chem. Comm., 742 (1968).
- 123. J. C. Tebby, Organophosphorus Chemistry, vol. 2, Specialist Periodical Reports, The Chemical Society, ed., London (1970) p. 252.
- 124. R. G. Bates, Determination of pH Theory and Practice, J. Wiley and Sons, Inc., N.Y., London, Sydney, (1964), p. 53.
- 125. H. S. Harned and B. B. Owen, The Physical Chemistry of Electrolytic Solutions, Reinhold Publishing Corp., N.Y., 3rd edition, (1958), p. 165.
- 126. L. Meites, Handbook of Analytical Chemistry, McGraw-Hill Book Co., N.Y., San Francisco, Toronto, London, Sydney, 1st edition, (1963), p. 1-21.
- 127. C. Cotton and J. Wilkinson, Advanced Inorganic Chemistry, Interscience, 3rd edition, p. 848.
- 128. J. J. Lingane, Chem. Rev. 29, 1 (1941).
- 129. D. D. DeFord and D. N. Hume, J. Am. Chem. Soc., 73, 5321 (1951).
- 130. S. Fronaeous, Acta Chem. Scand., 4, 72 (1950).
- 131. H. S. Harned and B. B. Owen, the Physical Chemistry of Electrolytic Solutions, Reinhold Publishing Corp., N.Y., 3rd edition, (1958), p. 738.

- 132. L. Meites, Handbook of Analytical Chemistry, McGraw-Hill Book Co., N.Y., San Francisco, Toronto, London, Sydney, 1st edition, (1963), p. 1-46.
- 133. P.-H. Heubel and J. Hoogerheide, "Constant Current Coulometer," (1977).
- 134. J. L. Dye and V. A. Nicely, J. Chem. Educ., <u>48</u>, 443 (1968).
- 135. F. A. L. Anet, J. Krane, J. Dale, K. Daasvatn, and P. O. Kristiansen, Acta Chem. Scand., 27, 3395, (1973).
- 136. A. Sabatini, A. Vacca, and P. Gans, Talanta, <u>21</u>, 53 (1974).
- 137. D. D. Traficante, J. A. Simms and M. Mulvay, J. Magn. Reson., 15, 484 (1974).
- 138. D. A. Wright and M. T. Rogers, Rev. Sci. Instr., 44, 1189 (1973).

